Copyright Warning & Restrictions

The copyright law of the United States (Title 17, United States Code) governs the making of photocopies or other reproductions of copyrighted material.

Under certain conditions specified in the law, libraries and archives are authorized to furnish a photocopy or other reproduction. One of these specified conditions is that the photocopy or reproduction is not to be "used for any purpose other than private study, scholarship, or research." If a, user makes a request for, or later uses, a photocopy or reproduction for purposes in excess of "fair use" that user may be liable for copyright infringement,

This institution reserves the right to refuse to accept a copying order if, in its judgment, fulfillment of the order would involve violation of copyright law.

Please Note: The author retains the copyright while the New Jersey Institute of Technology reserves the right to distribute this thesis or dissertation

Printing note: If you do not wish to print this page, then select "Pages from: first page # to: last page #" on the print dialog screen

ABSTRACT

Power Consumption in Single-Phase Agitated Vessels Provided with Multiple Impellers

by

Gwo-Ming Chang

A significant amount of data can be found in the literature on power consumption of single-impeller agitation systems. However, little and incomplete information is available for power consumption in multiple-impeller systems. Therefore, the main objective of this study is to experimentally determine the power consumed by multiple impellers in mixing vessels as a function of impeller type, impeller off-bottom clearance, impeller spacing, and agitation speed.

In this work, the power dissipated by combinations of one, two or three impellers of either identical types or different types was studied. The power drawn by each individual impeller was measured by means of strain gages. The results indicate that the power consumed by each impeller is strongly dependent on the combination of impeller types, spacing, clearance, and the presence of other impellers. For triple-disc turbine systems, the maximum power consumption was found when the intermediate impeller was spaced midway between the other two. In addition, the total power drawn was approximately equal to the sum of each individual power drawn when the spacing was about twice the impeller diameter.

POWER CONSUMPTION IN SINGLE-PHASE AGITATED VESSELS PROVIDED WITH MULTIPLE IMPELLERS

by
Gwo-Ming Chang

A Thesis
Submitted to the Faculty of
New Jersey Institute of Technology
in Partial Fulfillment of the Requirements for the Degree of
Master of Science in Environmental Engineering

Department of Civil and Environmental Engineering

May 1993

APPROVAL PAGE

Power Consumption in Single-Phase Agitated Vessels Provided with Multiple Impellers

Gwo-Ming Chang

Dr. Piero M. Armenante, Thesis Advisor (date)
Associate Professor of Chemical Engineering, NJIT

Dr. Angelo J. Perna, Committee Member (date)
Professor of Chemical and Environmental Engineering, NJIT

Dr. Paul N. Cheremisinoff, Committee Member (date)
Professor of Civil and Environmental Engineering, NJIT

BIOGRAPHICAL SKETCH

Author: Gwo-Ming Chang

Degree: Master of Science in Environmental Engineering

Date: May 1993

Undergraduate and Graduate Education:

- Master of Science in Environmental Engineering,
  New Jersey Institute of Technology, Newark, NJ, 1993
- Bachelor of Engineering in Chemical Engineering,
  National Taiwan Institute of Technology, Taipei, Taiwan, 1989
- Diploma in Chemical Engineering,
  National Taipei Institute of Technology, Taipei, Taiwan, 1984

Major: Environmental Engineering

This thesis is dedicated to my parents

ACKNOWLEDGMENT

I would like to express my sincere gratitude to my thesis advisor, Dr. Piero M. Armenante, for his timely help, guidance, and support. His efforts were truly appreciated.

I would like to acknowledge Dr. Angelo J. Perna and Dr. Paul N. Cheremisinoff for serving as the members of my thesis committee.

I appreciate the mixing laboratory members, Joseph Chou and Emad Abu-Hakmeh, for their suggestions and assistance.

TABLE OF CONTENTS

Chapter **Page**

LIST OF TABLES

LIST OF FIGURES

LIST OF APPENDICES

APPENDIX A Figures for Multiple-Impeller Systems

Figure Page

Figure Page

APPENDIX B Experimental Data for Multiple-Impeller Systems

Table Page

Table Page

NOMENCLATURE

A	impeller blade angle (radian)
B	baffle width (cm)
C	impeller off-bottom clearance (cm)
C_1	clearance between Impeller #1 and vessel bottom (cm)
C_2	clearance between Impeller #2 and vessel bottom (cm)
C_3	clearance between Impeller #3 and vessel bottom (cm)
D	impeller diameter (cm)
Fr	Froude Number, ND^2 / g (dimensionless)
H	liquid height (cm)
K_1	proportionality factor corresponding to Strain Gage #1 (watts • s/mV)
K_2	proportionality factor corresponding to Strain Gage #2 (watts • s/mV)
K_3	proportionality factor corresponding to Strain Gage #3 (watts • s/mV)
k	constant
L	impeller blade length (cm)
mV_1	signals corresponding to Strain Gage #1 (mV)
mV_2	signals corresponding to Strain Gage #2 (mV)
mV_3	signals corresponding to Strain Gage #3 (mV)
N	rotational speed (rps)
Ne	power number (dimensionless)
Ne_i	individual power number (dimensionless)
Ne_1	power number for Impeller #1 (dimensionless)
Ne_2	power number for Impeller #2 (dimensionless)
Ne_3	power number for Impeller #3 (dimensionless)
Ne*	power number for single impellers at C/D=1 (dimensionless)
Ne(tot)	total power number for multiple impellers (dimensionless)

n_b impeller blade number (dimensionless)

P power input (watts)

P_i individual power drawn (watts)

P_1 power drawn by Impeller #1 (watts)

P_2 power drawn by Impeller #2(watts)

P_3 power drawn by Impeller (watts)

Ptot power drawn by multiple impellers (watts)

P*single power drawn by single impellers at C/D=1 (watts)

p impeller pitch

Re Reynolds number, $\rho ND^2 / \mu$ (dimensionless)

S spacing between impellers(cm)

S_{12} spacing between Impeller #1 and Impeller #2 (cm)

S_{13} spacing between Impeller #1 and Impeller #3 (cm)

S_{23} spacing between Impeller #2 and Impeller #3 (cm)

T tank diameter (cm)

T_1 actual torque produced by impellers corresponding to Strain Gage #1 (Nm/s)

T_2 actual torque produced by impellers corresponding to Strain Gage #2 (Nm/s)

T_3 actual torque produced by impellers corresponding to Strain Gage #3 (Nm/s)

W impeller blade width (cm)

Greek Letters

ρ liquid density (kg/m^3)

μ liquid viscosity (kg/m s)

ω angular velocity (radian/s)

CHAPTER 1

INTRODUCTION

Mixing is an extremely common operation in the industrial practice. Power consumption is fundamental to any mixing process since energy is needed to homogenize the vessel content, disperse immiscible phases such as gases and liquids, suspended solids, increase gas-solid, solid-liquid or liquid-liquid mass transfer, and, in general, produce the desired mixing effect. Power consumption is not only dependent upon the type of impeller used and its rotational speed, but also on the physical properties of fluid and the geometric characteristics of the system, including the location of the impeller within the mixing vessel.

A significant amount of data can be found in the literature for power consumption in single-impeller agitation systems. However, little and incomplete information is available for power consumption in mixing tank provided with multiple impellers. These systems are often used in industry, especially in fermentation. The power consumed by multiple impellers and the characteristics of the flow that they generate are often estimated on the basis of the power consumed in single-impeller systems. However, this may not be correct in most applications. *Therefore, the main objective of this study is to experimentally determine the agitation power consumed by multiple-impeller agitation systems.*

In this work, the typical apparatus consisted of a vessel equipped with a centrally located shaft on which one or more impellers could be mounted. Strain gages were placed at different heights on the shaft to measure the torque resulting from the impellers mounted below any given strain gage. The signals from the strain gages were collected through a slip ring which was also mounted on the shaft, and sent to an external conditioner and amplifier. The fluid was always tap water. The rotation speed was measured independently using an optical sensor. A data acquisition system receiving all

these signals and used to calculate the resulting power consumption for each individual impeller.

Vessels of different height-to-tank diameter ratios were used. One, two, or three impellers of different types namely disc turbine, 45° pitched-blade turbine (down flow), flat-blade turbine, and curved-blade turbine were employed on the centrally located shaft. Combinations of identical impellers as well as impellers of different types were studied. The power consumption of each impeller was measured as a function of number of impellers, impeller type, rotational speed, off-bottom clearance, and spacing between impellers. The effects of two major parameters, namely spacing between impellers and off-bottom clearance, were studied in greater detail.

CHAPTER 2

LITERATURE SURVEY

The power consumed by an impeller is the energy per unit time transferred from the impeller to the fluid as a result of impeller rotation. Power is one of the most important parameters used to describe and quantify the intensity of mixing.

Many types of impellers are used for agitation and mixing of liquids in vessels. The power consumption is not only dependent upon the type of impeller used and the rotational speed, but also on the physical properties of the fluid and the geometric characteristics of the system, including the location of the impeller within the mixing vessel. A number of factors such as the shape, size of the impeller and vessel, extent of baffling, impeller off-bottom clearance, and spacing between impellers typically produce changes in the flow pattern of the fluid being mixed and influence the power drawn. The power requirement for an agitated vessel and the power relationships given below are based on experimental measurements and dimensional analysis considering the impeller-tank geometry factors which are applicable for scale up or scale down under the condition of geometric similarity.

The most common configuration of the mixing equipment used in industry consists of a vessel of a height nearly equal to the tank diameter where only one impeller is provided. However, agitated vessels having a value of height-to-diameter ratio greater than unity and equipped with multiple impellers are commonly used in processes where shear-sensitive or high viscosity materials are treated, or where a high vessel surface-to-volume ratio is required. (Fajner et al., 1982). Multiple-impeller mixing systems have attracted much attention in the last two decades, especially for gas-liquid operation and fermentation. However, the power consumed by multiple impellers and the characteristics of the flow they generate are often based on the single-impeller system under ungassed conditions. This may not be correct in most applications. Therefore, the

main objective of this study is to experimentally determine the agitation power consumed by multiple impeller agitation systems as a function of impeller type, rotational speed, off-bottom clearance, and spacing between impellers.

2.1 Power Number Theory

A number of investigators have reported impeller power characteristics in terms of two dimensionless groups, the Power Number, Ne, and the impeller Reynolds Number, Re. White and his coworkers (1934) were the first to point out the possibility and advantage of correlating impeller power using dimensional analysis. A general power relationship as a function of physical and geometrical parameters was reported as the following (Rushton, 1950; Bates et al., 1963):

$$\frac{P}{\rho N^3 D^5} = k\left(\frac{\rho N D^2}{\mu}\right)^a \left(\frac{N^2 D}{g}\right)^b \left(\frac{T}{D}\right)^c \left(\frac{H}{D}\right)^d \left(\frac{C}{D}\right)^e \left(\frac{p}{D}\right)^f \left(\frac{W}{D}\right)^g \left(\frac{L}{D}\right)^h \left(\frac{n_2}{n_1}\right)^i \qquad (2.1)$$

where the group on the left hand side is so called the impeller power number, Ne. The first group on the right hand side is known as the impeller Reynolds Number, Re, and the second group is known as the Froude Number, Fr. The remaining terms account for the effects of the tank geometry and impeller configuration. The Reynolds Number describes the hydrodynamic effect in the system. The Froude Number accounts for the effect of vortex in swirling systems. Bates et al., (1963) also pointed out that Equation (2.1) should be expended to include baffle number and width, spacing between impellers, and off-center impeller location. All of these additional geometrical parameters may be included in a form similar to that in Equation (2.1).

Chudacek (1985) proposed that the effect of vessel bottom shapes should be included in the above analysis, because the vessel bottom shape represents a significant geometrical factor with respect to the recirculation pattern and is also likely to influence the impeller power consumption.

However, the full form in Equation (2.1) is seldom used in practical power calculation. If geometrical similarity is assumed and if no vortex is present, the equation simplifies to

$$Ne = k\,(Re)^{a} \tag{2.2}$$

Furthermore, if the mixing process is carried out in a fully baffled turbulent region at a given geometry of configuration, Equation (2.1) reduces to

$$Ne = \frac{P}{\rho N^3 D^5} = \text{Constant} \tag{2.3}$$

Therefore, the dimensionless group of the power number, Ne, represents an important parameter since its knowledge enables the designer to predict the impeller power requirement for a given mixing operation.

2.2 Power Measurement and Power Relationships

2.2.1 Single-Impeller Systems

Agitation systems consisting of a single impeller and a mixing vessel with various impeller-tank geometry systems have been studied extensively, especially disc turbines (DTs) in vessels of standard geometry and in low viscosity fluid (Hudcova et al., 1988). Many investigators (Rushton, 1950; Bates et al, 1963; Gray et al., 1982; Shiue and Wong, 1984; Chudacek, 1985; Papastefanos, 1989; Rewatkar et al., 1990) have experimentally determined the power characteristics and behaviors of single impeller systems. All the results so obtained indicate that the impeller power number, Ne, reaches a constant value, for a given geometry, if the agitation intensity is high enough to produce turbulent flow (associated with Re>10,000).

White and Brenner (1934) were the first to determine the power law exponents. Their correlation was given as:

$$\frac{P}{D\mu N^2 T^{1.1} W^{0.3} H^{0.6}} = 0.000129\left(\frac{\rho N D^2}{\mu}\right)^{0.86} \tag{2.4}$$

Rushton et al. (1950) studied five impeller types for different impeller-tank geometries. For the case in which the impeller diameter-to-tank diameter ratio, D/T, was equal to 1/3, the liquid height-to-tank diameter ratio, H/T, was equal to 1, the off bottom clearance-to-impeller diameter ratio, C/T, was equal to 1, and the baffle width was 1/10 of the tank diameter, the power number was found by these investigators to be 6.3 for DTs and 1.65 for 45° pitched-blade turbines (PBTs). They also reported that the impeller off-bottom clearance had no effect if the value of C/D ranged from 0.7 to 1.6. No effect of liquid height was reported.

O'Connell and Mack (1950) investigated the power relationships for flat-blade turbines by varying the number of blades and impeller width-length ratios in both the laminar and turbulent regions under fully baffled condition. In the laminar region, they found that:

$$\frac{Pg_c}{\rho N^3 D^5} = k\left(\frac{\mu}{\rho N D^2}\right)\left(\frac{W}{D}\right)^b \tag{2.5}$$

and in the turbulent regime (Re>10,000):

$$\frac{Pg_c}{\rho N^3 D^5} = k\left(\frac{W}{D}\right)^b \tag{2.6}$$

where the constants k and b were dependent upon the number of blades.

Nagata et al. (1957) [from Tatterson, 1991] obtained an equation for Ne in the turbulent region for fully baffled tanks:

$$Ne = \frac{A}{R} + B\left(\frac{H}{T}\right)^{(0.35+W/T)} \tag{2.7}$$

where A, B, and R were determined from:

$$A = 14 + \left(\frac{W}{T}\right)\left[70\left(\frac{D}{T} - 0.6\right)^2 + 185\right]$$

$$\log_{10}(B) = 1.3 - 4\left(\frac{W}{T} - 0.5\right)^2 - 1.14\left(\frac{D}{T}\right)$$

$$R = \frac{25(D/T - 0.4)^2}{W/T} + \left(0.11 - \frac{0.0048T}{W}\right)^{-1}$$

Bates et al. (1963) reported a conventional log-log plot of the simplified power equation for some impeller types under the "standard conditions", D/T=1/3, C/T=1/3, H/T=1. The value of Ne that they reported for DTs was 4.8 for four T/12 baffles and 5.0 for four T/10 baffles. Flat-blade turbines (FBTs) and curved-blade turbines (CBTs) were shown, from the plot, to have similar power numbers in the turbulent region, while PBTs consumed the least power. Their measurements showed that the impeller off-bottom clearance has a definite effect on power consumption.

O'Kane (1974) investigated the effect on power consumption of blade width and number of blades. He demonstrated that it was not possible to find a value of exponents in the generalized power relationship (Equation 2.1) which could be applied to all types of impellers. The power number obtained at standard conditions for a DT and a 45° PBT with six blades was 5.05 and 1.52, respectively.

Gray et al., (1982) proposed a power correlation for DTs with six flat blades. The result was a constant power number of 5.17 representing the data for C/D>1.1. For C/D<1.1, Ne varied with $(C/D)^{0.29}$. The baffling effect was found to be negligible over the range of standard size baffling, $1/12 \leq W/T \leq 1/10$. The effect of D/T was small under these conditions.

Chudacek (1985) conducted a power study in profiled bottom vessels. For the standard flat bottom vessel, the 45° PBT exhibited a power number of 1.63.

Rao and Joshi (1988) studied the flow pattern and power consumption in liquid phase mixing with DTs, PBTs (downflow and upflow). For the case of DT, the measured power numbers were 5.18 and 4.40 for clearances equal to T/3 and T/6, respectively. At lower clearance, the impeller pumping action was greater, thereby increasing the power consumption. For the case of PBT (downflow), when the clearance was decreased from T/3 to T/4 and further to T/6, an increase in the value of Ne equal to 1.29, 1.35, and 1.61, respectively, was observed. Their reports also pointed out that the PBT (downflow) with D/T=1/3 was found to be most energy efficient out of all PBT impellers.

Rewatkar et al., (1990) conducted a series of measurements using PBT impellers and compared them to DT impellers. A number of geometrical factors, D, W, H, C, blade angle, and blade thickness, were studied in detail. The power number of the standard DTs (D/T=1/3, C=D) and PBTs was found to be 5.18, and 1.67, respectively. The power number was observed to have a strong dependence on the flow pattern generated by the impeller. In general, Ne increased for PBTs (pumping down) and decreased for DTs with a decrease in clearance. However, in practice, Ne decreased when the clearance was more than T/4 because of surface aeration. Without the effect of surface aeration, the liquid height was found to have little effect on power consumption. Rewatkar et al. obtained an overall correlation for the impeller power number for a PBT:

$$Ne = 0.653\left(\frac{T}{D}\right)^{0.11}\left(\frac{C}{T}\right)^{-0.23}(n_b)^{0.68}(A)^{1.82} \qquad (2.10)$$

for $6 \le T/D < 3$, $W/D=0.3$, $H/T=1$, $0.125 \le C/T \le 0.33$, $0.5 \le A$ (impeller blade angle, radian) ≤ 1.05, $4 \le n_b \le 8$

2.2.2 Multiple-Impeller Systems

Bates et al. (1963) studied the effect of some of the geometrical factors on power consumption of dual impellers, such as the type of impeller, impeller diameter, spacing between impellers, clearance, and extent of baffling. The results indicated that the dual 45°PBTs do not consume twice the power of a single turbine if $S/D \le 4$. Dual FBTs actually consumed a total power almost 25% greater than the sum of the two when $S/D < 1$. The combination of two impeller types, a PBT above a FBT, produced a combined power consumption equal to the sum of two single impellers at about S/D=1.

Nienow and Lilly (1979) conducted a research with two DTs in a vessel having H=T, C/T=1/4, D/T=1/4. Under ungassed conditions, the power number for a single impeller was 4.9 while that for the two impellers was found to be 10.2 for S/D=2. Their studies also pointed out that the power number for n impellers was approximately n times

the power number of single impeller provided the S/D≥1. In addition, the sum of their individual power numbers was unaffected by the impeller spacing used.

Kuboi and Nienow (1982) measured the power consumption by means of strain gages in dual-impeller systems. The experiments were conducted using some combinations of DT and 45°PBT mixed flow impellers in the vessel with H=T. Their studies indicated that the power numbers remain constant within 5% for $Re>4\times10^4$. The power drawn by single impellers was also measured in order to make a comparison and evaluate if the simple summation rule, total power input=$\sum$ (individual power input), was correct. For dual PBTs (bottom, downward; upper, upward) and the combination of a DT (bottom) and a PBT (top, upward) with C/D=1 and S/D=1, the total power drawn fall within 10% of the summation rule. However, the most surprising result that they found was for the dual DTs. For this system, these investigators found that Ne(tot)=7.5 (Ne=3.6 for the bottom impeller, and Ne=3.9 for the top impeller). This number should be compared with Ne=5 which is the value reported by many investigators for a single DT.

Roustan (1985) performed a study in non-standard vessels with hemispherical bottoms provided with two or three DTs. Under ungassed conditions, the measured power number was 10.4 for a dual-impeller system, which was equal to twice the power number for a single impeller in a standard vessel. However, the power number obtained for three DTs was 14.2 showing that the power dissipated with three impellers was not entirely proportional to the number of impellers used.

Machon et al. (1985) reported a comparison of single-impeller and dual-impeller configurations, i.e., a DT used in combination with a PBT (upward or downward). The data indicated that the total power input was less than the sum of the power input of the individual impellers with the two impellers spaced at a distance approaching the impeller diameter. At an impeller spacing equal to the vessel diameter, the resulting power number equaled the sum of the power numbers of the two impellers, even if the impellers

were of different types. The experiments were run in the fully turbulent region at different agitation speeds. They found that the reduction in Ne due to the increase in agitation speed was slight.

Smith et al. (1987) considered the flow conditions in a gas-liquid system in a vessel for which H/T=3, with triple DTs by changing the impeller spacing. Their results confirmed that, under ungassed conditions, the power consumed by two impellers was twice that of a single impeller provided that the S/D ratio was equal to 2. In triple-DT systems with each impeller evenly spaced at S/D=2.5, the total power input was 2.98 times that of a single turbine. They also reported that in the range S/D=1-1.5, the power demand increased steeply. When S/D=1.5, the additional power consumption was over 90% of that value obtained independently.

Abrardi et al. (1988) conducted a dynamic analysis of gas-sparged vessels agitated by two DTs in non-standard vessels, and compared their behavior to that of a standard vessel. This comparison showed that the hydrodynamic regimes of a dual-impeller system are more complicated than those of a single impeller one. In an ungassed system the dissipated power for two impellers with S/D=2 and C/D=1 was double that in a single impeller.

Nocentini et al. (1988) reported the ungassed power number in turbulent regime was 18.5 for four-impeller and 4.6 for single-impeller system. The reported values confirmed that the total power input for the multiple impellers was the sum of the power consumption of the individual impellers, at least when the impeller spacing was greater than the impeller diameter. Moreover, they also pointed that the power numbers were unaffected by the liquid height.

Hudcova et al. (1988) measured the power number for one and two DTs with D/T=1/3, H/T=1 or 2, C/T=1/3, and S/D=0.2 to 3. The dependence of the ratio Ptot/P*single and the individual power numbers at different spacing was closely related to the bulk flow patterns. When the impellers were touching (S/D=0.2), the flow pattern

was the same as that of a single impeller with twice the blade height, and the resulting Ptot/P*single value was equal to 1.29. When the spacing was in the range 0.5<S/D<~1.5, one circulation loop for each impeller was observed, with the value of Ptot/P*single=1.54 to 1.91. For S/D>~2, each impeller developed its typical radial flow pattern and the power drawn approximated twice that of a single one. They also confirmed that the top impeller drew slightly more power.

Abrardi et al. (1990) reported that the power dissipated by a multiple-impeller system was the sum of that dissipated by each impeller in a single impeller configuration under the condition of impeller spacing equal to 1.5-2D.

Chiampo et al. (1991) conducted a study on the effect of impeller spacing by taking into considerations mixed flow impellers in association with a DT. The experiments were carried out with a variable liquid height, maintaining a steady height of the liquid above the upper impeller, C'=D. Four dual-impeller combinations were tested with C/D=1, S/D varied from 0.2 to 4. The impeller spacing heavily affected the power consumption of dual-impeller systems. In unaerated systems, four hydrodynamic situations were identified by these investigators for the case of dual DTs:

(a) The power drawn increased moderately with spacing up to S/D=0.6.

(b) The power drawn increased slightly in the range 0.6<S/D<1.3.

(c) For S/D>1.3, the zone between two impellers became turbulent and a steep increase in power drawn was observed.

(d) At high speeds (>450 rpm), the power drawn was approximately twice that of a single impeller at S/D equal to 1.6, while at low speeds, it was necessary to wait till S/D was equal to 1.9.

For the arrangement of a PBT (top, downflow) and a DT (bottom), the power drawn increased in the range 1.6<S/D<2.8, and each impeller acted independently for S/D>2.8. They also showed that the power drawn by each impeller was a function of speed, but that this effect was not remarkable.

Lu and Yao (1991) reported the power consumption of each impeller in a triple-DT system. For a single impeller system, the average power number was found to be 4.5. The total power consumption caused by three impellers was approximately three times that of the power drawn by a single impeller. However, they found that in the region $Re>3.8\times10^4$, the average power number of top impeller was 5.05, that of the middle impeller was 5.5, while the bottom impeller had the lowest value of 3.75.

CHAPTER 3

EXPERIMENTAL APPARATUS AND METHOD

A schematic of the basic experimental set-up is shown in Figure 1. The work was carried out in open, flat bottomed, cylindrical, plexiglass vessels with different liquid height-to-tank diameter ratios. Each vessel was equipped with four baffles spaced 90° apart. Table 1 gives the details of the vessel dimensions. All the experiments were performed at room temperature. The fluid used in this work was always tap water. Its physical properties were taken at 19° C (Machon et al., 1985).

Four types of impellers, i.e. disc turbine (DT), flat-blade turbine (FBT), 45° pitched-blade turbine (PBT, always pumping down), and curved-blade turbine (CBT) were used in the experiments. Their shapes and dimensions are listed in Table 2. All impellers had six blades with a bore diameter of 1.27 cm. One, two, or three impellers of different types were mounted on the shaft, depending on the experiment. The off-bottom clearance, C, spacing between the impellers, S, and the rotational speed, N, were varied with each experiment. The off-bottom clearance was measured from the vessel bottom to the bottom edge of the disc for DTs. For FBTs, PBTs and CBTs, the clearance was measured from the vessel bottom to the bottom edge of the blade. A sketch of the agitated vessel is shown in Figure 2.

Table 1 Vessel Dimensions

Vessel #	Vessel Diameter, T (cm)	Liquid Height, H (cm)	Vessel Height, T (cm)	Baffle Width, B (cm)	H/T	B/T (%)
1	28.89	28.89	38.6	2.86	1	10
2	28.89	57.78	68.8	2.54	2	8.8

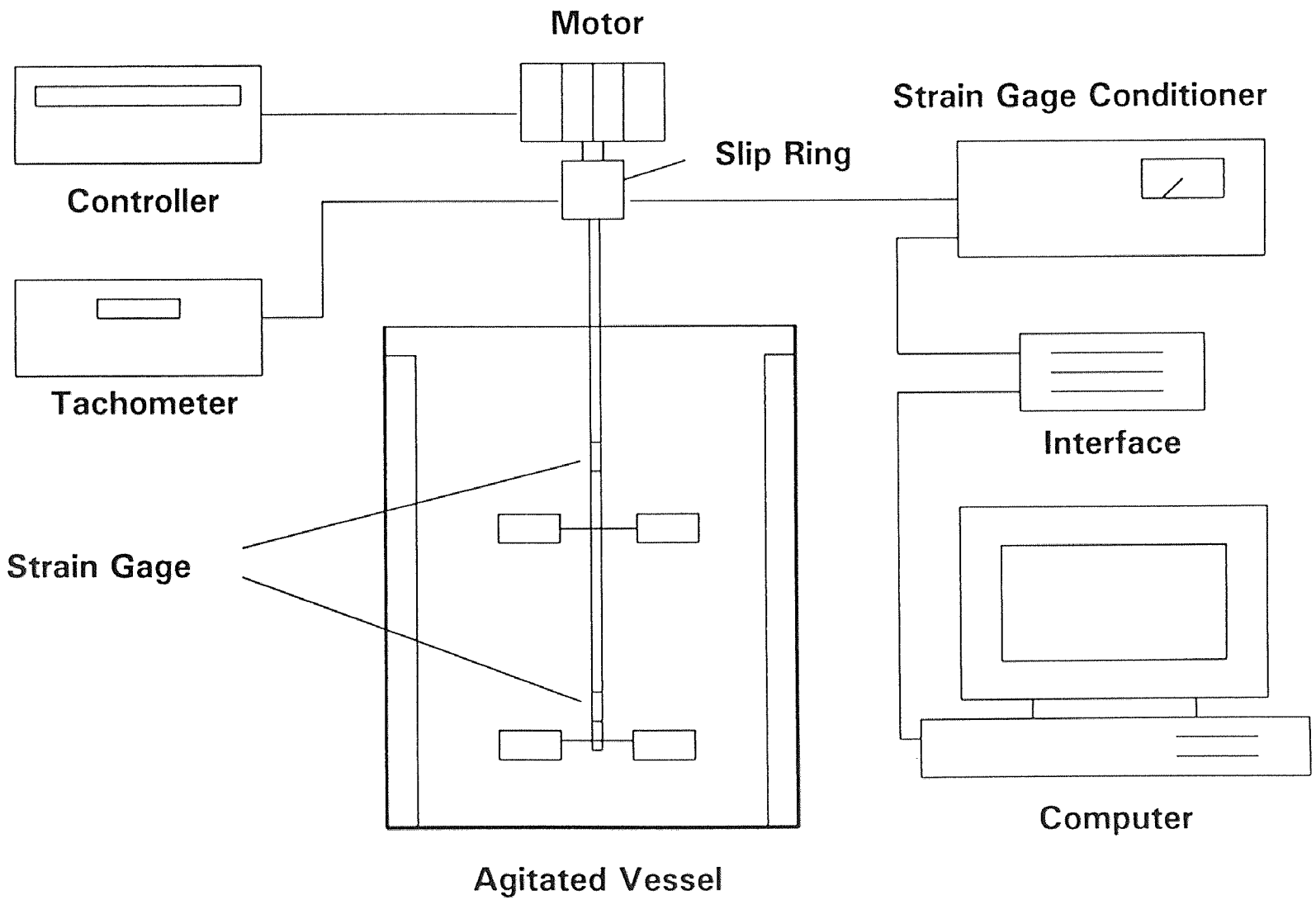

Figure 1 Experimental Set-up

Table 2 Impeller Types and Dimensions

Impeller Type	Diameter, D (cm)	Blade Width, W (cm)	W/D
Disc Turbine	7.62	1.45	0.19
	10.16	1.91	0.19
Flat-Blade Turbine	7.62	0.95	0.125
	10.16	1.27	0.125
45° Pitched-Blade Turbine	7.62	0.95	0.125
Curved-Blade Turbine	7.62	0.95	0.125

The agitation was provided by a 2.0 HP variable speed motor (G.K. Heller Corp.) with a maximum speed of 1,800 rpm. The rotational speed was measured independently using a digital tachometer with a photoelectric pick-up sensor (Cole Parmer) and was accurate within ± 1 rpm. Two or three strain gages (Measurements Group Co, CEA-06-187UV-350) were carefully mounted on aluminum hollow shafts having an O.D. of 9.5 mm and a wall thickness of 1.65 mm. Before attaching the strain gages to the shaft, metal collars having an internal diameter equal to the O.D. of the shaft and an external diameter equal to the bore diameter of impellers were slid onto the shaft between the points where the strain gages were to be inserted. After attaching the strain gages, these collars, having a length of 2.54 cm, could be moved along the shaft between two strain gages. This arrangement was designed so that the impellers could be mounted on the shaft without touching the protruding strain gages. In addition, this arrangement enabled the impeller-collar assemblies to be moved along the shaft thus permitting to vary the distances between impellers.

Shafts of different lengths were used in this work. Their lengths and the distance of each strain gage from the bottom of the shaft are given in Table 3. Shaft #1 and #2 were only used with Vessel #1 and #2, respectively.

The strain gages were connected with insulated lead wires passing through the hollow core of the shaft to a signal conditioner and amplifier system (2120A system, Measurement Group Co.). A data acquisition system (Labtech Notebook) connected to a computer was used to analyze the gage signal (mV) from the strain gage conditioner, receive the signal from the tachometer, and calculate the power drawn by each impeller. Each strain gage measured the cumulative torque produced by all impellers below it.

Table 3 Shaft Length and Strain Gage Location

Shaft #	Length (cm)	Distance of Each Strain Gage from the Bottom of the Shaft (cm)		
		Bottom Gage	Middle Gage	Top Gage
1	61	3.3	-	26.4
2	83.8	3.1	34.0	49.3

The power drawn by each individual impeller was determined using the following equations:

$$\begin{aligned} P_1 &= \omega \cdot T_1 = 2\pi N \cdot T_1 = N \cdot K_1 \cdot mV_1 \\ P_2 &= \omega \cdot (T_2 - T_1) = N \cdot (K_2 \cdot mV_2 - K_1 \cdot mV_1) \\ P_3 &= \omega \cdot (T_3 - T_2) = N \cdot (K_3 \cdot mV_3 - K_2 \cdot mV_2) \end{aligned} \qquad (3.1)$$

where P_1, P_2, P_3 are the powers drawn by the bottom, the middle, and the top impeller, respectively;

ω is the angular velocity;

T_1, T_2, T_3 are the actual torques produced by the impellers associated with Strain Gages #1, #2, #3, respectively;

N is the agitation speed in rps;

mV_1, mV_2, mV_3 are the signals corresponding to Strain Gages #1, #2, #3, respectively;

K_1, K_2, K_3 are the proportionality factors for Strain Gages #1, #2, #3, respectively

(obtained from calibration).

The sampling frequency of the data acquisition system was 30 times/60 seconds, and the representative power drawn was determined by calculating the average of the 30 readings. The corresponding Power Number (or Newton Number), Ne, was calculated with the following equation (Rushton et al., 1950):

$$Ne = \frac{P}{\rho N^3 D^5} \tag{3.2}$$

The system was calibrated periodically (when the impeller system was changed, i.e. typically every ten days) to assure the reliability and accuracy of the strain gage response. The calibration process consisted in placing the shaft horizontally so that it was supported by two stands. An impeller was mounted on the shaft, closed to each strain gage and a known weight was suspended from the edge of impeller blade so as to create a torque of known intensity. The torque was measured by the strain gage conditioner which gave a reading in mV. The same procedure was repeated with weights of different masses (30 to 500 g). The signals from the strain gages (in mV) were sent to the same data acquisition system used in the actual experiments. Torque-mV calibration curves were constructed. These curves were typically linear so that the proportionality factors, K_1, K_2, K_3 in Equation 3.1 could be determined. Examples of calibration curves for strain gages are given in Figure 3. The reproducibility of the results for the proportionality factors, K's, obtained from the calibration curves was within $\pm 5.2\%$ and $\pm 4.0\%$ for K_1 and K_2 (for Shaft #1), respectively, and $\pm 4.1\%$, $\pm 3.2\%$ and $\pm 5.1\%$ for K_1, K_2, and K_3 (for Shaft #2), respectively.

The distance between the impeller and the strain gage could, in principle, affect the value of the proportionality factor, K. To test this hypothesis a series of calibration curves were constructed for different values of such a distance, and the resulting K values were plotted as a function of the impeller-strain gage distance. The results, shown in Figure 4, indicate that the K value decreases slightly as a function of the distances. However, this

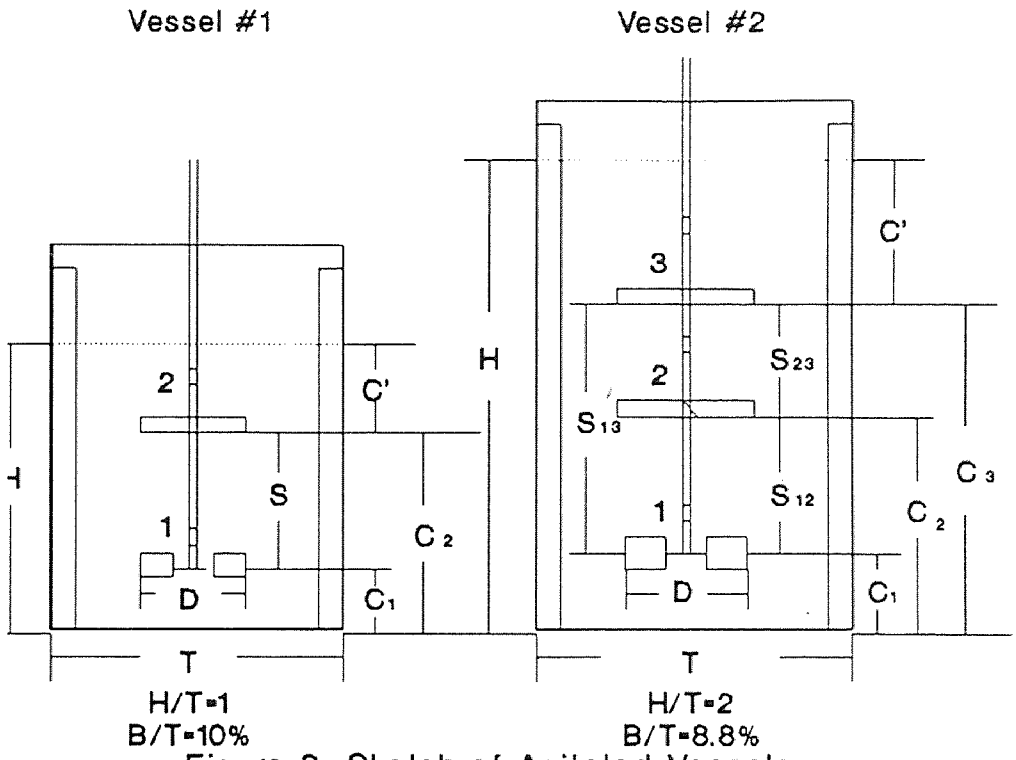

Figure 2 Sketch of Agitated Vessels

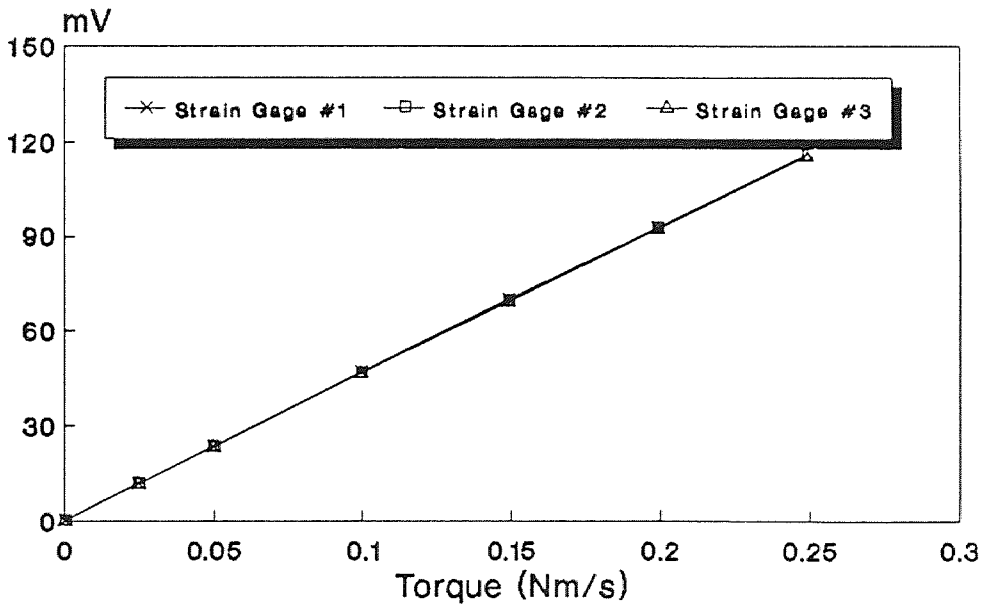

Figure 3 Calibration Curves on Strain Gage #1, #2, #3 for Shaft #2

could also result from bending moment effects. Therefore, another experiment was conducted in which the power consumption for the same speed, and impeller-vessel geometry was measured as a function of the impeller-strain gage distance. The results, reported in Figure 5, indicate that the power is unaffected by such a distance.

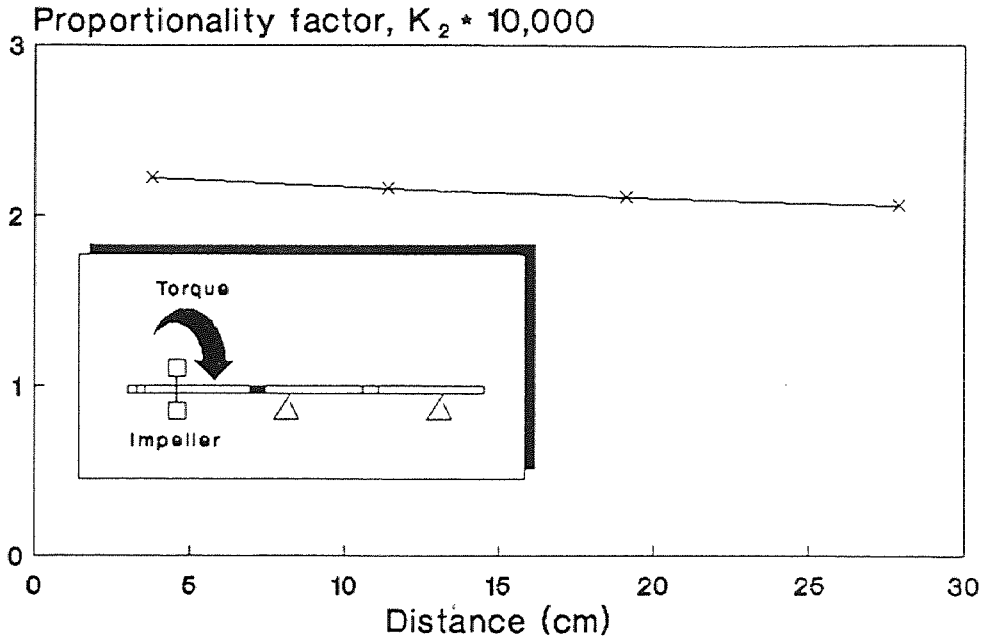

Figure 4 Effect on K_2 of Distance between Impeller and Strain Gage (Middle Strain Gage on Shaft #2)

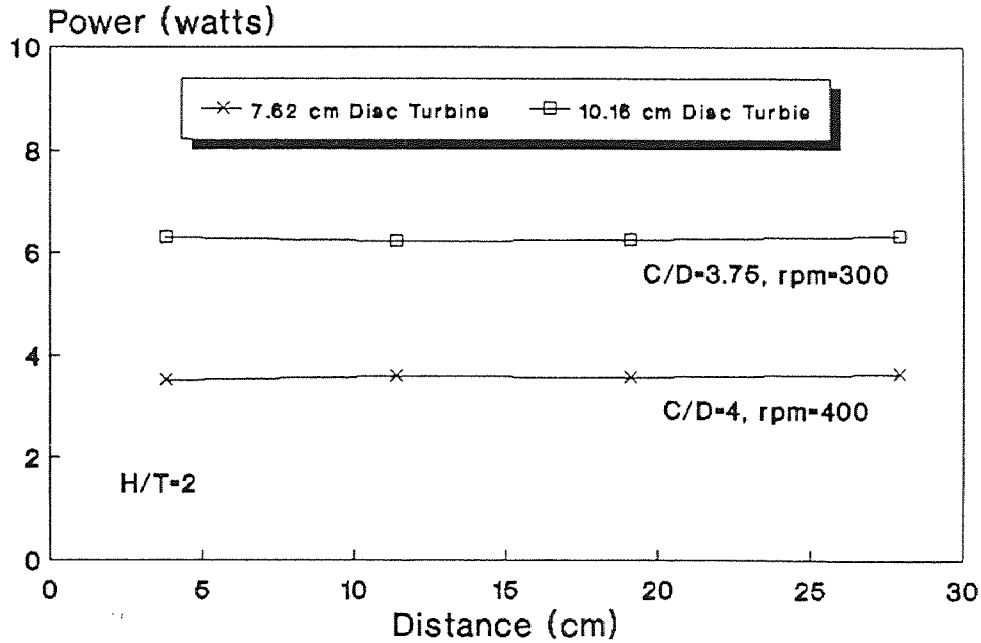

Figure 5 Effect on Power of Distance between Impeller and Strain Gage (Middle Strain on Shaft #2)

CHAPTER 4

EXPERIMENTAL PROCEDURE

The vessel was filled with tap water to the desired height, i.e., H/T=1 and H/T=2, for Vessel #1 and #2, respectively. The vessel was located on a tank support system that could be translated vertically so as to change the distance between the (fixed) shaft with the impellers mounted on it and the tank bottom. Then, the vessel was fixed in its final position. Two or three strain gages had been previously mounted on Shaft #1 and Shaft #2, respectively. Shaft #1 and Shaft #2 used only with Vessel #1 and Vessel #2, respectively. The shaft was centrally located in the vessel and was connected to the motor. The strain gages were connected with wires through the hollow core of the shaft to a slip ring. The slip ring, which was also mounted on the shaft, was connected to the external gage conditioner and amplifier. An optical sensor with a tachometer was used to measure the rotation speed.

One, two, or three impellers were mounted on the shaft. Four type of impellers namely disc turbine, 45° pitched-blade turbine, flat-blade turbine, and curved-blade turbine were used with the identical type or combinations of different types of impellers. In single-impeller systems, the off-bottom clearance, C, was varied in the range $1/6 \leq C/D \leq 5/2$ and $1/6 \leq C/D \leq 5$ corresponding to Vessel #1 and Vessel #2, respectively. The dual-impeller system studies were carried out with Vessel #1. The value of C/D was varied in the range 1/6 to 5/2, and the impeller spacing, S, was varied in the range $2/3 \leq S/D \leq 7/3$. The triple-impeller system studies were conducted in Vessel #2. The spacing between the top impeller and the bottom one was maintained constant for each series of experiments. The middle impeller was moved along the shaft between the other two impellers with each run. The clearance was varied in the range $1/6 \leq C/D \leq 3/2$.

The data acquisition system was connected to collect data on line and was used to analyze all the signals from the strain gages and the optical sensor. The sampling

frequency was 30 times/60 seconds. The representative power drawn was determined by the average of the 30 readings. The power consumed by each individual impeller was calculated using Equation (3.1). The corresponding power number was determined using Equation (3.2). The power consumption was measured at different rotational speeds (in the range 300 to 500 rpm) for any given S and C.

A strain gage calibration process was conducted each time the impeller agitation system was changed (typically every 10 days). No significant changes in the calibration curves were observed over time.

CHAPTER 5

RESULTS AND DISCUSSION

5.1 Results for Single-Impeller Agitation Systems

In this work, four types of impellers, i.e., disc turbine (DT), 45°pitched-blade turbine (DT), flat-blade turbine (FBT), and curved-blade turbine (CBT), were used under the condition of H/T=1 in Vessel #1, and H/T=2 in Vessel #2. The power number, Ne, was calculated by taking the average of the powers measured at two different agitation speeds, i.e., 400 and 500 rpm ($Re>3.8\times10^4$). The difference between the two resulting power numbers was always less than 4.3% of the average value.

5.1.1 Effect of Clearance on Power Number

The impellers were tested in a system for which D/T=0.264 and having a ratio C/D in the range 1/6 to 5/2 for Vessel #1 and 1/6 to 5 for Vessel #2. Some types of impellers, with D/T=0.352, were also used to compare the effect of impeller diameter. For Vessel #1, where H/T=1, the effect of clearance on power number for each type of impeller is shown in Figure 6, and the data for some specific conditions are shown in Table 4.

For the case of disc turbines (DT), it was observed that the power number increased untill it reached a constant value of 5.10 at C/D=2. The variation in power number value can be interpreted in terms of flow pattern (Rao and Joshi, 1988). At low clearance, C/D=1/6, the bottom circulation of disc turbines is reduced, producing a smaller power consumption (Ne=3.34). However, with a little change of clearance, C/D=1/6 to 1/3, a steep increase in power number was observed (Ne=4.30). In the range $1/3\leq C/D\leq 1$, there was a moderate increase in the power number. The reason could be the transition state of flow pattern around the impeller blades. When the clearance was equal to the impeller diameter, C/D=1, the power number increased to 4.90, while it increased to 5.10 at C/D=2. The power numbers obtained here are very close to the most

acceptable literature value of 5.0 at the standard conditions (Kuboi and Nienow, 1982). The reason could be that the flow pattern generated by the impeller was fully developed when the value of C/D was greater than 1, therefore dissipating more power. For the case of DTs with D/T=0.352, the power number was almost the same as that with D/T=0.264 when C/D>1. Some deviations were observed in the range 1/3<C/D<1, known as the transitional region, where unstable flow patterns are known to occur.

The 45° pitch-blade turbine (PBT) exhibits both radial and axial flow patterns. The effect of clearance on power number was different due to the mixed-flow pattern. Contrary to the behavior of DT, when the clearance was increased from C/D=1/6 to C/D=2, a decrease in PBT power number from 1.90 to 1.34 was observed (more details are given in Figure 6 and Table 4). At low clearance, the impeller stream hits the vessel bottom with higher velocity causing a sharp change in flow direction which dissipates more energy (Rao and Joshi, 1988). As a result, an increased power number was obtained.

For the case of the flat-blade turbine (FBT), various effects of power drawn were displayed by changing the clearance. The power number decreased with clearance, from C/D=1/6 to 1/2. Furthermore, for C/D=5/6, Ne reached the minimum value of 2.09, as shown in Figure 6 and Table 4. In the range 5/6<C/D≤3/2, Ne increased moderately, and then decreased when C/D>3/2. The change of power numbers show the subtle effects of flow patterns around the impeller blades. Because of the variations in the arrangement of impeller-tank geometry, these flow patterns cause changes in the impeller-fluid relative velocity thereby affecting the power drawn (Tatterson, 1991). The behavior of the power drawn for the FBT in this work was similar to that obtained by Bates et al. (1963).

For the case of the curved blade turbine (CBT) or the backswept turbine, the influence of clearance on power drawn was not very remarkable. In general, the power number decreased when the clearance was increased. The results are plotted in Figure 6

and tabulated in Table 4. The power number decreased moderately in the range 1/6 (Ne=2.26)≤C/D≤3/2 (Ne=1.99), and then increased slightly when C/D≥3/2.

Table 4 Effect of Clearance on Power Number (Vessel #1)

T=28.89 cm, H/T=1

C/D	Power Number, Ne				
	D/T=0.264				D/T=0.352
	DT	PBT	FBT	CBT	DT
1/6	3.34	1.90	2.57	2.26	3.52
1/2	4.35	1.64	2.16	2.13	4.69
1	4.90	1.49	2.39	2.06	4.87
3/2	4.96	1.39	2.39	1.99	4.92
2	5.10	1.34	2.14	2.05	4.96

The liquid height has been shown previously to have no significant effect on power consumption when there is no surface aeration, or air entrainment (Rushton, 1950; Rewatkar, 1990). This conclusion was confirmed here when Vessel #2 (having a H/T equal to 2) was used. For Vessel #2, the effect of clearance on power number for each type of impeller is shown in Figure 7 and Table 5. A comparison of these values with those in Table 4 (H/T=1), shows that, in general, the power drawn in Vessel #2 is similar to that of Vessel #1 for every type of impellers. However, the slight differences in power number could be due to the effect of baffling and minor changes in the impeller-tank geometry system. The extent of baffling, represented by the B/T ratio, is 10% and 8.8% for Vessel #1 and #2, respectively. Both are in the range of standard size baffling 1/12<B/T<1/10 which is commonly used in industrial operations. The effect of baffling is small over this range (Gray et al., 1982).

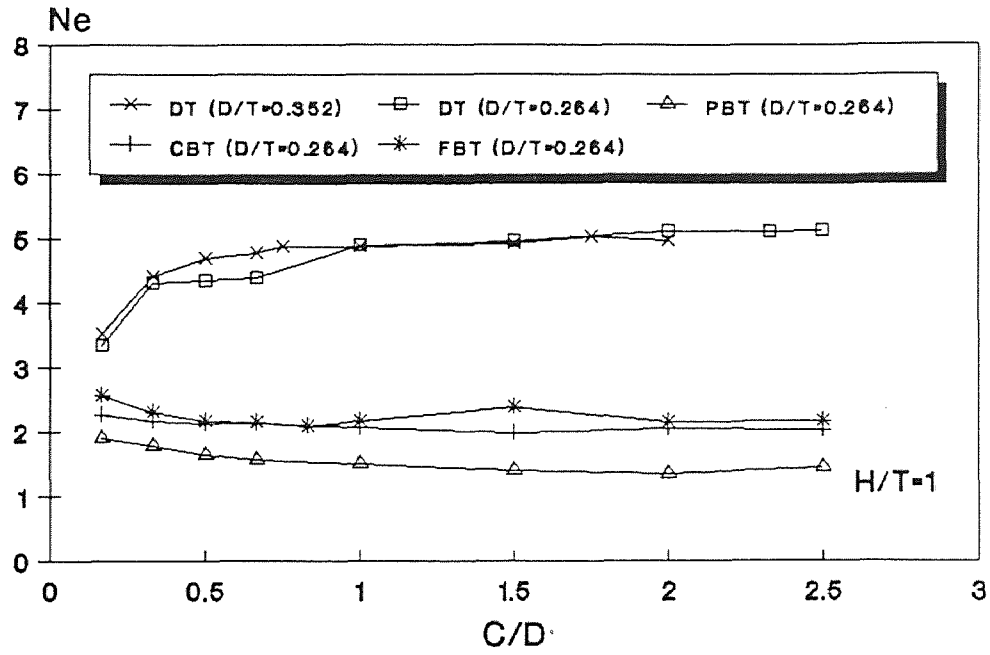

Figure 6 Effect of C on Ne (Vessel #1)

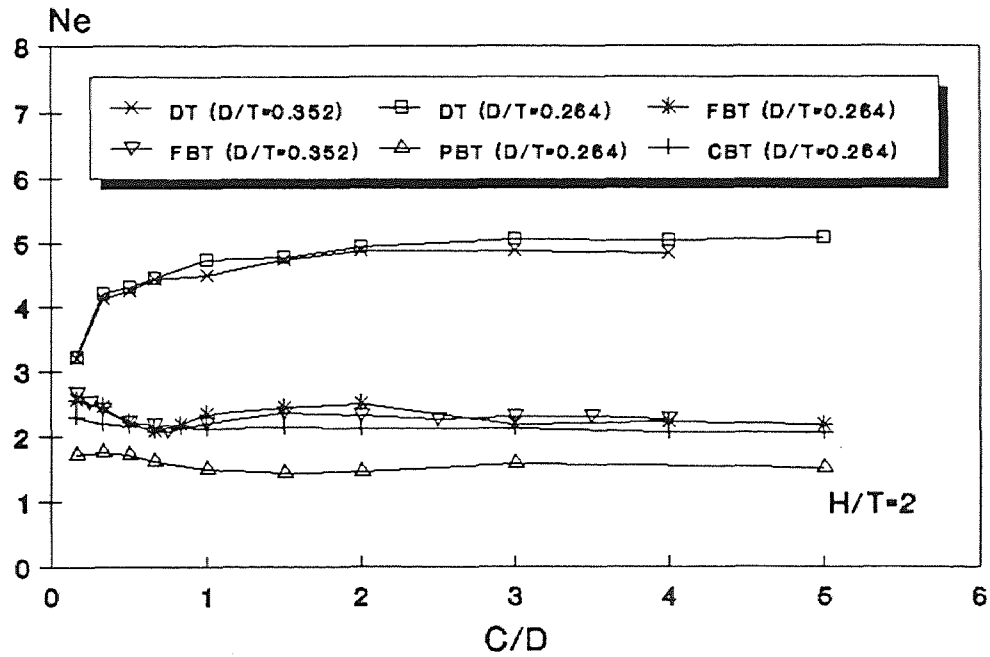

Figure 7 Effect of C on Ne (Vessel #2)

Table 5 Effect of Clearance on Power Number (Vessel #2)

T=28.89 cm, H/T=2

C/D	Power Number, Ne					
	D/T=0.264				D/T=0.352	
	DT	PBT	FBT	CBT	DT	FBT
1/6	3.23	1.71	2.56	2.30	3.21	2.67
1/2	4.31	1.72	2.22	2.17	4.25	2.22
1	4.74	1.49	2.35	2.13	4.48	2.21
3/2	4.78	1.44	2.45	2.15	4.73	2.36
2	4.93	1.45	2.51	2.12	4.88	2.32
5	5.07	1.51	2.19	2.08	-	-

The results obtained for both vessels indicate that the effect of impeller off-bottom clearance on power consumption was found to be very significant, especially when the impeller clearance was smaller than the impeller diameter. The power drawn also depends on the type of impeller. The DT draws the largest power among all types of impellers. The power dissipated by the FBT is similar to that of the CBT in the range $1/2 \leq C/D \leq 1$, but in general, the FBT draws a little more power than the CBT. The pitched blade turbine displayed the least power consumption due to the different flow pattern it created.

5.1.2 Effect of Rotational Speed on Power Consumption

The effect of speed on power drawn for each type of impeller is shown in Figure 8 in which logarithmic coordinates are used for both axes. The slope obtained was close to three, in the range 2.79 to 3.06, for each impeller in Vessel #1 and Vessel #2. From power number theory, Ne equals a constant in the fully turbulent region, and Equation 2-3 applies to any impeller (Rushton et al., 1950). This Equation shows that the power is

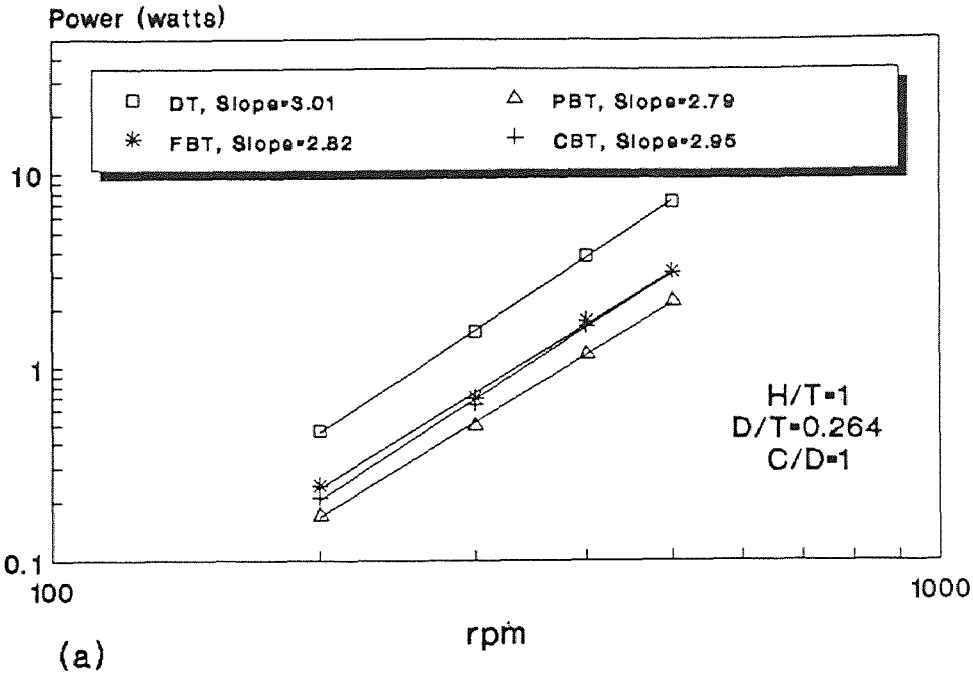

(a)

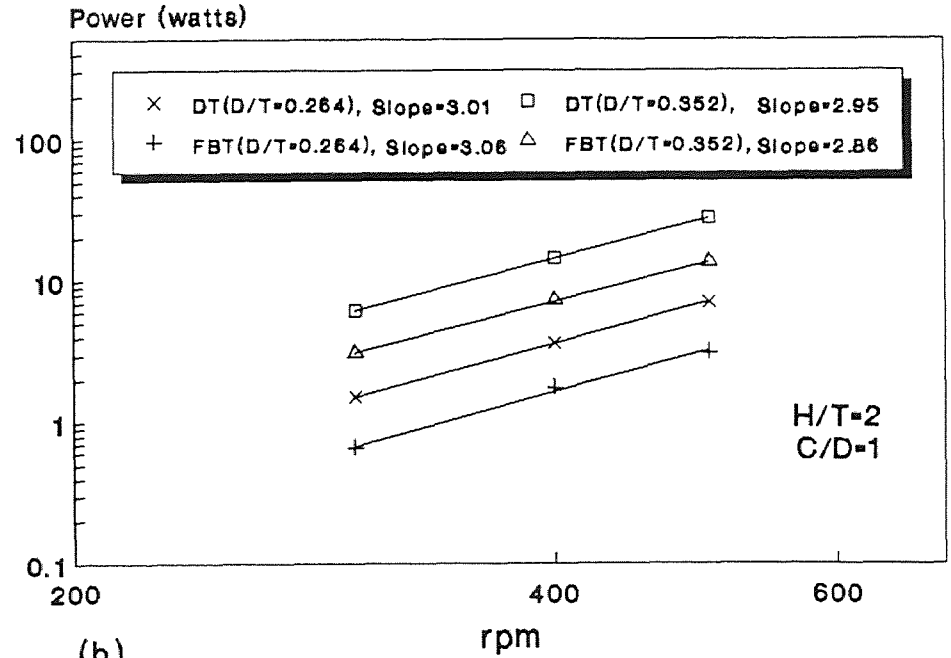

(b)

Figure 8 Effect of Agitation Speed on Power

proportional to the agitation speed raised to the power of 3. The results obtained here indicate a good agreement with the power relationship of Equation 2.3 for geometrically similar systems.

Power numbers at three rotational speeds are shown in Table 6 and Table 7 for Vessel #1 and #2, respectively. The values are within ±4.2% from the mean. In practice, increasing the rotational speed will somewhat reduce the power number due to the effect of surface aeration (especially at high off-bottom clearance or high D/T ratio) which induce air bubbles into the liquid (Greaves, 1981; Nocentini et al., 1988; Rewatkar et al., 1990). The results of this work indicate a reduction of Ne with increasing rotational speed for the impeller with D/T=0.352. The same is not always true for the case in which D/T=0.264. However, the effect is not significant in each case, and some deviations could be due to errors in the measurement procedure.

Table 6 Effect of Agitation Speed on Power Number (Vessel #1)

T=28.89 cm, H/T=1, C/D=1

rpm	Power Number, Ne				
	D/T=0.264				D/T=0.352
	DT	PBT	FBT	CBT	DT
300	4.74	1.52	2.15	2.0	4.94
400	4.95	1.51	2.25	2.04	4.91
500	4.85	1.47	2.08	2.08	4.75

Table 7 Effect of Agitation Speed on Power Number (Vessel #2)

T=28.89 cm, H/T=2, C/D=1

rpm	Power Number, Ne					
	D/T=0.264				D/T=0.352	
	DT	PBT	FBT	CBT	DT	FBT
300	4.67	-	2.05	-	4.50	2.27
400	4.77	1.55	2.29	2.15	4.46	2.25
500	4.70	1.44	2.10	2.12	4.38	2.12

5.2 Results for Multiple-Impeller Agitation Systems

The effects of impeller spacing, S, and off-bottom clearance, C, on power consumption were reported here in terms of Ptot/P*single or Ptot/$\sum$P*single for combinations of identical or different types of impellers, respectively. In this study, Ptot refers to the total combined power drawn by all multiple impellers, and P*single refers to a reference power drawn by a single impeller of the same type at $C_1/D=1$.

In dual-impeller systems, the power dissipated by each impeller is reported as a ratio of P_2 / P_1, where P_1 and P_2 refer to the power drawn by the bottom impeller and the top impeller, respectively. In triple-impeller systems, the power dissipated by each impeller is expressed as P_i%, where i varies from 1 to 3, referring to the bottom, the middle, and the top impeller, respectively.

The resulting power numbers are expressed as Ne_i for each individual impeller. Ne(tot) refers to the sum of their power numbers, $\sum Ne_i$. The reference power number for a single impeller is expressed as Ne*, and refers to the same type of impeller for which $C_1/D=1$.

5.2.1 Effect of Impeller Spacing and Clearance on Power Consumption in Dual-Impeller Systems

In this work, four types of impellers with a diameter of 7.62 cm and D/T=0.264, were used in dual-impeller systems. The power numbers were calculated by taking the average of the power numbers in correspondence of two agitation speeds, i.e., 400 and 500 rpm ($Re>3.8\times10^4$). The deviations between the resulting power numbers were typically between 2 to 5%, with a maximum deviation of 8% from the mean. The presence of air entrainment was annotated in the figures and typically occurred when the distance, C', between the liquid surface and the top impeller was less than the impeller diameter, D. When C'/D<1, the measured power drawn could be not reliable due to surface aeration.

5.2.1.1 Results for Dual-Disc Turbine Systems

The effect of spacing between impellers on power consumption is shown in Figure 9(a). These results indicate that power dissipation is strongly affected by the impeller spacing, and that the effect is more pronounced at lower clearance. In general, the power consumption increased when the spacing was increased. At lower clearance ($C_1/D\leq2/3$), a steep increase in Ptot was observed in the range $1<S/D<5/3$, while a moderately increase was observed when $S/D<1$ or $S/D>4/3$. At $C_1/D=1$, Ptot increased slightly up to S/D=3/2. A sharp increase in Ptot was found in the range $3/2<S/D<5/3$, with a Ptot/P*single value of 1.84 at S/D=5/3.

From the available literature data on dual-impeller systems, the spacing needed to make the power drawn twice that of a single impeller is at least for S/D>3/2 or 2 (Abrardi et al. 1990; Chiampo et al. 1991). In this work, at $C_1/D=1$, $S/D\geq2$ was not available due to the effect of air entrainment. However, the results obtained indicate that when S/D=5/3, the power dissipated by dual disc turbines was not twice that of the single one.

The power dissipated by each individual impeller is also a function of spacing, as shown in Figure 9(b). The effect of spacing is more evident when the clearance value is small. When $C_1/D<2/3$, P_2/P_1 dropped sharply with S for $S/D<3/2$. This variation was due to a significant increases in P_1, for the bottom DT, when S was increased. When $C_1/D \geq 2/3$, this effect was not appreciable, and the ratio P_2/P_1 tended to reach a value of 1.

The effect of clearance on power drawn was conducted for various spacing between impellers, as shown in Figure 10(a). When $S/D \leq 1$, Ptot increased with C_1, similarly to that of a single impeller. A steep increase in Ptot was observed in the range $1/2<C_1/D<2/3$. As shown in figure 10(b), the P_2/P_1 ratio decreased sharply in the range $C_1/D<2/3$, with the top impeller drawing much more power than the bottom one. The decrease in P_2/P_1 value was due to a steep increase in P_1 by the bottom DT. The most surprising results were observed in the range $4/3 \leq S/D \leq 3/2$. Ptot increased with clearance up to $C_1/D=2/3$ (Ptot/P*single=1.79), but, contrary to the case of a single DT, a decrease in Ptot was observed when increasing the C_1/D value from 2/3 to 1 (Ptot/P*single=1.6). A separate experiment conducted independently under the same conditions confirmed this change. However, when a larger spacing was provided ($S/D \geq 5/3$), no reduction in Ptot was found in the range of clearances examined. The variation of Ptot in the range $4/3 \leq S/D \leq 3/2$ and $2/3 \leq C_1/D \leq 1$ could be caused by an unstable hydrodynamic state resulting in a drop in the power drawn.

The variation of power number as a function of impeller spacing, at $C_1/D=1$, is shown in Figure 11. The sum of each power number, Ne(tot), increased with S as a result of the increased Ne_i by both impellers. The top impeller dissipated more power than the bottom one, but both Ne_1 and Ne_2 were found to be smaller than Ne*. The effect of spacing on power consumption is due to the change of flow patterns between impellers. When the spacing is increased, a larger amount of liquid occupies the zone between the impellers. This increases the solid body rotation, thereby increasing the power drawn

(Chiampo et al. 1991). Each impeller tends to operate as a single one, at least for S/D>5/3, when the distance between impellers is rather significant. Figure 12 shows the effect of C_1 on Ne. The results indicate that the decrease in Ne(tot) when $C_1/D>2/3$ was mainly due to the decrease in Ne_2, for the top impeller.

5.2.1.2 Results for Dual-Pitched Blade Turbine Systems

This type of impeller pumps the fluid in both the axial (downward) and radial directions. The dependence of Ptot on S in shown in Figure 13(a). The effect of spacing is more pronounced at smaller clearance values. In general, Ptot increased with S up to S/D=~3/2, and then decreased for S/D>3/2. A greater power drawn was observed at lower clearance and when S/D=3/2. The effect of S on the ratio P_2 / P_1 is shown in Figure 13(b). In general, the ratio decreased when spacing was increased. When S/D<~1, it was observed that $P_2 > P_1$. However, when S/D>~1, $P_2 < P_1$ was found.

The effect of clearance on power drawn by dual-PBT systems is somewhat similar to that of single-impeller systems, as shown in Figure 14(a). In general, Ptot decreased with increasing clearance. Various changes of the P_2 / P_1 ratio were observed at lower clearance ($C_1/D<2/3$), as shown in Figure 14(b).

For $C_1/D=1$, the variation of Ne as a function of S is shown in Figure 15. Ne_1, for the bottom impeller, increased slightly, while Ne_2, for the top impeller, decreased in the same way. Both effects nearly offset each other. Hence, Ne(tot) was only slightly affected by S.

The effect of C_1 on Ne, at S/D=3/2, is shown in Figure 16. Both individual power numbers dropped slightly with C_1, and caused a decrease in Ne(tot). However, it should be noted, as stated by Papastefanos and Stamatoudis (1989), that the power drawn by PBT is less than that drawn by the other types of impellers, and that the axial or radial flow direction can be switched under certain conditions. This causes an unstable situation and hence increases the experimental error. In addition, this type of impeller produces a

more significant surface aeration, since the downward flow tends to introduce air into the liquid when top impeller is close to the liquid surface, especially at higher rotational speeds.

5.2.1.3 Results for Dual-Flat Blade Turbine Systems

For this type of impeller, the effect of S on Ptot is not significant, as shown in Figure 17(a). In general, Ptot decreased with S to a minimum value at S/D=~3/2 and then increased slightly for S>3/2. At C/D=1, the total power drawn was approximately twice that of a single impeller. The effect of S on the P_2 / P_1 ratio is shown in figure 17(b). P_2 / P_1 reached a maximum at S=D due to a smaller power drawn by the bottom impeller. However, P_1 is approximately equal to P_2 in most cases.

The effect of C_1 on Ptot is significant, as shown in Figure 18(a). This effect for the dual FBTs is similar to that for a single FBT. The smallest power drawn was observed when C_1 / D value was approximately equal to 1. The effect of C_1 on P_2 / P_1 is complicated, as shown in Figure 18(b).

As shown in Figure 19, no significant effect on Ne(tot) was found when changing S. Compared to a single FBT, Ne_1 was less than Ne*. However, Ne_2 was greater than Ne*, thus making Ne(tot) nearly a constant. Figure 20 shows the effect of clearance on Ne, at S/D=3/2. An interesting change occurred at C_1/D=1/2 when the power drawn by the bottom impeller (and hence the total power consumption) decreased to a minimum.

5.2.1.4 Results for Dual-Curved Blade Turbine Systems

The effect of spacing on power drawn is shown in Figure 21(a). In spite of an unstable change which occurred at C_1/D=2/3, Ptot seemed unaffected by the spacing for S/D≥3/2. A moderate increase in Ptot with S was observed for S/D>3/2. Under the condition of S/D=5/2 and C_1/D=1, the ratio Ptot/P*single was found to be 1.87. The effect of S on P_2 / P_1 is shown in Figure 21(b). In general, when C_1/D≤1/3, the P_2 / P_1 ratio dropped

slightly. However, when C/D≥2/3, the ratio increased slightly. Each P_2 / P_1 curve tended toward an asymptotic value of 1.2 when spacing was increased.

The effect of clearance on Ptot is shown in Figure 22(a). The minimum power drawn was observed in the range $1/2 \leq C_1/D \leq 2/3$. However, in general, Ptot increased with C_1. The sharp change in power consumption implies that a sudden change of flow pattern occurred at that condition. It should be noticed that the flow pattern generated by a double impeller system is significantly different and more complex than that generated by a single impeller. In general, a larger power drawn was observed for smaller impeller spacing and higher clearance. The change of P_2 / P_1 with clearance is shown in Figure 22(b), indicating that the variation of P_2 / P_1 is significant when S≤D, but negligible for S/D≥3/2.

Figure 23 displays Ne as a function of S/D for $C_1/D=1$. No remarkable effect was found. The effect of clearance on Ne is shown in Figure 24. Both Ne_1 and Ne_2 increased (and hence Ne(tot) increased) with clearance when $C_1/D>2/3$. In addition, both values are less than Ne*.

These results indicate that the effect of spacing and clearance on Ptot obtained for the dual-CBT systems is similar to that of the dual-FBT systems. However, the FBT dissipates more power than the CBT.

5.2.1.5 Results for Combinations of a Disc Turbine and a Pitched-Blade Turbine Systems

For the combination of a PBT (top) and a DT (bottom), the effect of S on Ptot is shown in Figure 25(a). This effect was more pronounced at lower clearance (C/D=1/3). However, no significant change in Ptot was observed for C/D≥2/3. The P_2 / P_1 ratio decreased with S moderately in most cases, as shown in Figure 25(b)

The effect of clearance on Ptot is shown in Figure 26(a). Ptot increased with clearance. This phenomenon was the result of much more significant power drawn by the

DT than the PBT. Therefore, the resulting Ptot was dominated by the DT. Similarly to single DT systems, the power drawn by the DT increased with clearance. At S/D=3/2, C_1/D=1, the combined power drawn was about 86% of the sum of both impeller. As shown in Figure 26(b), the P_2 / P_1 ratio decreased moderately with clearance. This was primarily due to the bottom impeller, DT, which drew more power when the clearance was increased.

Figure 27 shows the variation of Ne as a function of spacing. Ne(tot) was nearly unaffected by the spacing. Figure 28 shows the effect of clearance on Ne. A significant increase in Ne_1, for the bottom DT, with C_1 was observed when $C_1/D \geq 2/3$. This caused Ne(tot) to increase for $C_1/D \geq 2/3$.

Chiampo et al. (1991) reported that $S/D \geq 2.8$ was needed to make Ptot=$\sum$P*single. However, the results from this work confirms that the spacing has no significant effect for $S/D \geq 3/2$. Under this condition, Ne(tot) was less than the sum of both individual power numbers.

5.2.1.6 Results for Combinations of a Pitched-Blade Turbine and a Flat-Blade Turbine Systems

For this case, a PBT (top) and a FBT (bottom) were used. The effect of spacing on Ptot is shown in Figure 29(a). These results indicate that Ptot decreased slightly with S in most cases. At C_1/D=1, Ptot was equal to 92% of the sum of the power drawn by the corresponding single individual impellers, and no significant effect of spacing was noticed. The effect of S on P_2 / P_1 is shown in Figure 29(b). The variation of the P_2 / P_1 ratio with spacing was complicated. However, this effect was not significant.

The effect of clearance on Ptot is shown in Figure 30(a). The changes in Ptot observed at each S/D value are consistent along the range of clearance examined. Ptot decreased moderately with clearance for $C_1/D \leq 1$, when a minimum value of Ptot/$\sum$P*single (0.92) was observed. When plotting P_2 / P_1 vs. C_1/D, a maximum value

was observed in the range $1/2<C_1/D<2/3$ for a given S/D value, as shown in Figure 30(b). In general, P_2/P_1 increased with C_1 up to $C_1/D=\sim 2/3$, and then decreased for $C_1/D>2/3$.

The effect of spacing on Ne is shown in Figure 31. At $C_1/D=1$, this effect was not remarkable. Figure 32 shows the effect of clearance on Ne. A decrease in Ne(tot) with C_1 was observed. This was mainly due to the decrease in Ne_1 for $C_1/D \leq 2/3$.

5.2.2 Effect of Impeller Spacing and Clearance on Power Consumption in Triple-Impeller Systems

For the triple-impeller configurations, the power number of each impeller was determined by taking the average of the power numbers in corresponding of two rotational speeds, i.e., 400 and 500 rpm ($Re>3.8\times10^4$) for impellers with D=7.62 cm (D/T=0.264). For impellers with D=10.16 cm (D/T=0.352), Ne was calculated at 300 and 400 rpm ($Re>5.1\times10^4$). The difference between the total power numbers, Ne(tot), calculated at the two speeds was very small (typically between 1 and 3%, with a maximum value of 4.2%). The diameter of the impeller, D, the ratio D/T, and the ratio S_{13}/D (where S_{13} is the spacing between the top and the bottom impeller) used in all experiments are listed in Table 8.

Table 8 Configurations Used for the Triple-Impeller Systems

	DTs	PBTs	FBTs	CBTs	DTs+PBTs
D (cm)	7.62	7.62	10.16	7.62	7.62
D/T	0.264	0.264	0.352	0.264	0.264
S_{13}/D	5	5	3.5	4.67	5

5.2.2.1 Results for Triple-Disc Turbine Systems

Figure 33(a) shows the effect of S_{12} (i.e., spacing between the middle and the bottom impeller) on Ptot (i.e., the total power consumption). From this figure it is apparent that when the middle impeller was placed midway between the others, the power drawn reached the maximum value at any given clearance. At $C_1/D=1$, the Ptot/P*single ratio was observed to be 3.1. For $S_{12}/D=S_{23}/D=5/2$, the spacing was large enough for each impeller to draw full power (Abrardi et al, 1990; Chiampo et al., 1991). Therefore, maximum power consumption was observed. Figure 33(b) shows the variation of the combined power number, Ne(tot), and the individual power number, Ne_1, as a function of S_{12}, for $C_1/D=1$. Under this condition, Ne(tot) was found to be 14.8. The individual power numbers were $Ne_3=5.35$ for the top DT, $Ne_2=5.12$ for the middle one, and $Ne_1=4.37$ for the bottom DT. From the curves in the figure, some variations can be observed. When $S_{12}/D \leq 1$, the power number increased moderately with spacing. For $1 \leq S_{12}/D$(or $S_{23}/D) \leq 3/2$, Ne(tot) increased very moderately. A steep increase in Ne(tot) was observed in the range $3/2 \leq S_{12}/D$(or $S_{23}/D) \leq 2$. For $2 \leq S_{12}/D$(or $S_{23}/D) \leq 3$, Ne(tot) reached its maximum.

The effect of spacing observed in these experiments is similar to that found in dual-DT systems. For triple-DT systems, the Ptot/P*single ratio obtained by Smith et al. (1987) was equal to 2.98 under the condition of $S_{12}/D=S_{23}/D=5/2$. The results from this work confirm that the total power input is approximately equal the sum of the three individual power numbers, when S/D≥~2.

The effect of S_{12} on the individual power drawn, represented by $P_i\%$, is shown in Figure 34. In general, it was observed that $P_3\% > P_2\% > P_1\%$. When the middle impeller was moved toward to the top one, $P_1\%$ increased and $P_3\%$ decreased. The change in $P_2\%$, for the middle impeller was not remarkable in most cases. However, for $S_{12}/D>7/2$, each of the three impellers had a similar value of $P_i\%$.

The effect of off-bottom clearance, C_1, on Ptot is shown in Figure 35(a). The results indicate that this effect was pronounced when the middle impeller was rather close to the bottom one. In general, Ptot increased with clearance. However, Ptot decreased with C_1/D value from 1/2 to 1 for $S_{12}/D=3/2$. A similar phenomenon was also observed in dual-DT systems. The results obtained here confirm this change. The variation of Ne as a function of C_1/D is shown in Figure 35(b). An increase in Ne(tot) with clearance was observed due to the increase in Ne_1. Both Ne_2 and Ne_3 were unaffected by clearance. Figure 36 shows the effect of clearance on $P_i\%$. For a lower value of S_{12}/D, both $P_2\%$ and $P_3\%$ decreased with C_1 while $P_1\%$ increased. For a higher value of S_{12}/D, the effect of clearance was not significant.

From the results obtained in this work, it can be concluded that the position of the middle impeller has a significant effect on the total and the individual power consumptions. In addition, the effect of clearance is also very important, as observed previously in single impeller systems.

5.2.2.2 Results for Triple-Pitched Blade Turbine Systems

For the case of three 45° pitched-blade turbines, the effect of S_{12} on Ptot is shown in Figure 37(a). This effect was found to be more pronounced at lower clearance values. In the range $1 \leq S_{12}/D \leq 3/2$, a greater power consumption was observed. A maximum value of Ptot was found under the conditions $S_{12}/D=3/2$ and $C_1/D=1/6$ (Ptot/P*single=2.99). Figure 37(b) shows the variation of Ne as a function of S_{12} for $C_1/D=1$. Although the variation in Ne(tot) was not significant, it was noticed that Ne_2, for the middle impeller, dropped as S_{12}/D increased from 2/3 to 3/2. Ne_1 increased with spacing up to $S_{12}/D=3/2$. No remarkable change was found for Ne_3. However, all the power numbers were unaffected by the position of the middle impeller when $S_{12} > S_{23}$. The effect of S_{12} on $P_i\%$, is complicated, as shown in Figure 38. In general, the variation was more pronounced at lower values of S_{12}/D.

The effect of C_1 on Ptot is shown in Figure 39(a). All the curves in this figure indicate a moderate decrease of Ptot with C_1. This effect is similar to that observed in single-PBT systems. The variation of Ne as a function of C_1 at $S_{12}/D=5/2$ is shown in Figure 39(b). Ne(tot) decreased moderately as C_1/D changed from 1/6 to 1/2, and then decreased slightly when C_1/D increased from 1/2 to 1. At $C_1/D=1$, Ne(tot) was observed to be 3.91 ($Ne_1=1.19$, $Ne_2=1.39$, $Ne_3=1.33$). A significant variation of the individual power numbers was observed at lower clearances, $C_1/D<1/2$. Under this condition, Ne_1 dropped but Ne_2 increased with clearance. When $C_1/D>1/2$, no significant effect was found. Figure 40 shows the effect of C_1 on $P_i\%$. $P_1\%$ decreased in most cases when the clearance was increased. In general, this effect was more remarkable at lower clearance.

5.2.2.3 Results for Triple-Flat Blade Turbine Systems

The effect of impeller spacing on Ptot is complicated, as shown in Figure 41(a). A larger power drawn was observed when the middle FBT was close to either the bottom or the top impeller. Furthermore, a significant increase in Ptot was found at S_{12}/D around 3/2. At $C_1/D=1$, Ptot/P*single reached a value about 2.95 when the middle FBT was close to either one impeller. The effect of S_{12} on Ne(tot) and Ne_i is shown in Figure 40(b). In general, the variation of Ne(tot) and Ne_i were not significant. Under the condition of $S_{12}=S_{23}$ and $C_1/D=1$, Ne(tot) was found to be 6.42 ($Ne_1=2.09$, $Ne_2=2.07$, $Ne_3=2.26$). Figure 42 shows the variation of $P_i\%$ as a function of spacing. This effect was complicated at lower clearance. However, for $C_1/D\geq 1/2$, each $P_i\%$ value tended to be similar when $S_{12}>S_{23}$. $P_3\%$ was likely to be the largest value in most cases.

The effect of C_1 on Ptot is shown in Figure 43(a). In general, Ptot decreased with an increase in C_1 when $C_1/D<\sim 1/2$. However, in most cases, a slight increase in Ptot was observed when $C_1/D>\sim 1/2$. Figure 43(b) shows the variation of Ne as a function of C_1 under the condition $S_{12}=S_{23}$. When the clearance was increased, a significant decrease in Ne(tot) was observed for $1/4<C_1/D<1/2$. For $C_1/D>1/2$, Ne(tot) increased very

moderately with C_1. Figure 44 shows the effect of C_1 on P_i%. In general, changing the clearance had a little effect on all the P_i% values.

5.2.2.4 Results for Triple-Curved Blade Turbine Systems

For this case, the effect of spacing on Ptot is shown in Figure 45(a). In general, the value of Ptot increased with S_{12}. However, a larger power consumption was observed when the middle impeller was spaced at S_{12}=S_{23}, and when it was rather close to the top one. Under the condition S_{12}=S_{23} and C_1/D=1, the ratio Ptot/P*single was found to be 3. The effect of S_{12} on Ne is shown in Figure 45(b). Ne(tot) was equal to 6.39 under the same conditions, with Ne_1=1.84, Ne_2=2.13, and Ne_3=2.42. No significant change in each individual power number with spacing was observed. The effect of S_{12} on P_i% is shown in Figure 46. The top impeller (P_3%) contributed the largest part of power consumption at a given Ptot. P_1%, for the bottom CBT, was found to have the smallest value, regardless of the position of the middle impeller between the others.

The effect of C_1 on Ptot was strongly affected by the location of the middle impeller, as shown in Figure 47(a). In general, when S_{12}<S_{23}, Ptot increased with C_1; when S_{12}>S_{23}, Ptot decreased with C_1. However, the variation in Ptot due to this effect was not significant. The variation of Ne, at S_{12}=S_{23}, as a function of C_1, is shown in Figure 47(b). A moderate increase in Ne(tot) was observed when C_1/D>2/3. This was mainly due to a slight increase in Ne_1. Figure 48 shows the effect of C_1 on P_i%. The top impeller had the largest value of P_3% (about 40%) while P_1% for the bottom impeller was found to have the smallest value of about 23%-29%. Each P_i% value was nearly unaffected by the clearance.

5.2.2.5 Results for Combinations of Disc Turbines and Pitched-blade Turbines Systems

In this work, the following three combinations of disc turbines (DT) and 45° pitched-blade turbines (PBT) were tested.

Combination A: PBT (top) + DT (middle) + DT (bottom)

Combination B: DT (top) + PBT(middle) + DT (bottom)

Combination C: PBT (top) + PBT (middle) + DT (bottom)

(a) Combination A

The effect of spacing on Ptot is shown in Figure 49(a). These results indicate that Ptot increased when moving the middle DT apart from the bottom DT up to the point when $S_{12}/D=2.5$, i.e., $S_{12}=S_{23}$. When $S_{12}>S_{23}$, Ptot was nearly a constant. For $S_{12}=S_{23}$ and $C_1/D=1$, the value of $Ptot/\sum P^*single$ was obtained to be 0.96, i.e., the total power demand was approximately equal to the sum of that of three individual impellers. The effect of S_{12} on Ne is shown in Figure 49(b). For $S_{12}<S_{23}$, the variation of Ne for the lower two DTs was very similar to that observed in triple-DT systems. A pronounced increase in Ne(tot), as well as Ne_1 and Ne_2, was observed when increasing the S_{12}/D value from 3/2 to 2. The variation of Ne_3, for the top PBT, had only a small effect on Ne(tot) because its power number was rather small compared to that of DT. For $S_{12}=S_{23}$ and $C_1/D=1$, Ne(tot) was found to be 10.49 ($Ne_1=4.58$, $Ne_2=4.82$, $Ne_3=1.09$). Figure 50 shows $P_i\%$ as a function of S_{12}. When S_{12} was increased, $P_1\%$ increased but $P_2\%$ decreased. However, both values tended to be the same when $S_{12}>S_{23}$. Some noticeable changes in $P_3\%$ were observed when the middle DT was close to either the bottom or the top impeller.

The effect of C_1 on Ptot is shown in Figure 51(a). In most cases, the value of Ptot was proportional to the clearance. Figure 51(b) refers to the effect of C_1 on Ne. Ne(tot) increased with clearance since Ne_1 and Ne_2 increased for both DTs. Ne_3, for the top

PBT, was not affected by the clearance. The change of P_1% as a function of C_1 is shown in Figure 52. These results indicate that when the middle DT was close to the bottom one, P_1% was heavily affected by the clearance. When it was moved closer to the top PBT, the effect of clearance was not significant.

(b) Combination B

For the combination of a DT (top), a PBT (middle), and a DT (bottom), the effect of S_{12} on Ptot is shown in Figure 53(a). These results indicate that changing the location of the middle PBT had no significant effect on Ptot. In general, Ptot decreased very moderately with S_{12}. At $S_{12}/D= S_{23}/D= 2.5$ and $C_1/D=1$, the value of $Ptot/\sum P^*single$ was equal to 0.98. The variation of Ne due to this effect is shown in Figure 53(b). Under this condition, Ne(tot) was found to be 10.81 (Ne_1=4.66, Ne_2=0.97, and Ne_3=5.18). A noticeable decrease in Ne_3 was observed for $S_{12}/D>3.5$ (i.e., $S_{23}/D<1.75$). Figure 54 is the plot of P_i% vs. S_{12}/D. In general, P_3% decreased and P_1% increased slightly with S_{12}. A very moderate increase in P_2% for the middle PBT was observed when it was moved closer to the top impeller. However, the results indicate that $P_3\%>P_1\%>P_2\%$ in most cases.

The effect of C_1 on Ptot is shown in Figure 55(a). Regardless of the location of the middle PBT between the other two impellers, Ptot increased with clearance up to $C_1/D=1/3$, and, again, from $C_1/D=2/3$ to 1. Figure 55(b) shows the effect of C_1 on Ne. No significant variation was found in the individual power number for the top DT and the middle PBT. Ne_1, for the bottom DT, increased sharply from $C_1/D=1/6$ to 1/3, and then increased moderately with clearance. Because the DT drew much more power than the PBT, the variation of Ne(tot) as a function of clearance was mainly dominated by the two DTs, especially the bottom one.

Figure 56 shows the variation of P_1% as a function of C_1. In general, P_3% decreased and P_1% increased with clearance. In most cases, P_2% tended to decrease slightly when increasing the clearance.

(c) Combination C

This was the case in which a PBT (top), a PBT (middle), and a DT (bottom) were used. Figure 57(a) shows the dependence of Ptot on S_{12}. No significant variation was observed. The results indicate that the ratio Ptot/$\sum$P*single was less than unity in all cases. At C_1/D=1, the ratio was in the range 0.86-0.9. Ne as a function of S_{12} is plotted in Figure 57(b). Ne(tot) did not change appreciably when the location of the middle PBT was varied. A slight increase in Ne_1, for the bottom DT, was observed when increasing S_{12}. Ne_2 and Ne_3, for both the PBTs, were likely to have the same power number. The effect of S_{12} on P_1% is negligible as shown in Figure 58.

The effect of C_1 on Ptot is shown in Figure 59(a). Ptot increased with clearance in most cases. Figure 59(b) shows the variation of Ne as a function of C_1. A noticeable increase in Ne(tot) with C_1 was observed for $1/2<C_1/D\leq 1$. This change was mainly due to an increase in Ne_1, for the bottom DT. The effect of C_1 on P_1% is shown in Figure 60. In general, P_1% increased with clearance. No significant effect was observed on both P_2% and P_3%.

CHAPTER 6

CONCLUSIONS

1. In the turbulent agitation regime, the agitation rotation speed and the liquid height were found to have no significant effect on power number.
2. For multiple-DT systems, the total power consumption was approximately equal to the sum of each individual power consumption when the spacing was about twice the impeller diameter.
3. In general, for any multiple-DT systems, the power consumption was proportional to the impeller off-bottom clearance and spacing. However, for S/D (or S_{12}/D)=~3/2 and C_1/D>~1/2, Ptot decreased with C_1. In both dual- and triple-impeller systems, the uppermost DT was found to draw more power than the lower DTs, i.e., (P_3>)P_2>P_1.
4. In both the triple-DT and the triple-PBT systems, Ptot and P_1 were found to be strongly dependent on the location of the middle impeller and off-bottom clearance. For triple-DT systems, the maximum power consumption was found when the intermediate DT was spaced midway between the others for any given clearance. In general, for multiple-PBT systems, Ptot decreased when C_1 was increased. The maximum power drawn was observed at a lower clearance and when S/D (or S_{12}/D)=~3/2. However, for combinations of DTs and PBTs in triple-impeller systems, the location of the middle PBT was found to have no significant effect on the power consumption. The variation of Ptot due to the effect of spacing and clearance was mainly caused by the DTs.
5. For multiple-CBT systems, the impeller spacing was found to have little effect on Ptot and P_1. In general, (P_3>)P_2>P_1 .

APPENDIX A

FIGURES FOR MULTIPLE-IMPELLER SYSTEMS

This appendix includes the figures showing the effects of impeller clearance and spacing on the power consumption in multiple-impeller systems. For dual-impeller systems, these figures include:

Dual-DT systems (Figure 9-Figure 12)

Dual-PBT systems (Figure 13-Figure 16)

Dual-FBT systems (Figure 17-Figure 20)

Dual-CBT systems (Figure 21-Figure 24)

Combination of a DT and a PBT systems (Figure 25-Figure 28)

Combination of a PBT and a FBT (Figure 29-Figure 32)

For triple-impeller systems, these figures include:

Triple-DT systems (Figure 33-Figure 36)

Triple-PBT systems (Figure 37-Figure 40)

Triple-FBT systems (Figure 41-Figure 44)

Triple CBT systems (Figure 45-Figure 48)

Combinations of DTs and PBTs (Figure 49-Figure 60)

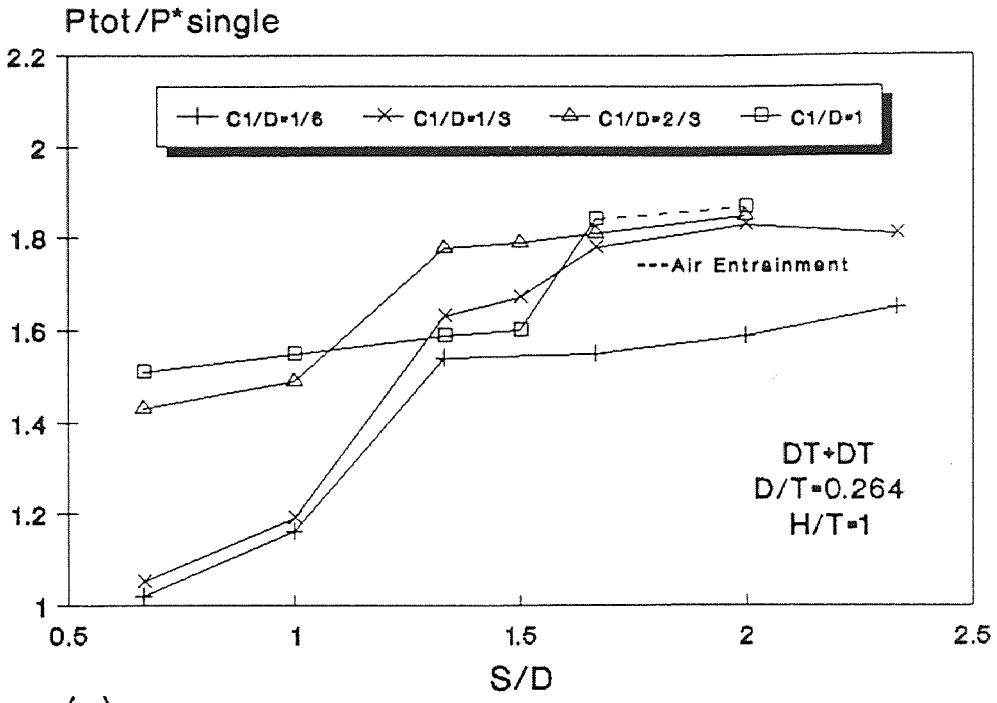

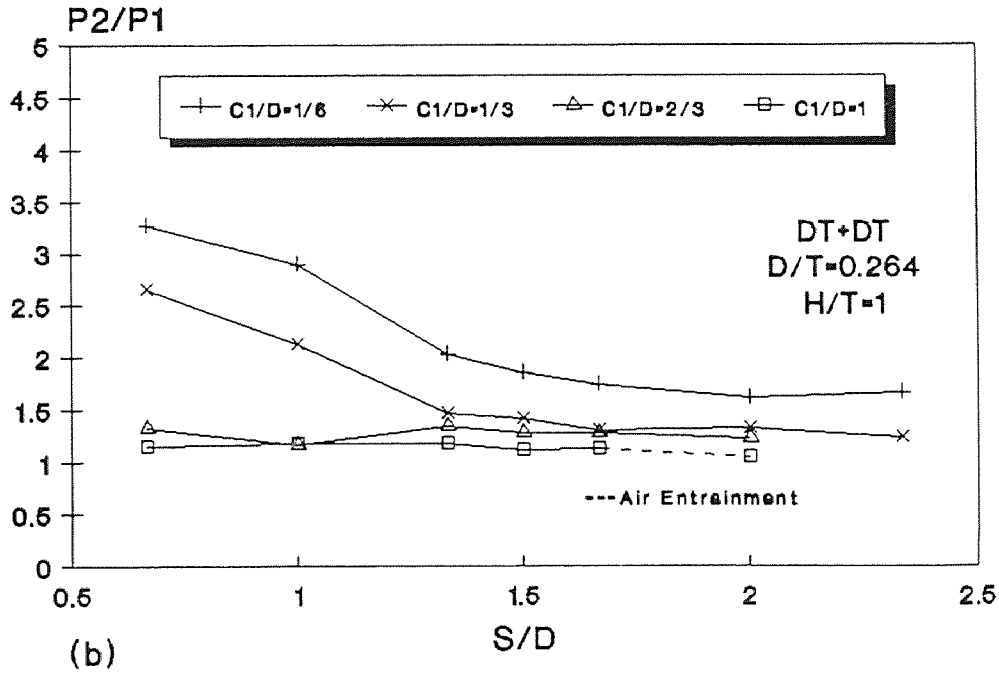

Figure 9 Effect of S on Power

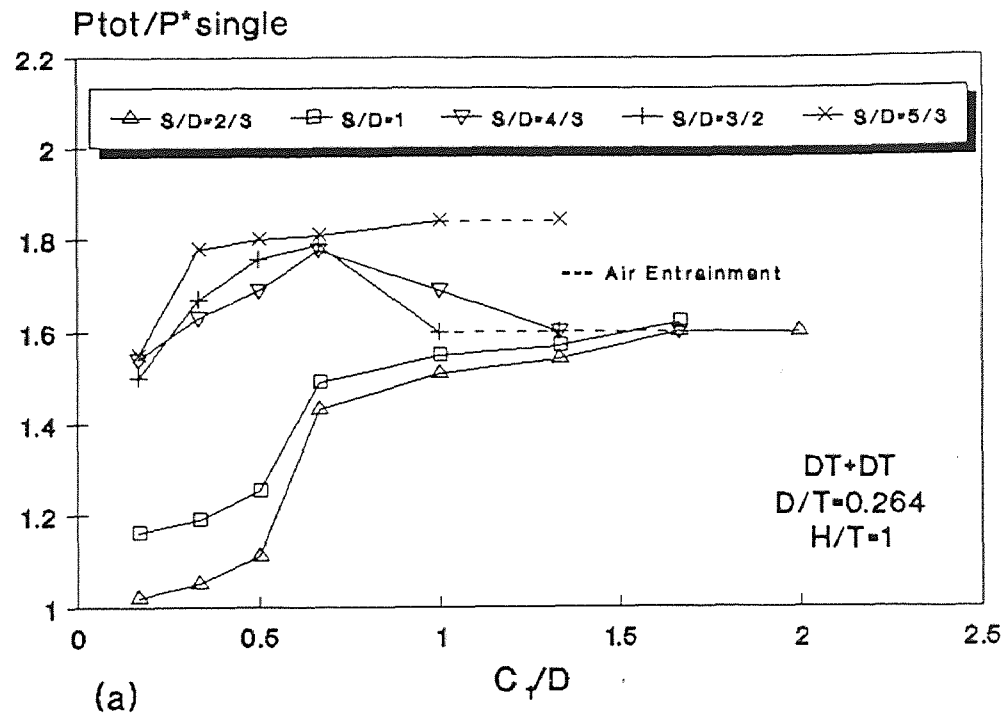

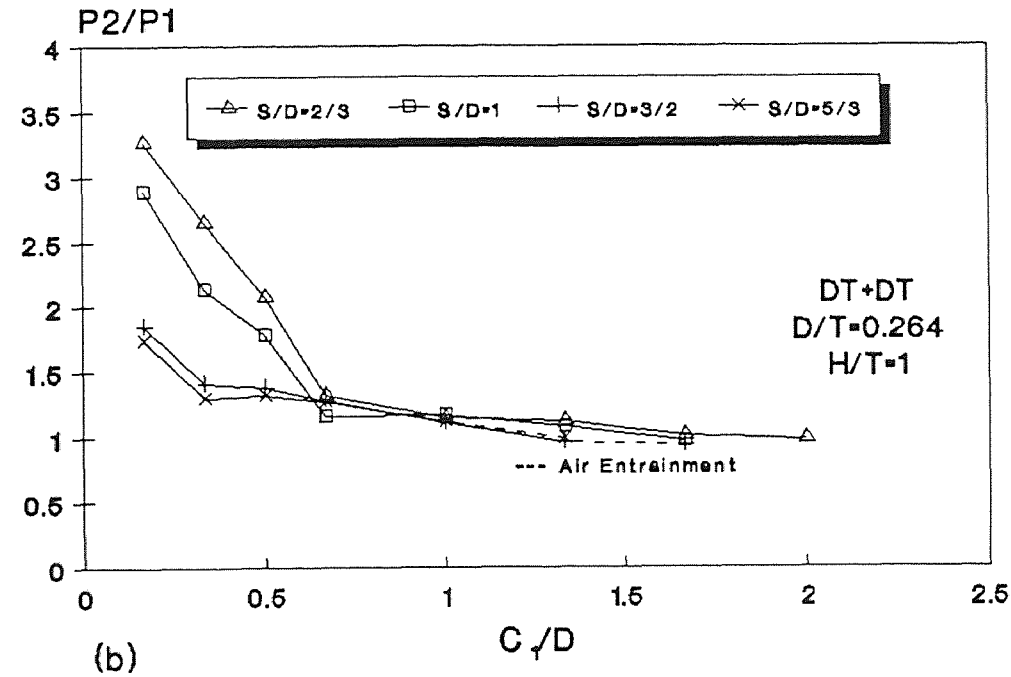

Figure 10 Effect of C_1 on Power

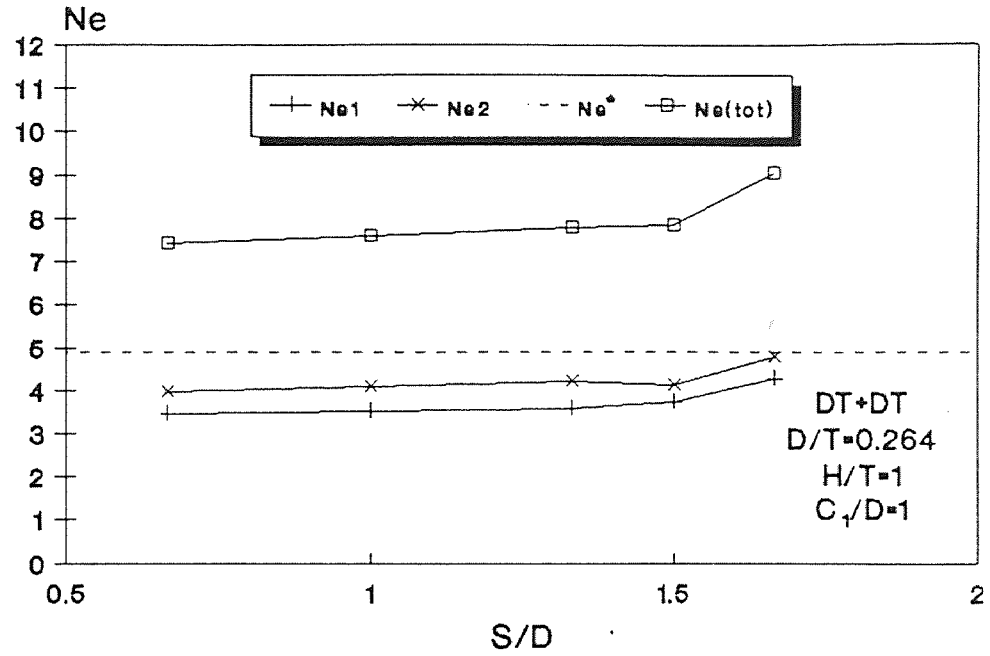

Figure 11 Effect of S on Ne

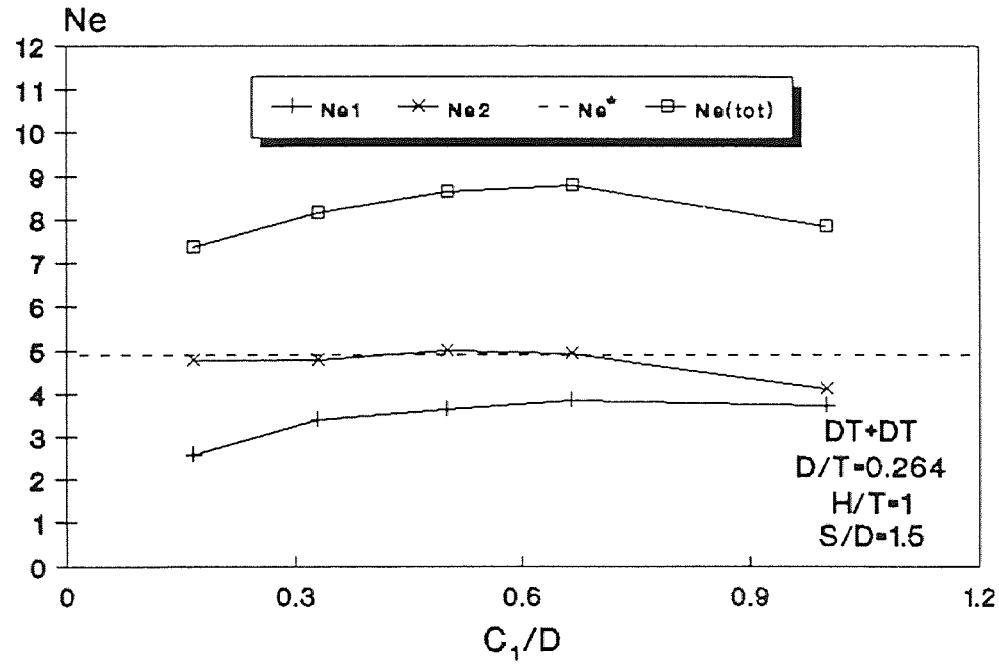

Figure 12 Effect of C_1 on Ne

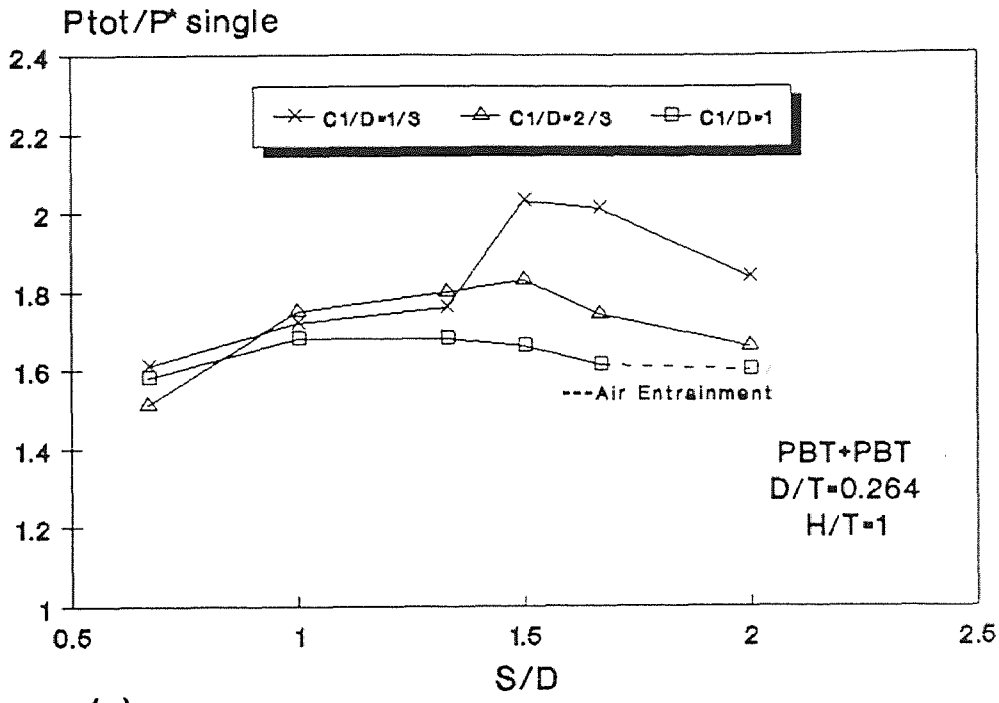

(a)

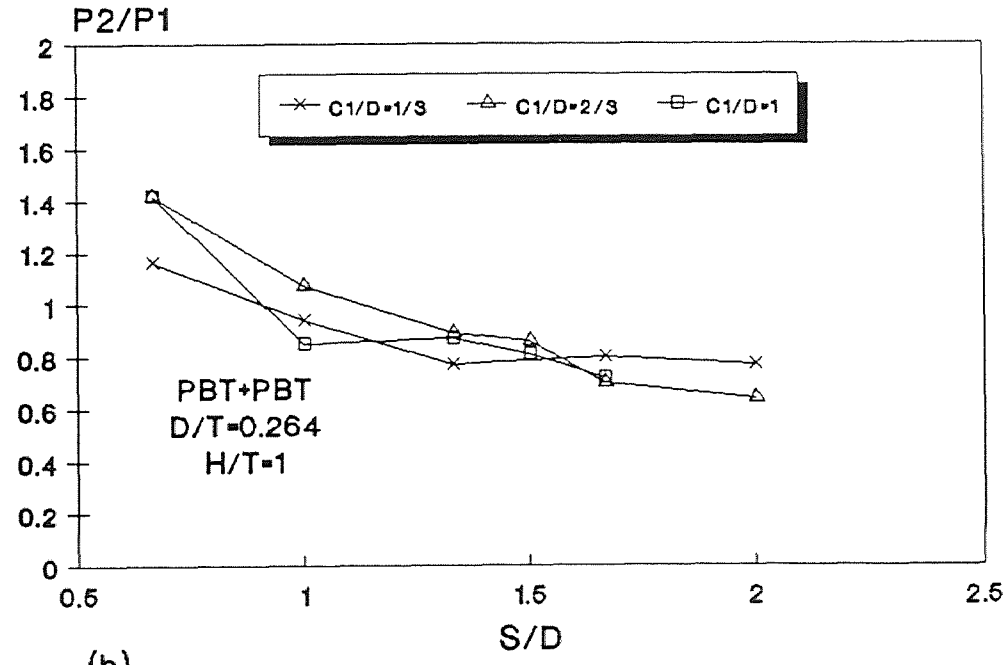

(b)

Figure 13 Effect of S on Power

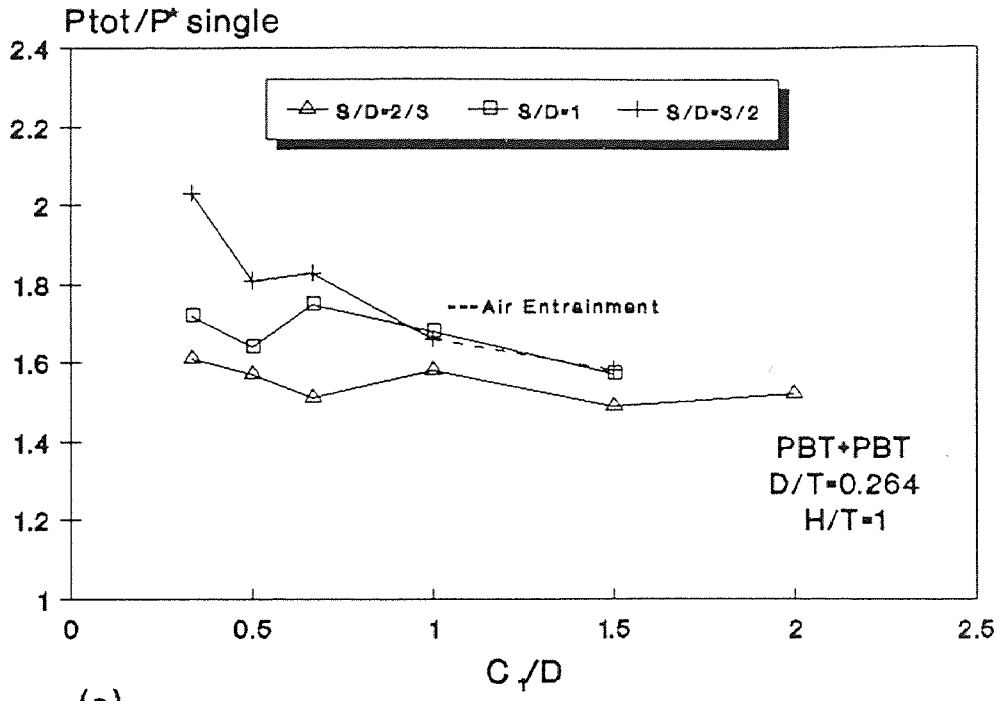

(a)

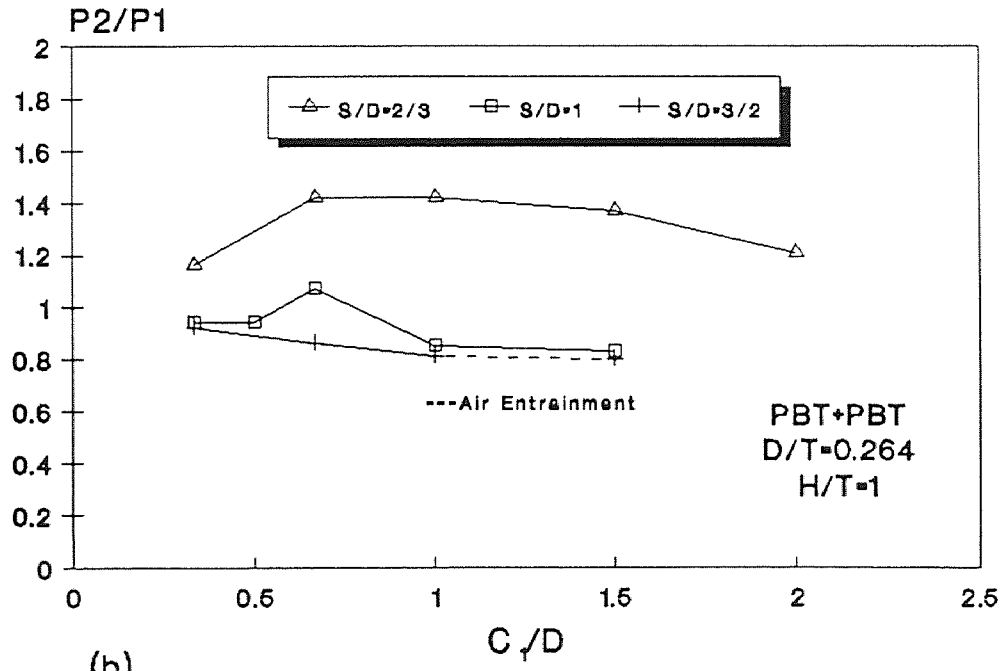

(b)

Figure 14 Effect of C_1 on Power

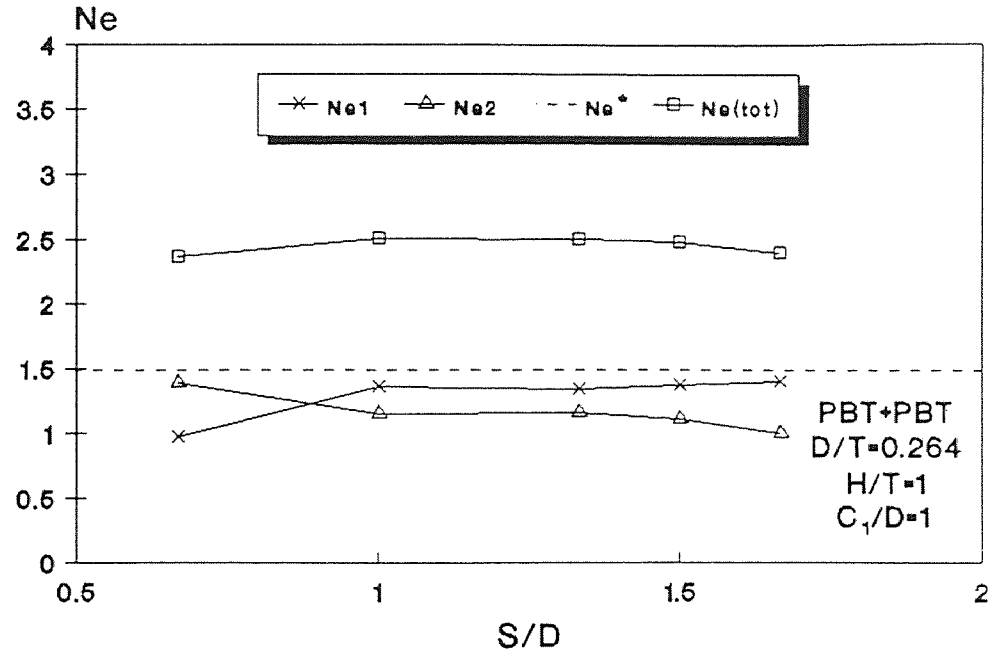

Figure 15 Effect of S on Ne

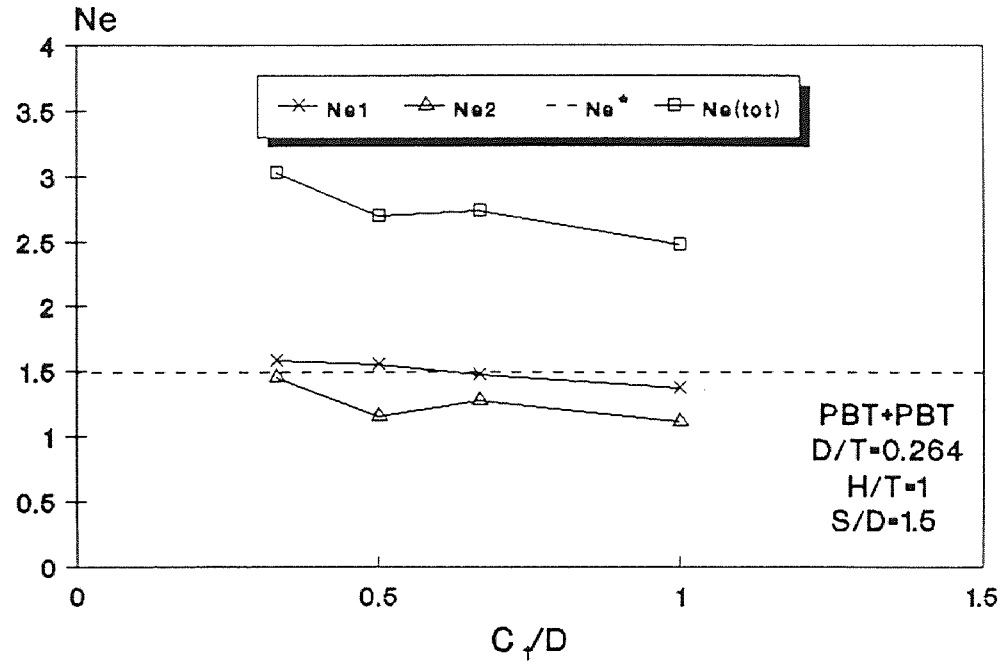

Figure 16 Effect of C_1 on Ne

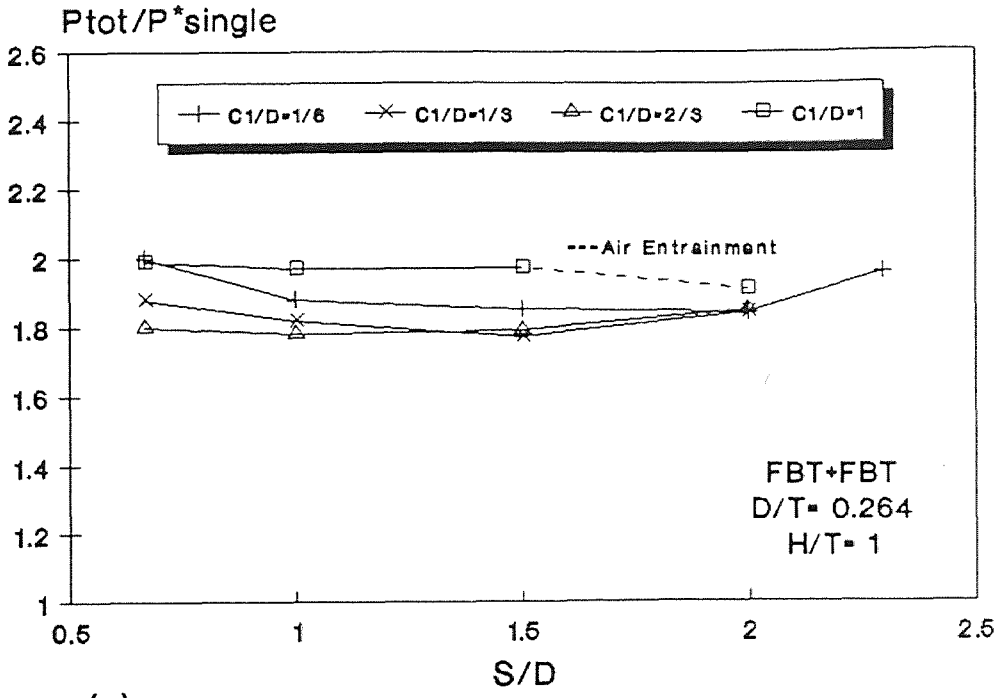

(a)

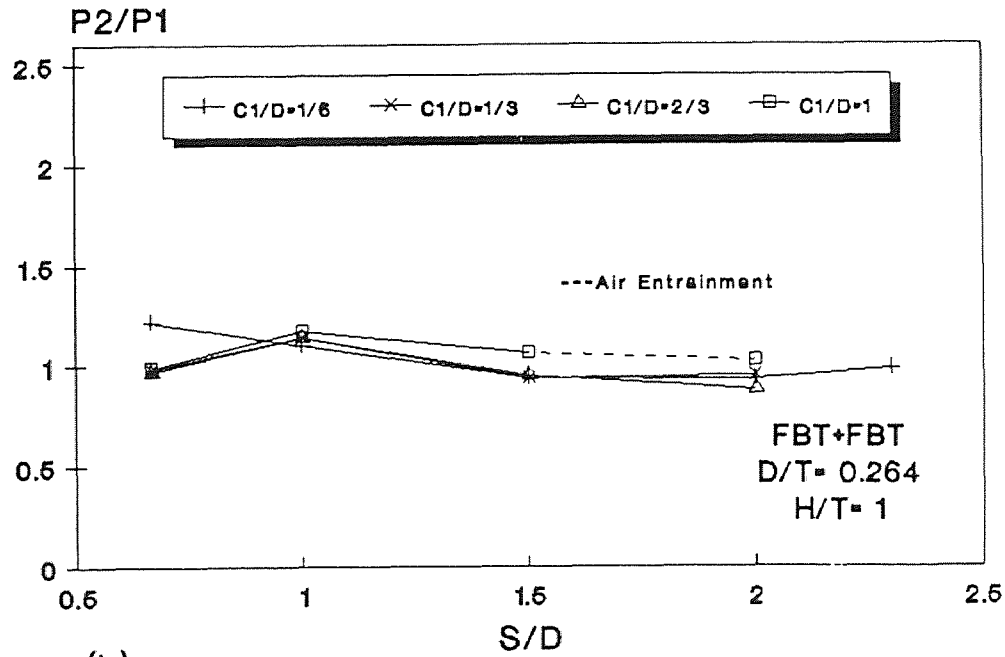

(b)

Figure 17 Effect of S on Power

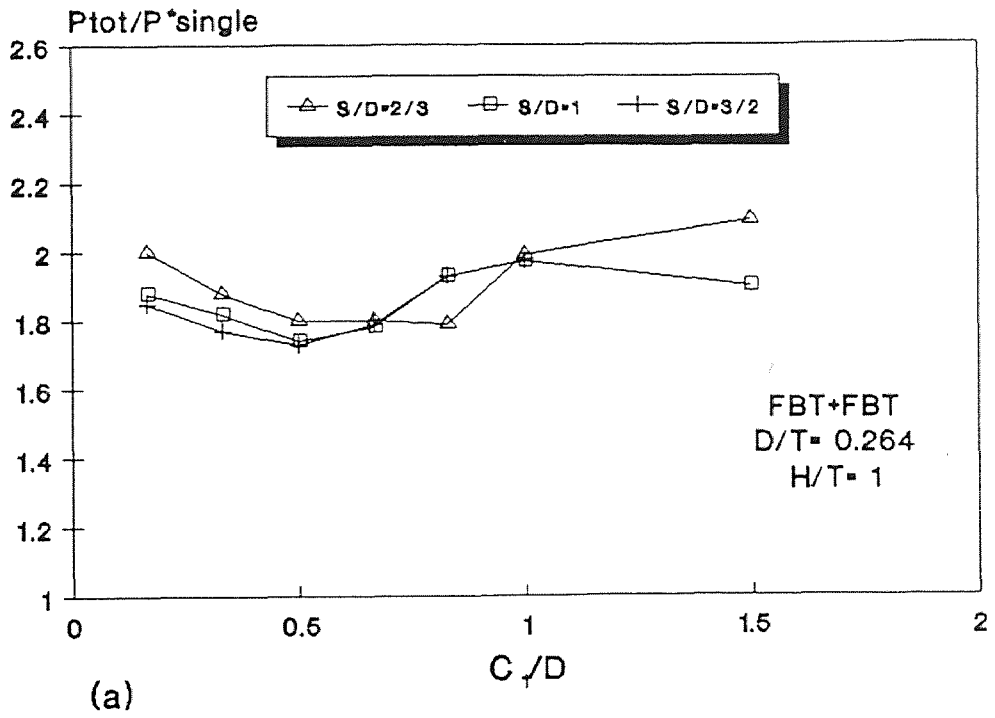

(a)

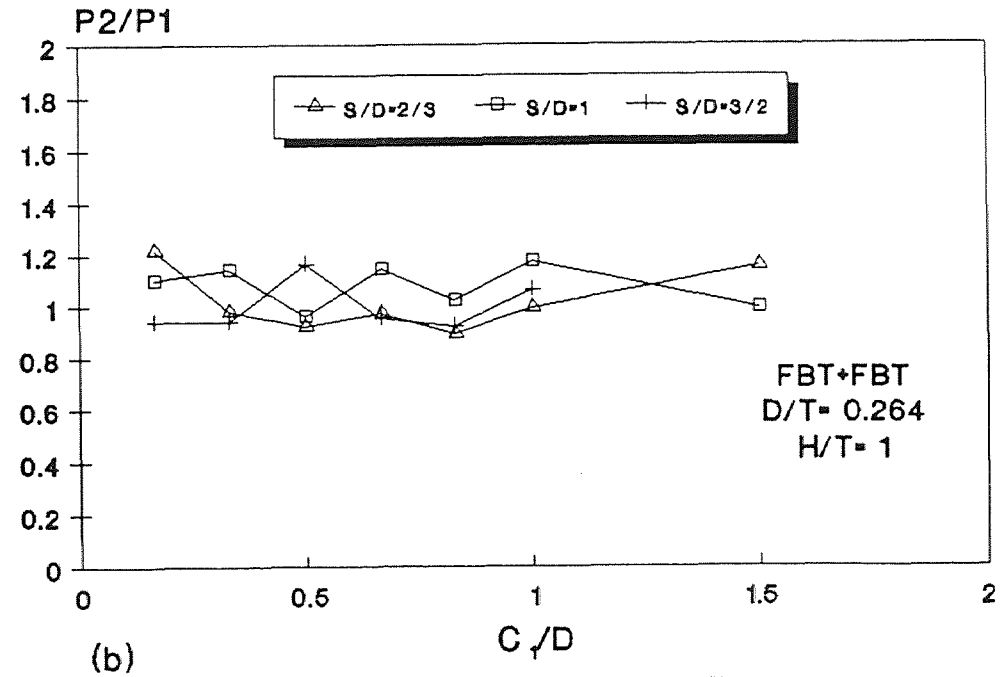

(b)

Figure 18 Effect of C_1 on Power

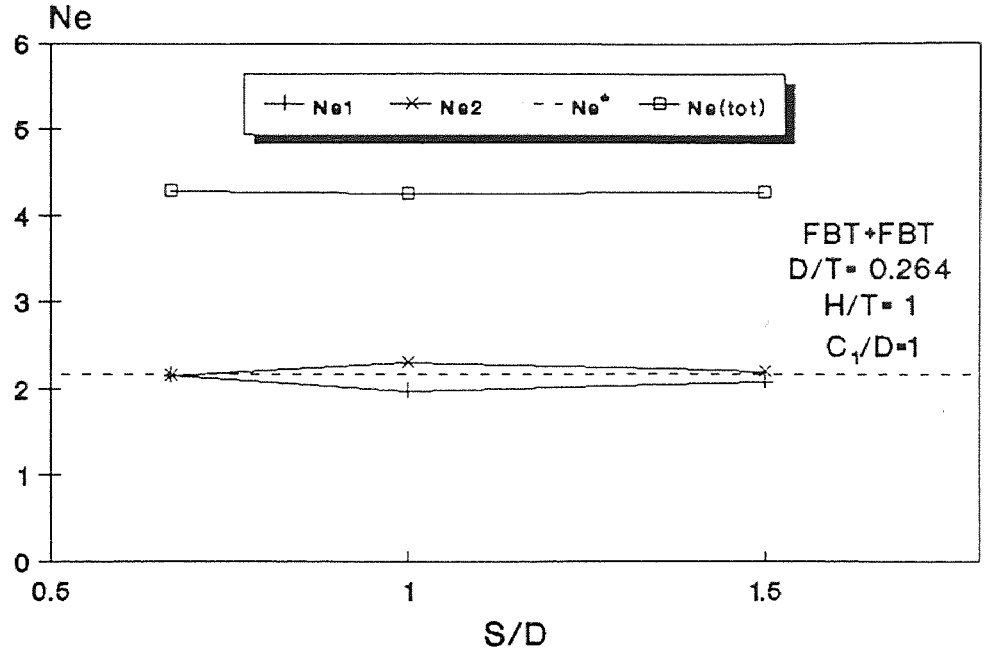

Figure 19 Effect of S on Ne

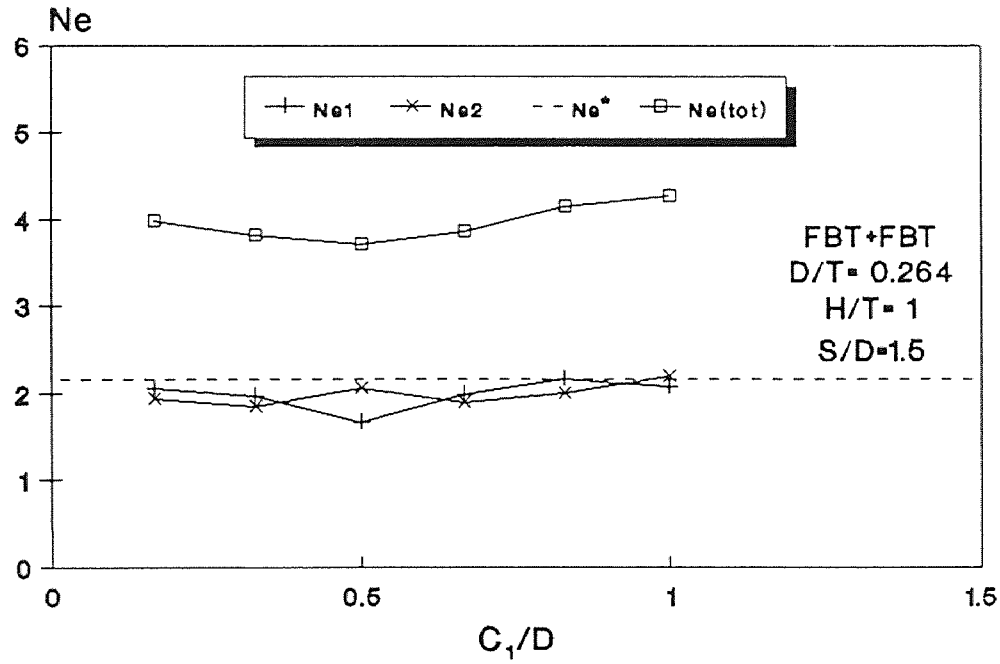

Figure 20 Effect of C_1 on Ne

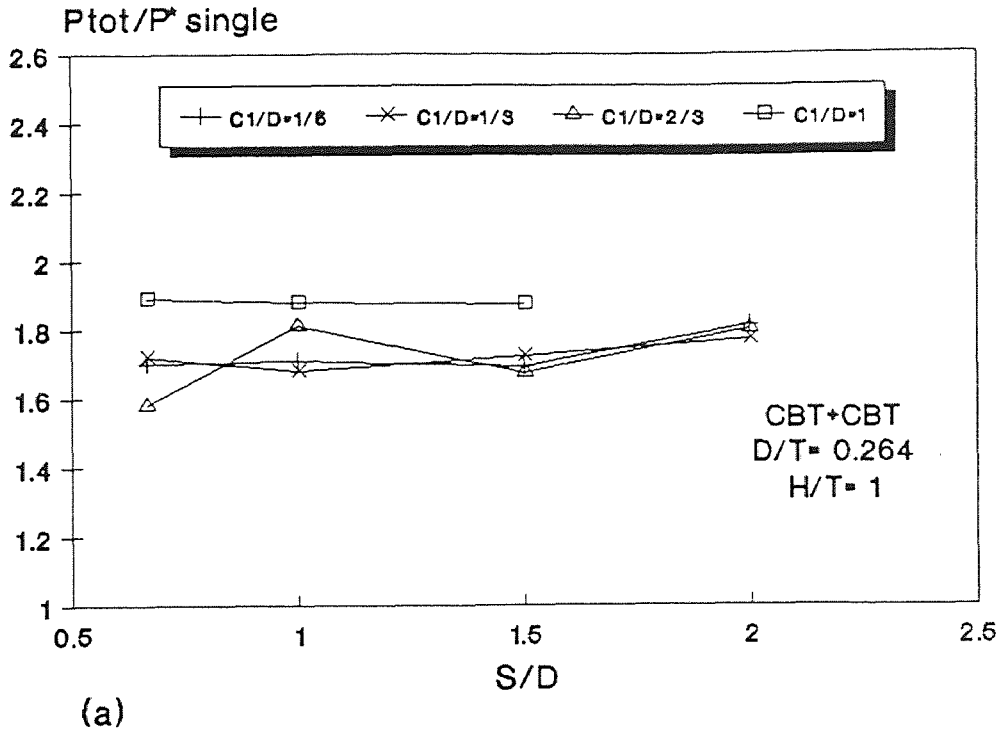

(a)

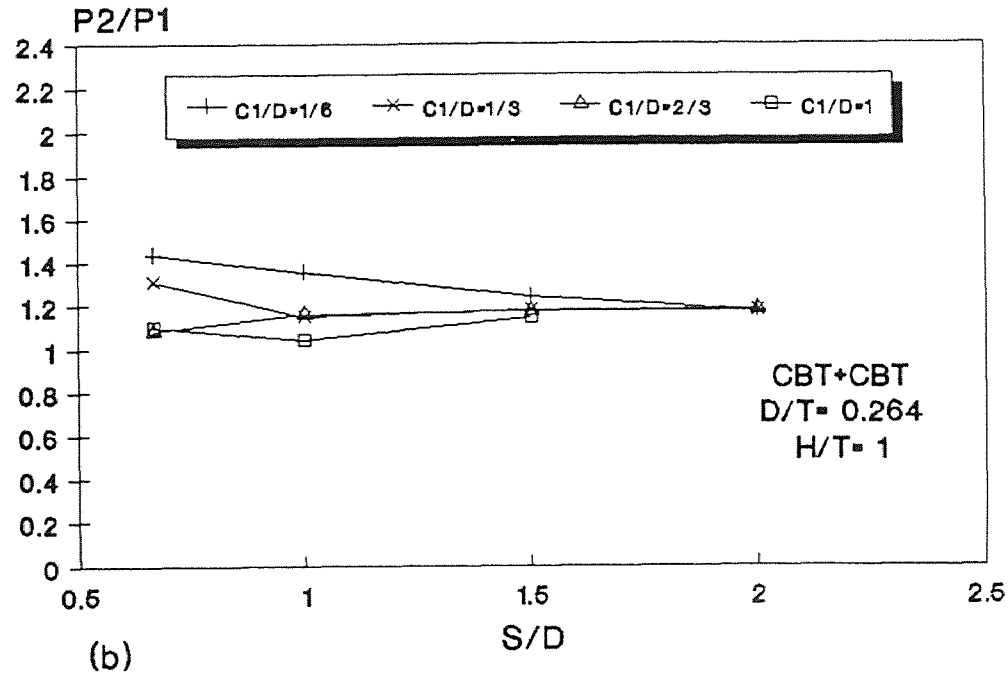

(b)

Figure 21 Effect of S on Power

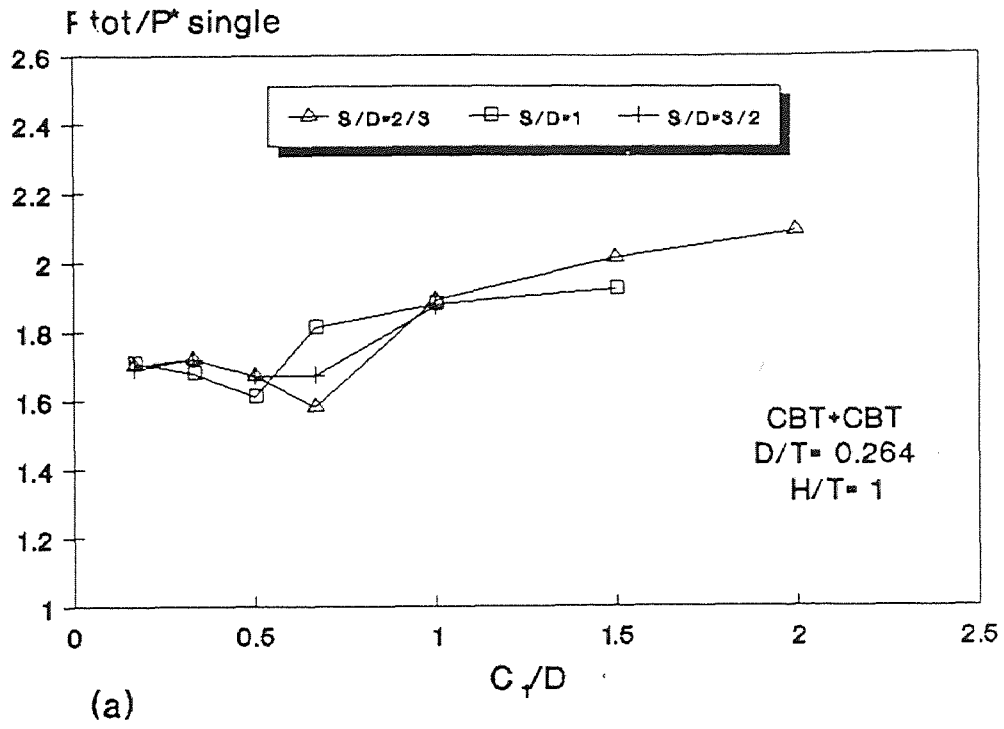

(a)

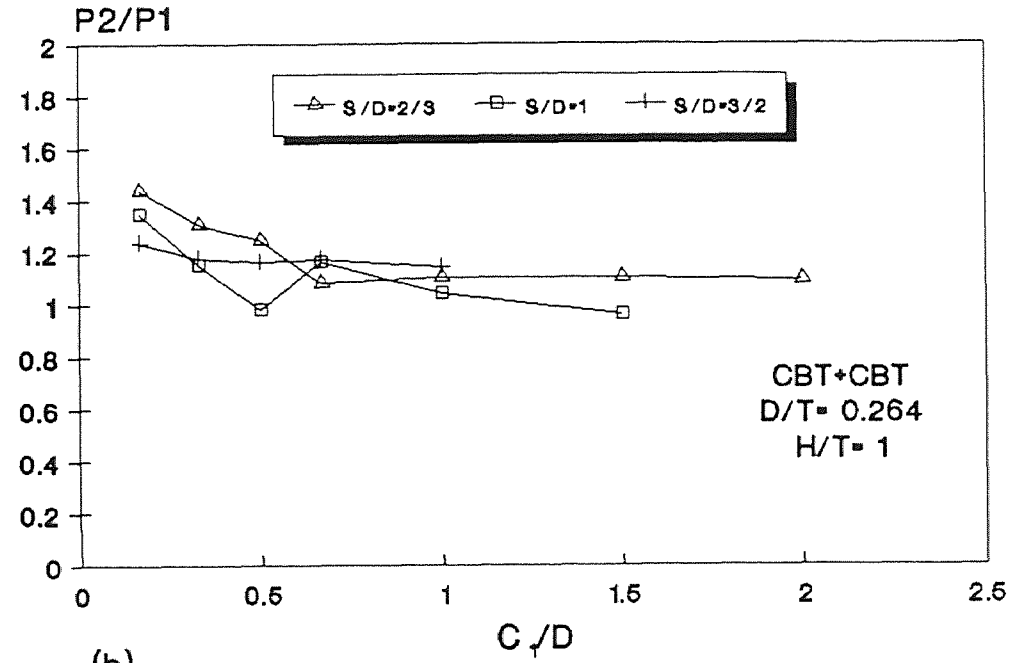

(b)

Figure 22 Effect of C_1 on Power

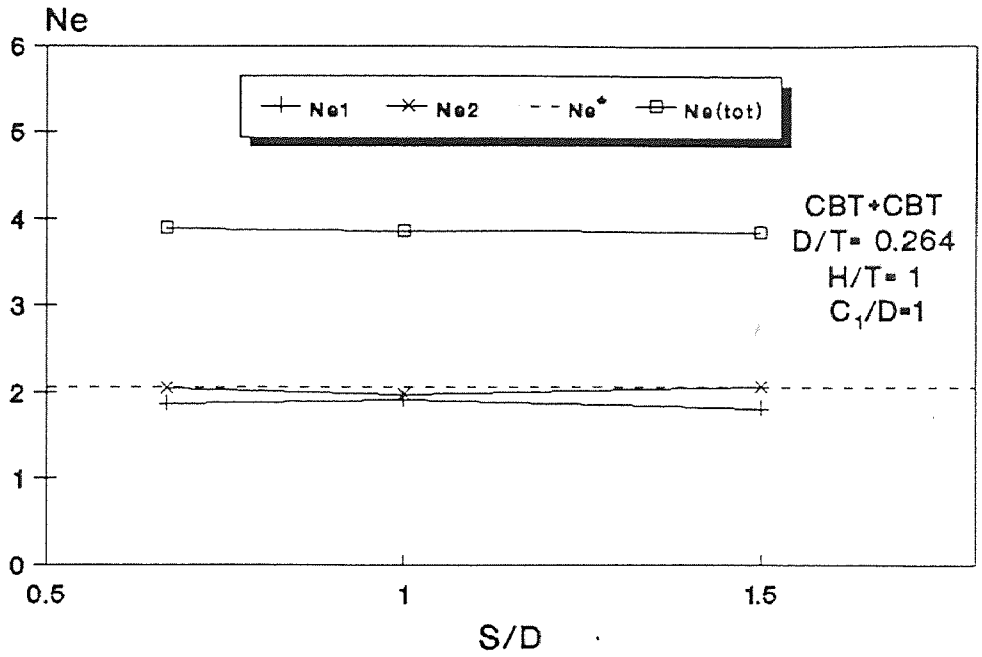

Figure 23 Effect of S on Ne

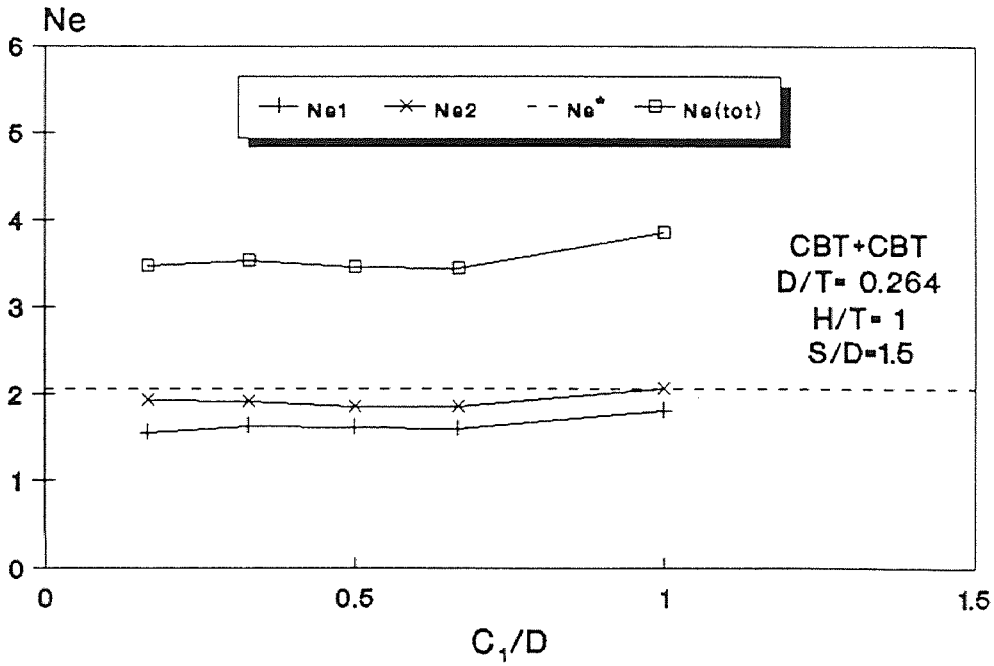

Figure 24 Effect of C_1 on Ne

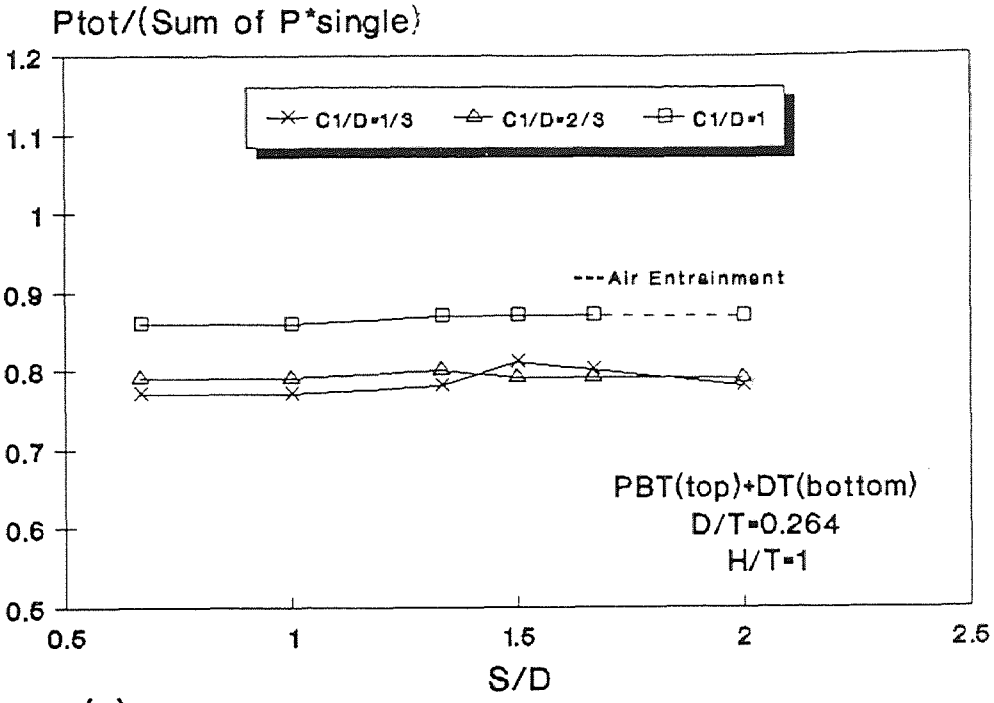

(a)

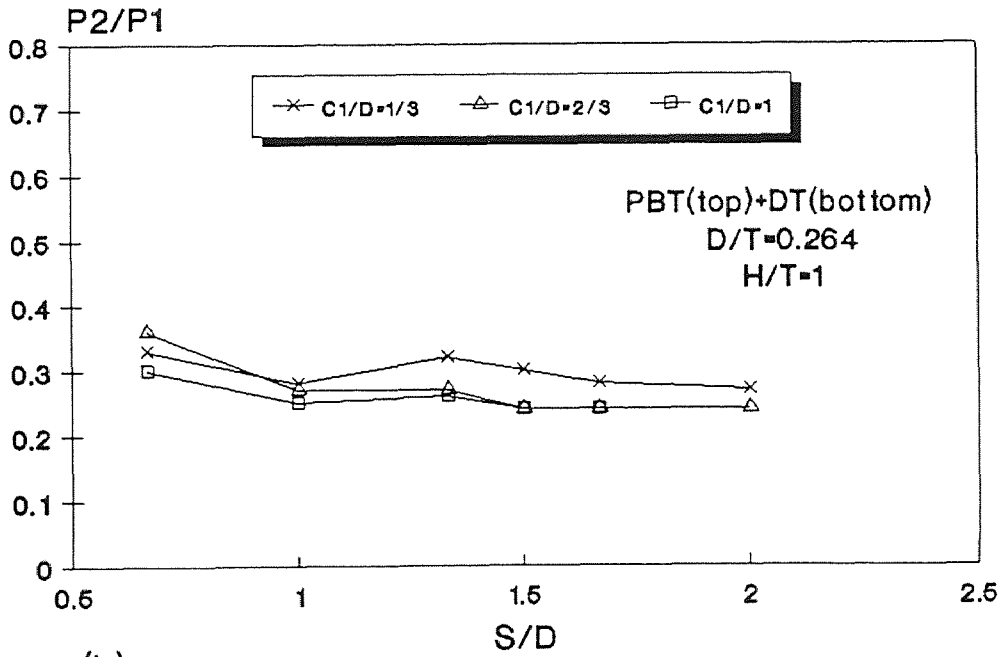

(b)

Figure 25 Effect of S on Power

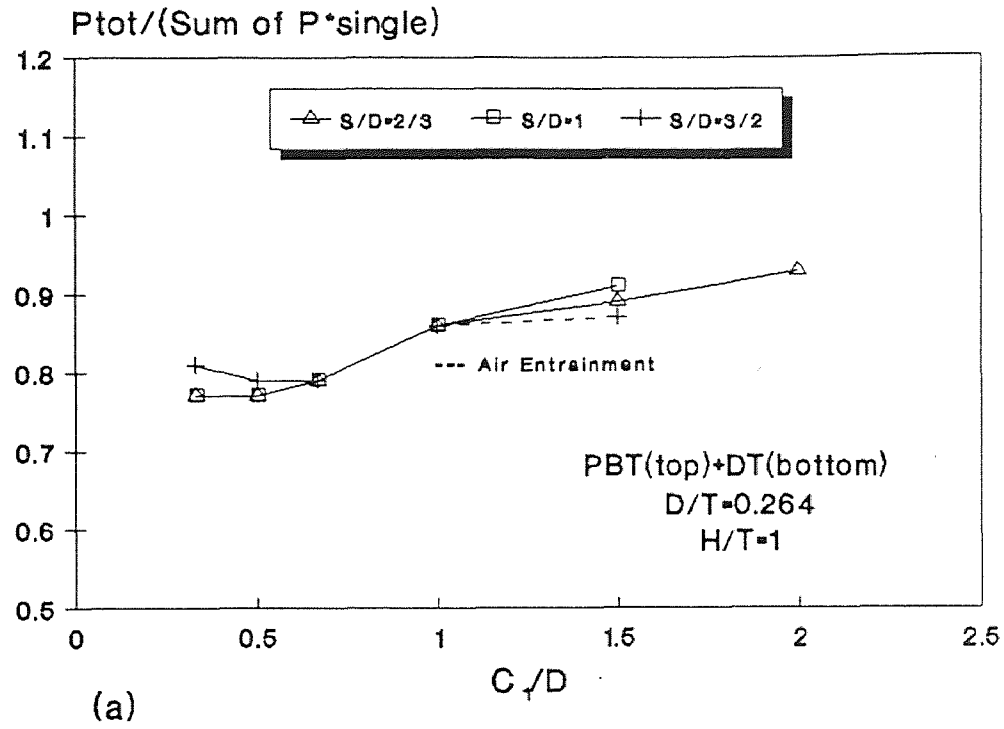

(a)

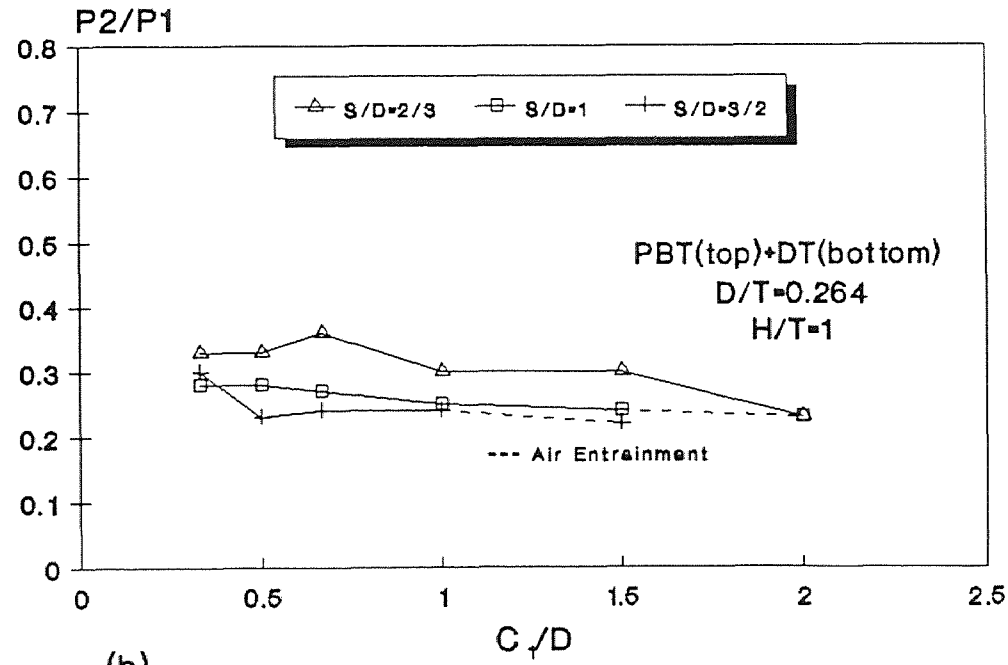

(b)

Figure 26 Effect of C_1 on Power

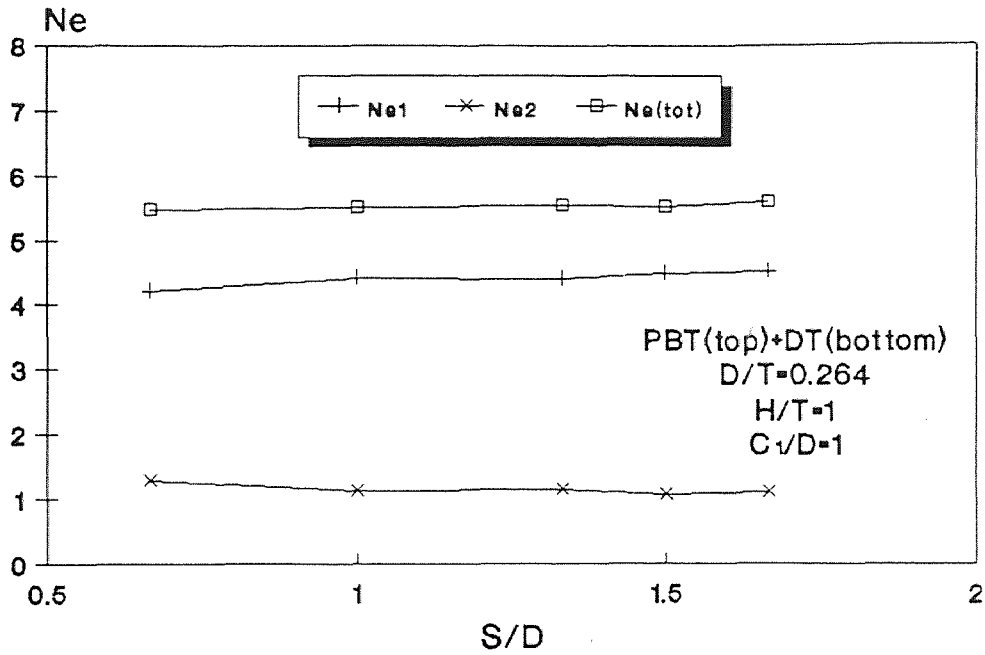

Figure 27 Effect of S on Ne

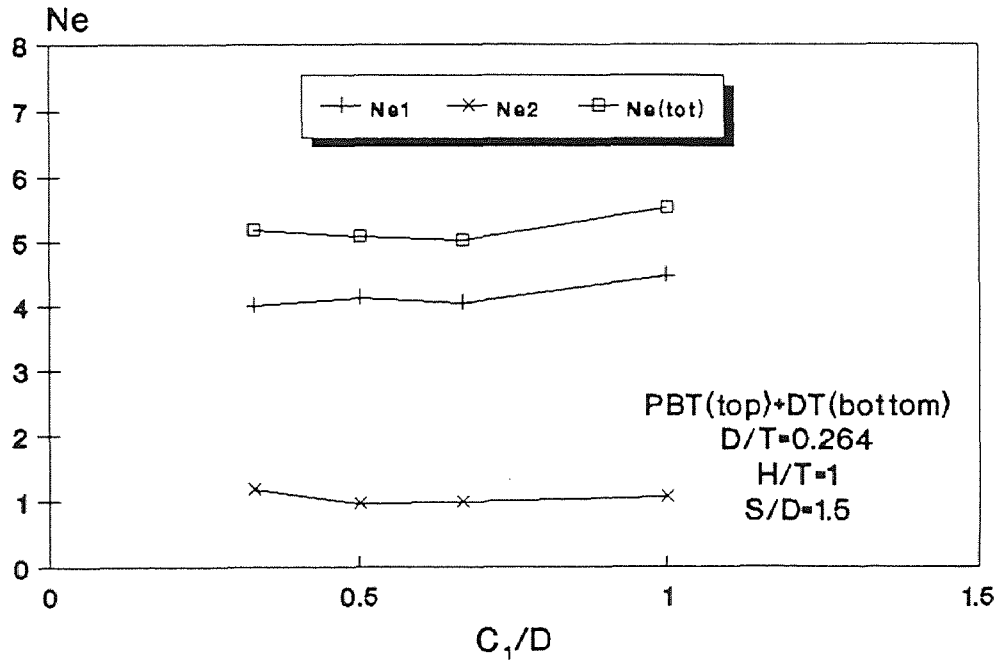

Figure 28 Effect of C_1 on Ne

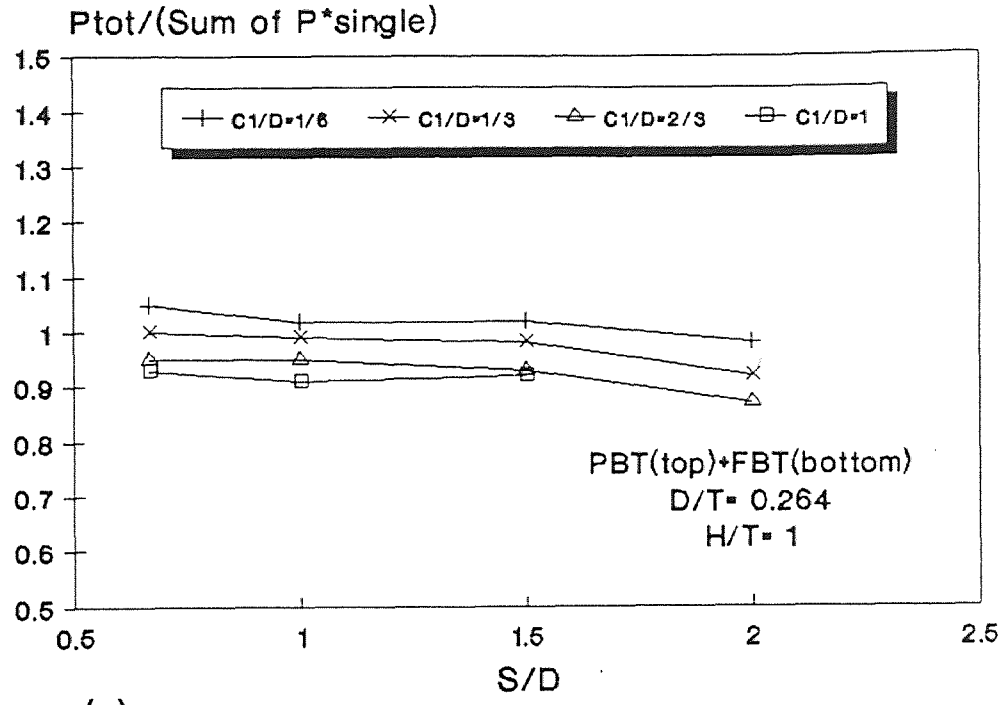

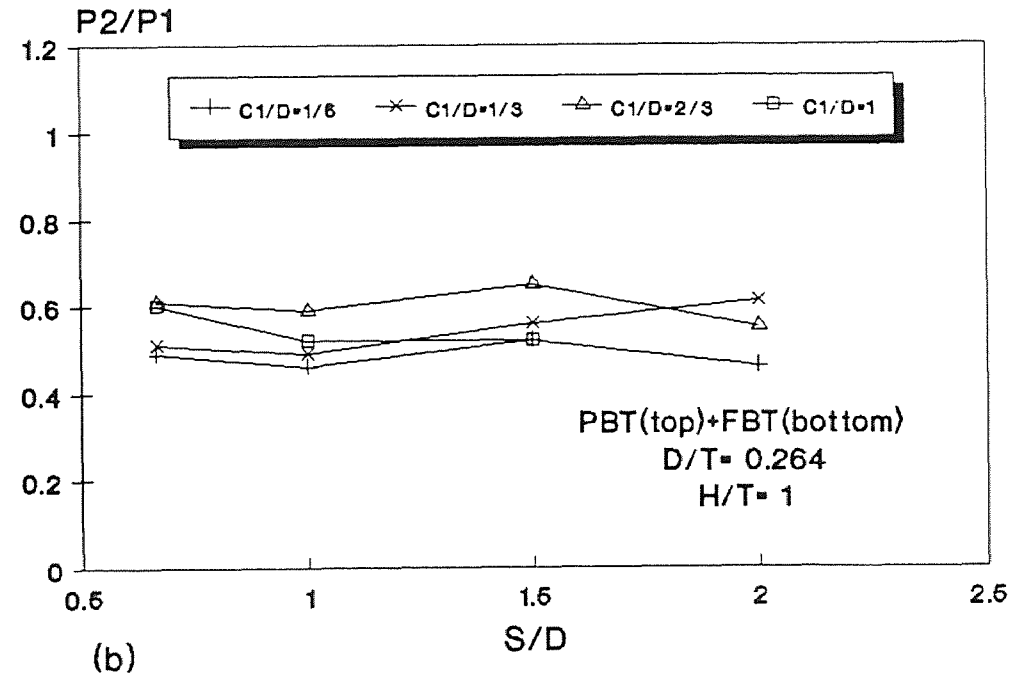

Figure 29 Effect of S on Power

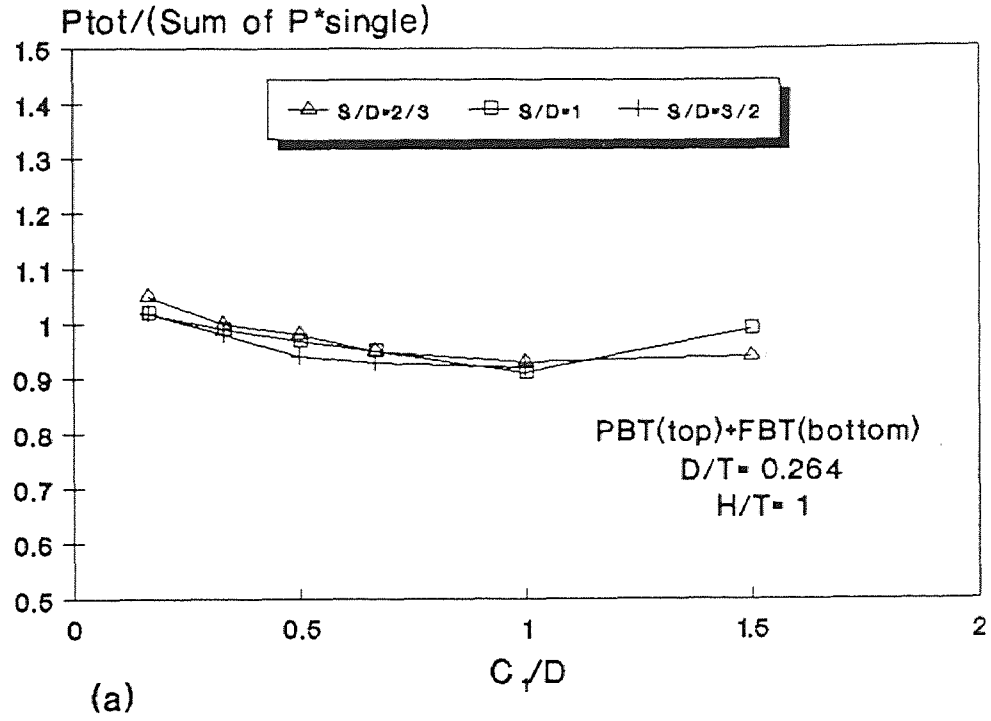

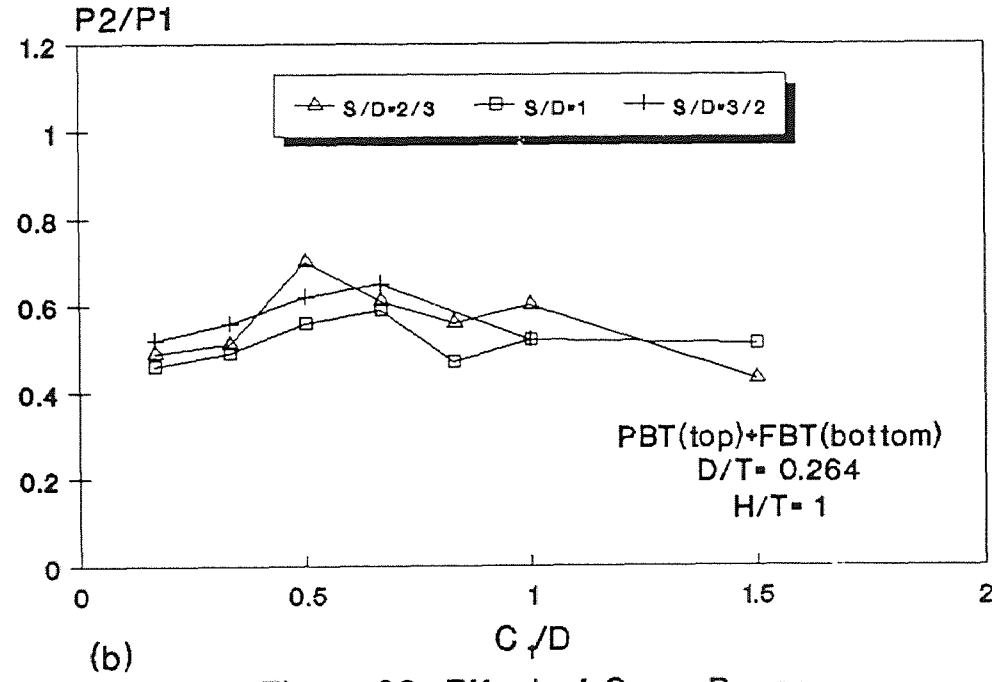

Figure 30 Effect of C_1 on Power

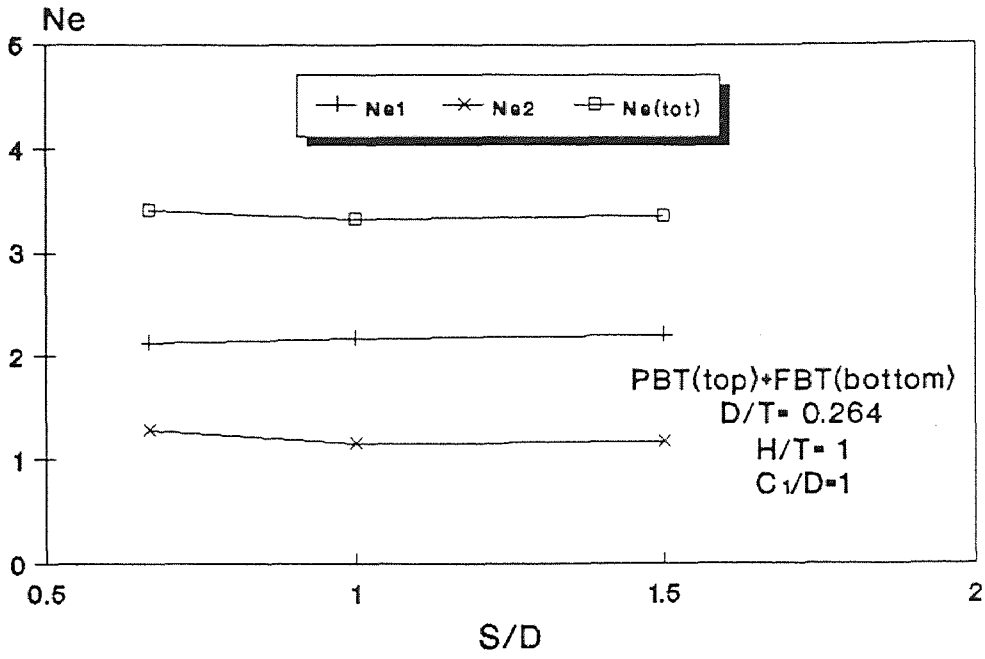

Figure 31 Effect of S on Ne

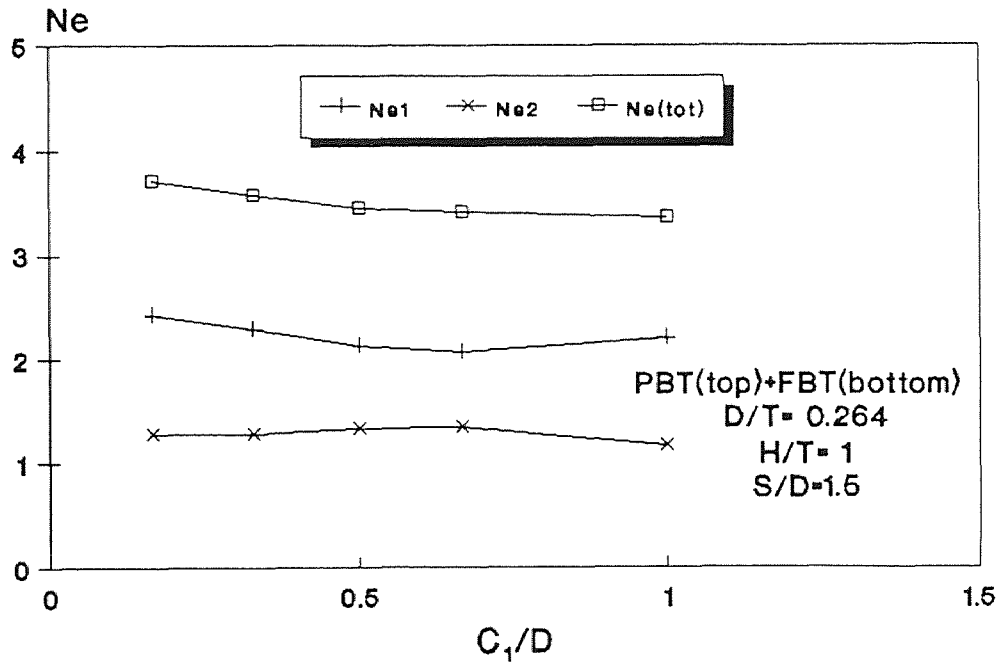

Figure 32 Effect of C_1 on Ne

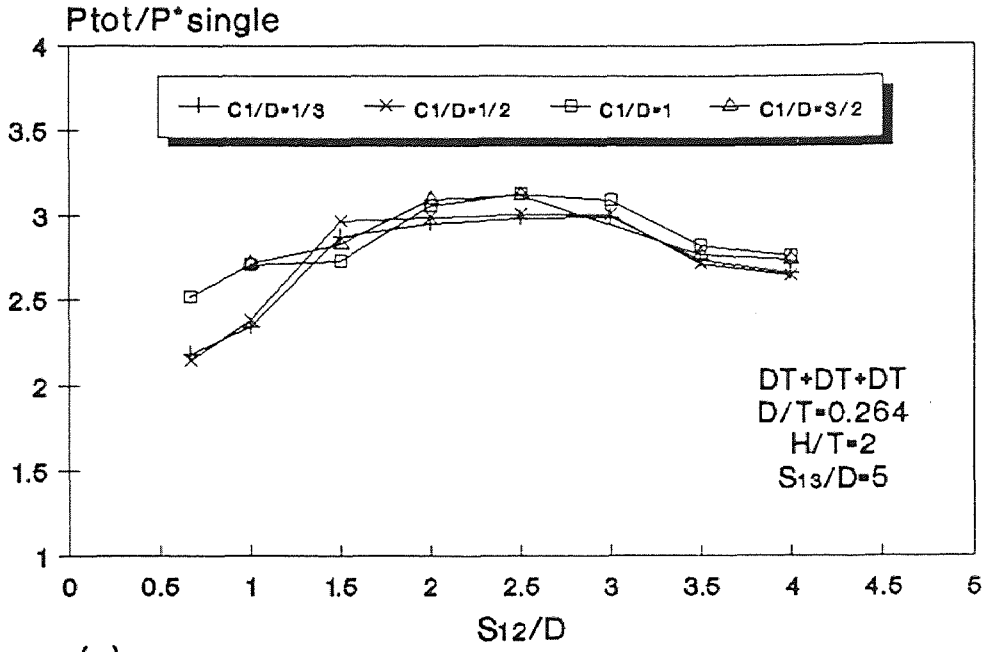

(a)

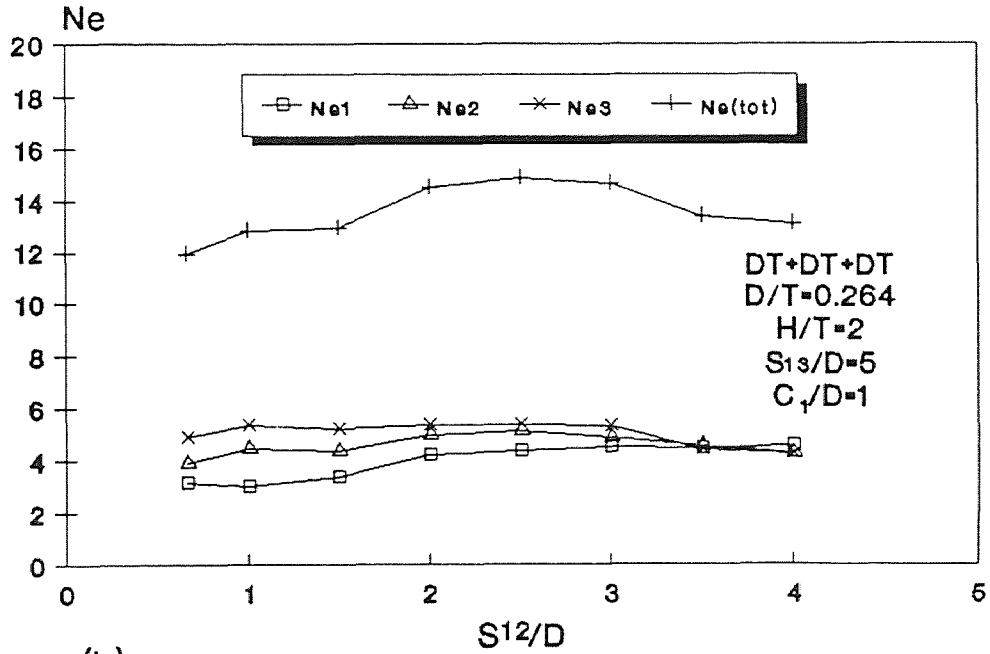

(b)

Figure 33 Effect of S on Ptot and Ne

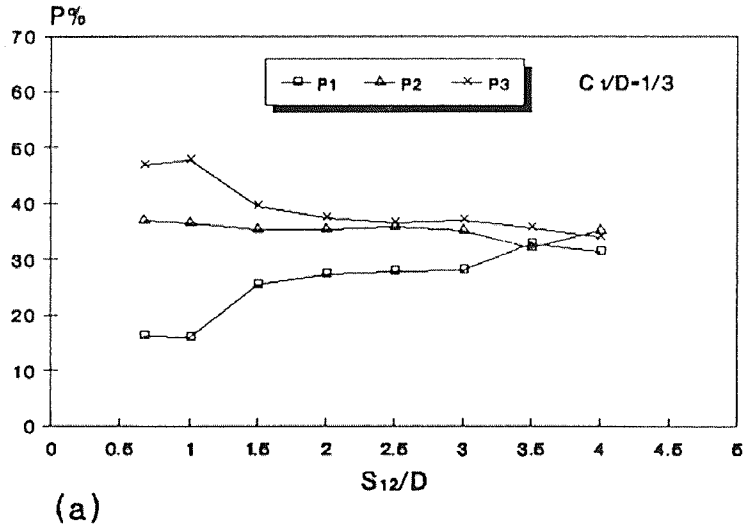

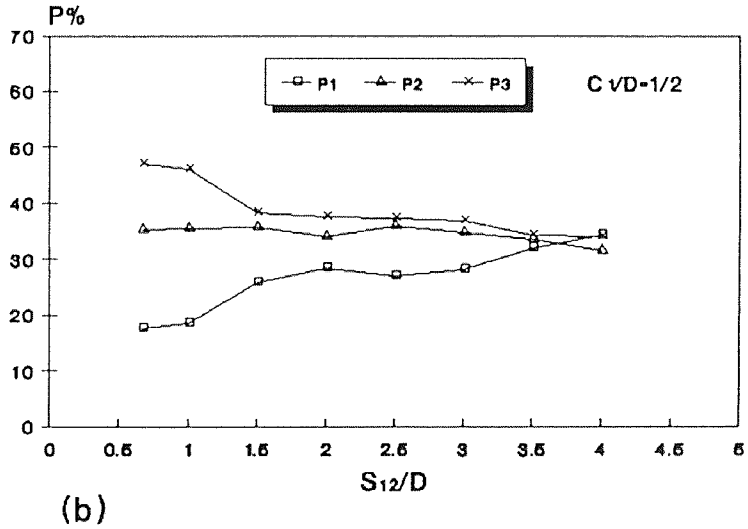

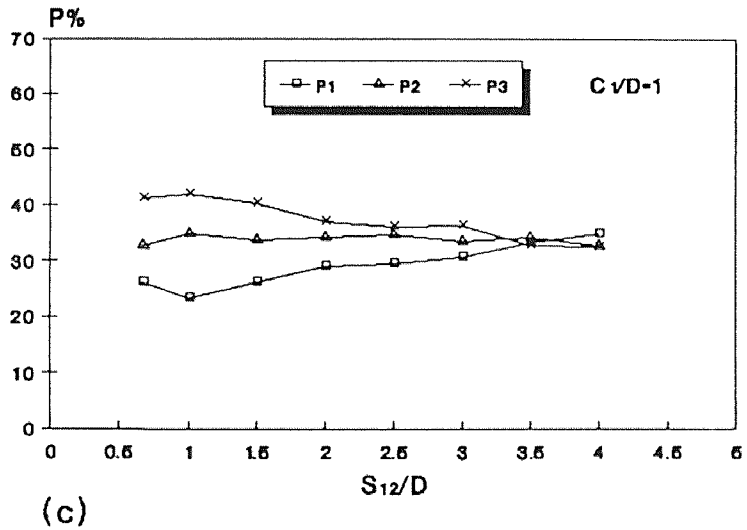

DT+DT+DT
D/T=0.264
H/T=2
S 13/D=5

Figure 34 Effect of S on PI

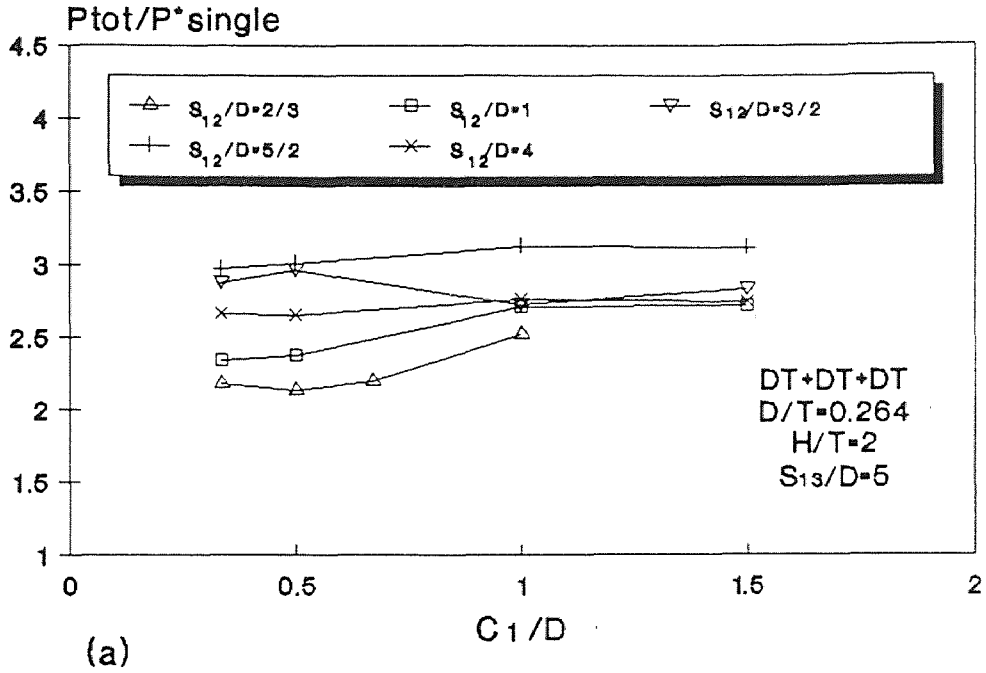

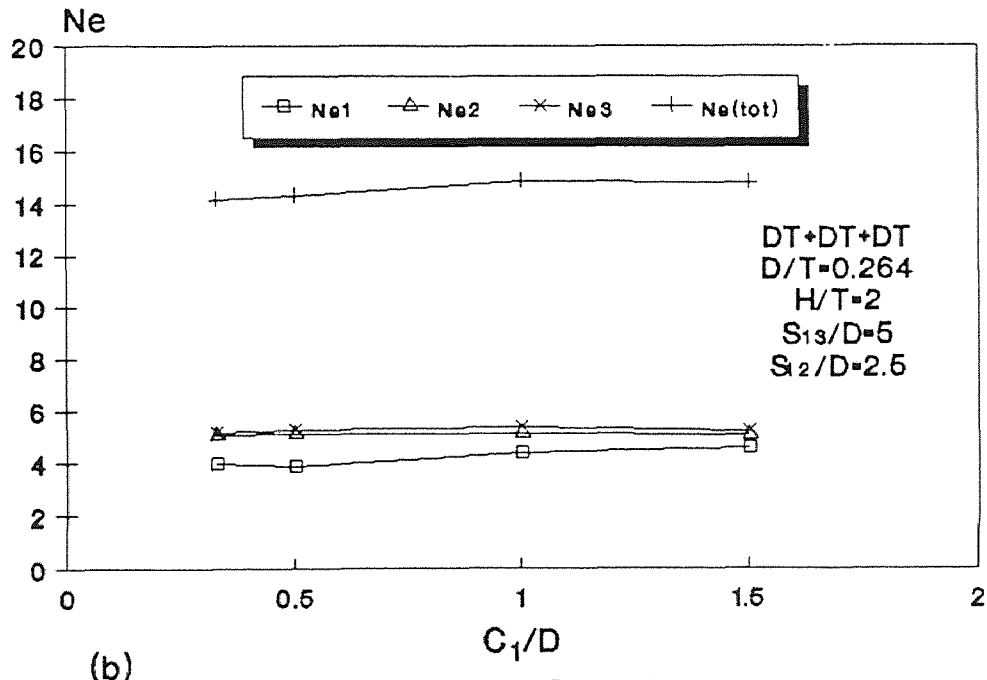

Figure 35 Effect of C_1 on Ptot and Ne

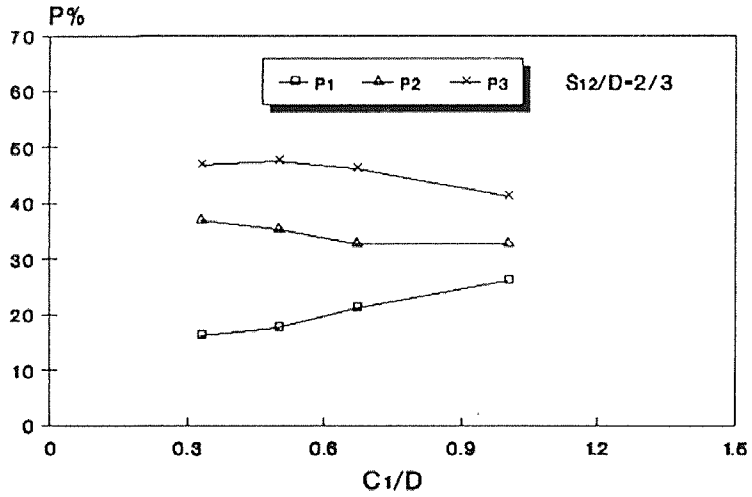

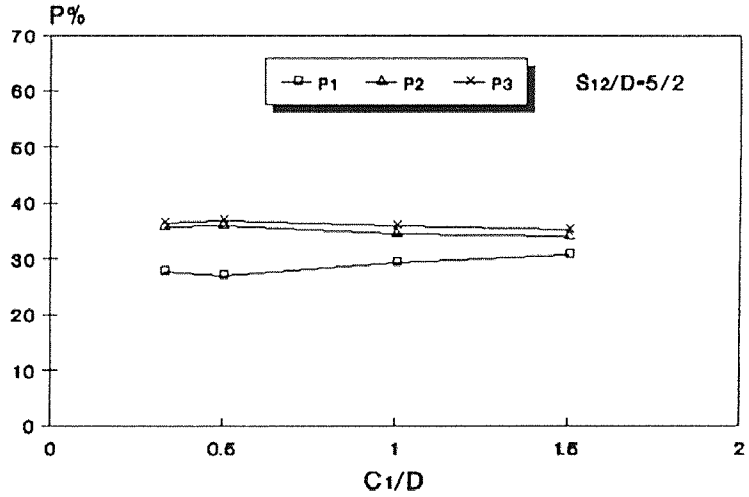

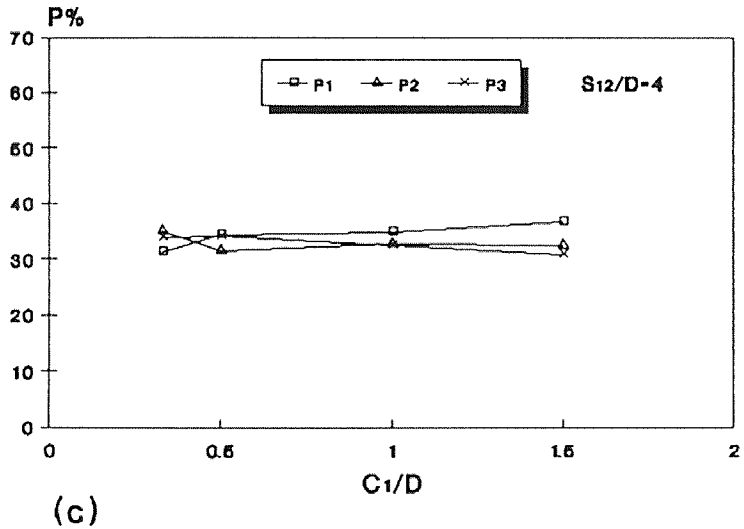

DT+DT+DT
D/T=0.264
H/T=2
$S_{13}/D=5$

Figure 36 Effect of C_1 on PI

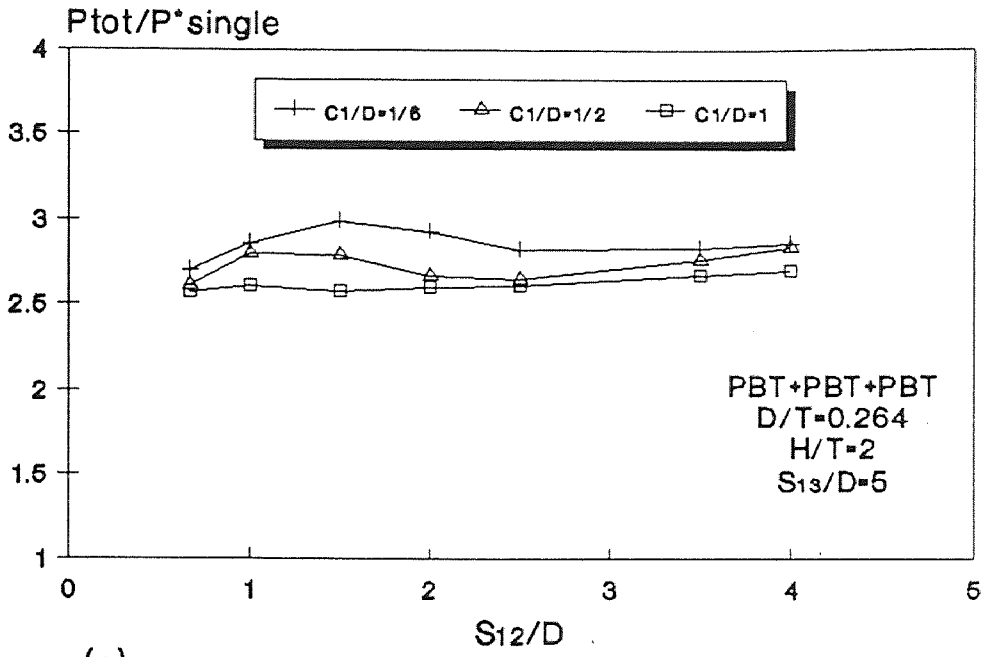

(a)

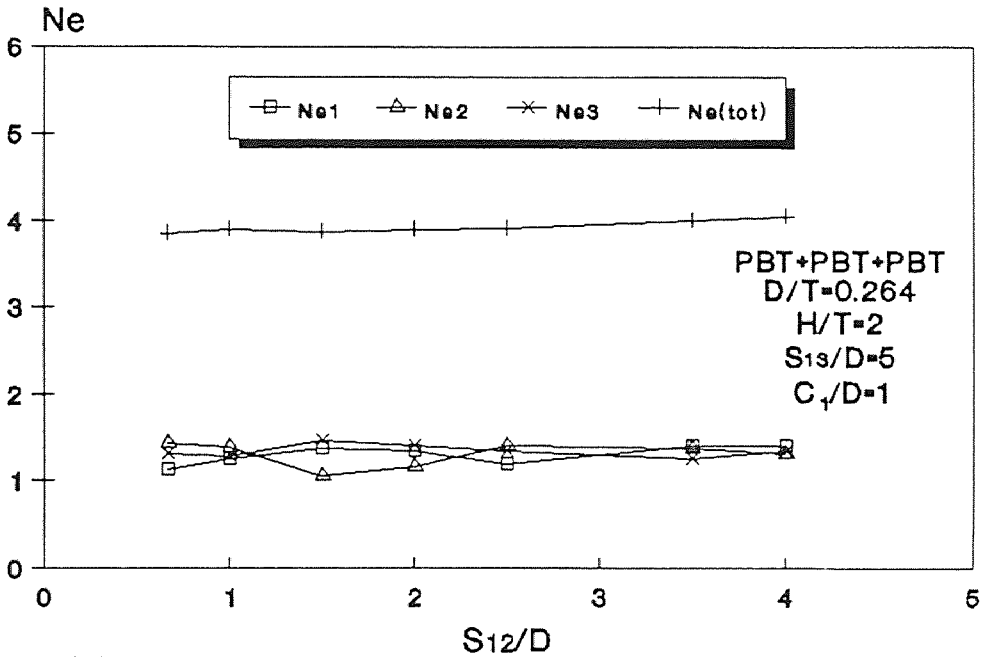

(b)

Figure 37 Effect of S on Ptot and Ne

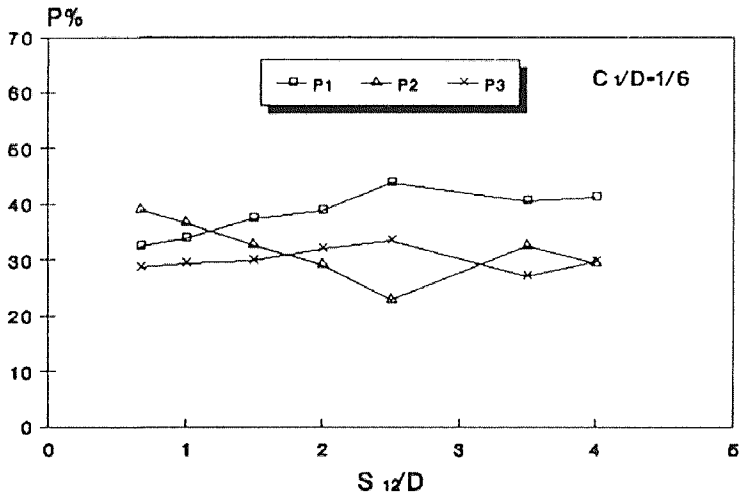

(a)

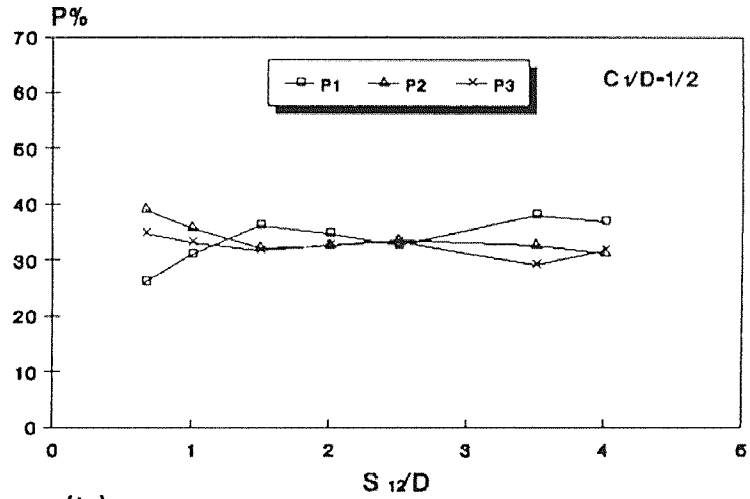

(b)

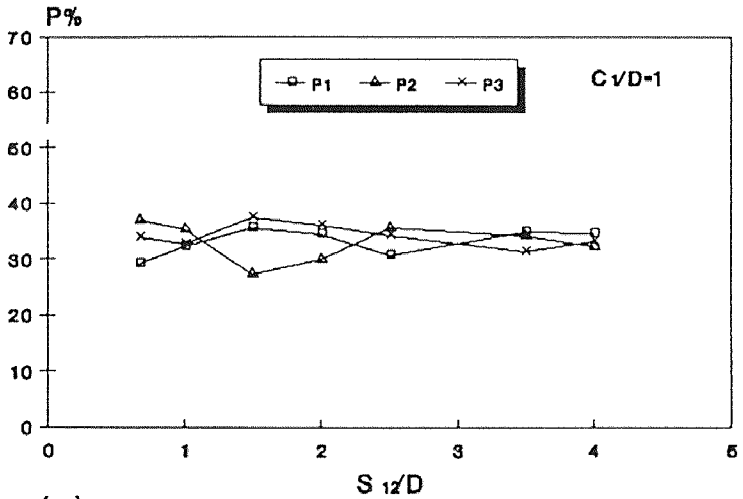

(c)

PBT+PBT+PBT
D/T=0.264
H/T=2
$S_{13}/D=5$

Figure 38 Effect of S on PI

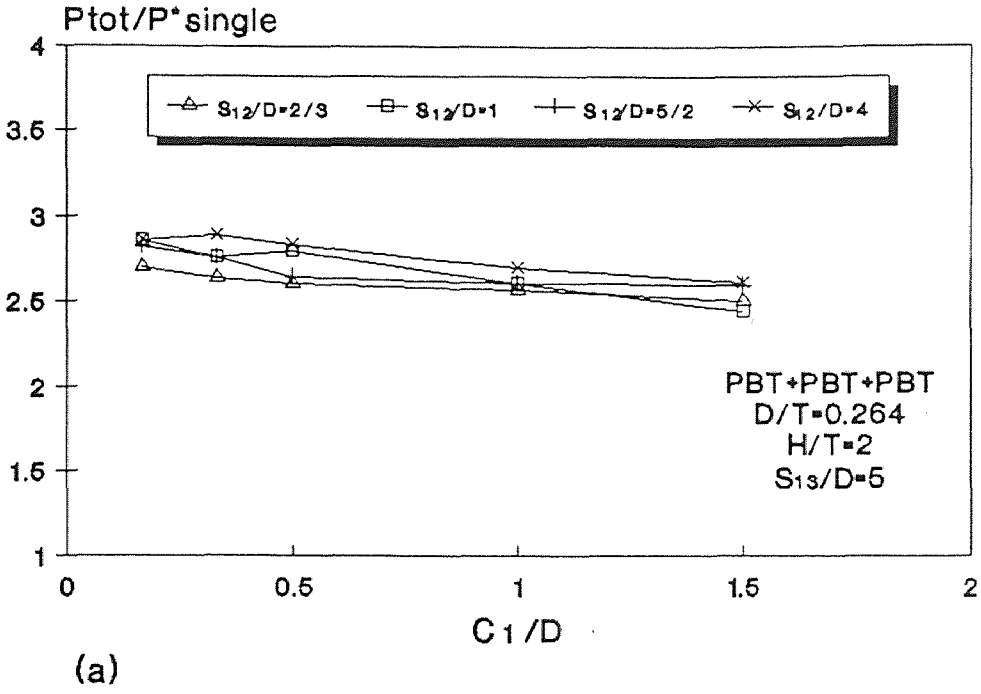

(a)

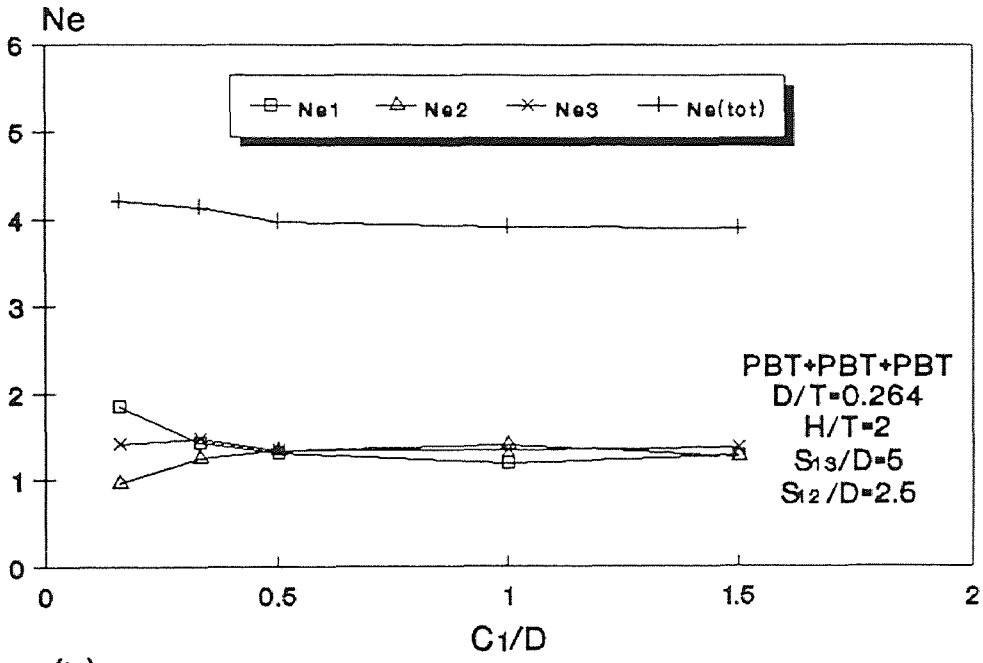

(b)

Figure 39 Effect of C_1 on Ptot and Ne

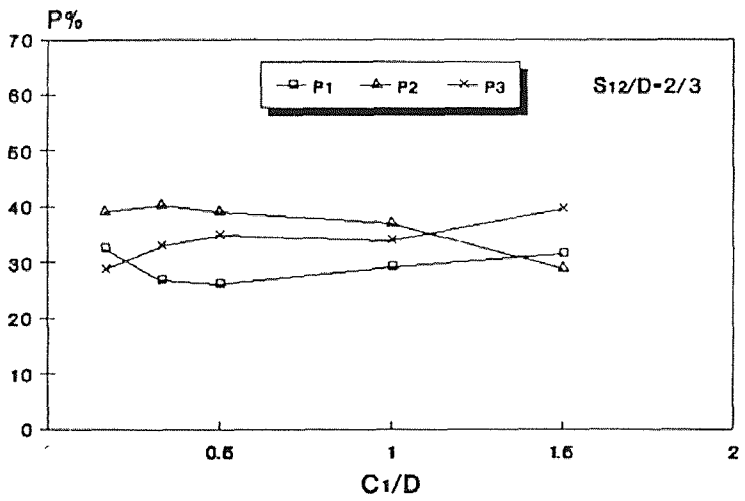

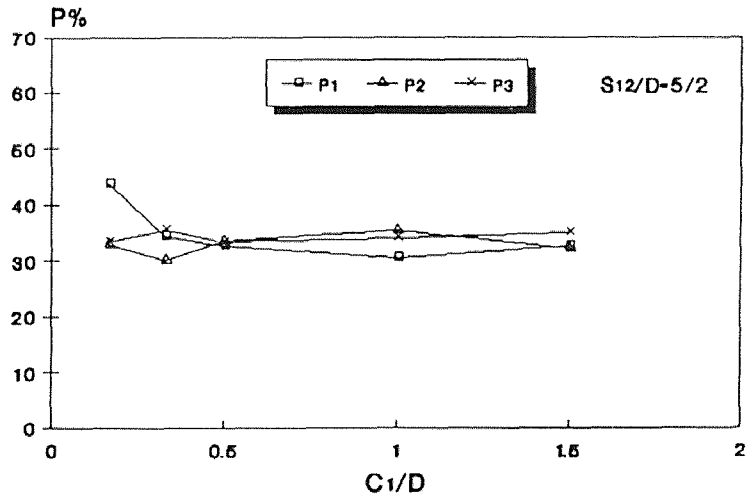

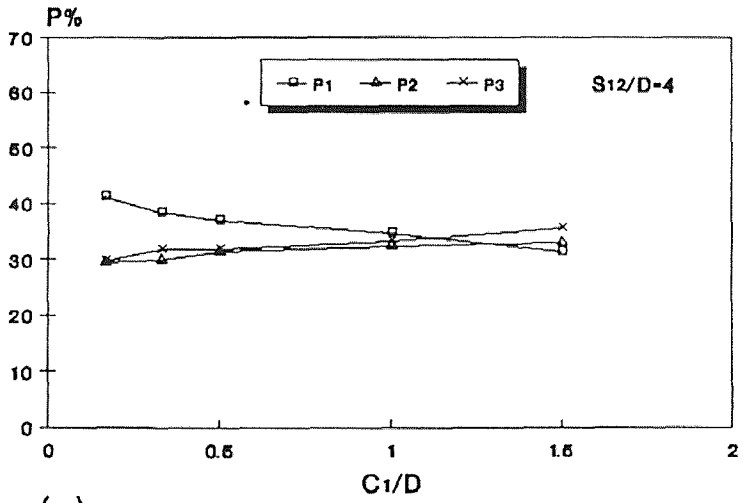

PBT+PBT+PBT
D/T=0.264
H/T=2
$S_{13}/D=5$

Figure 40 Effect of C_1 on PI

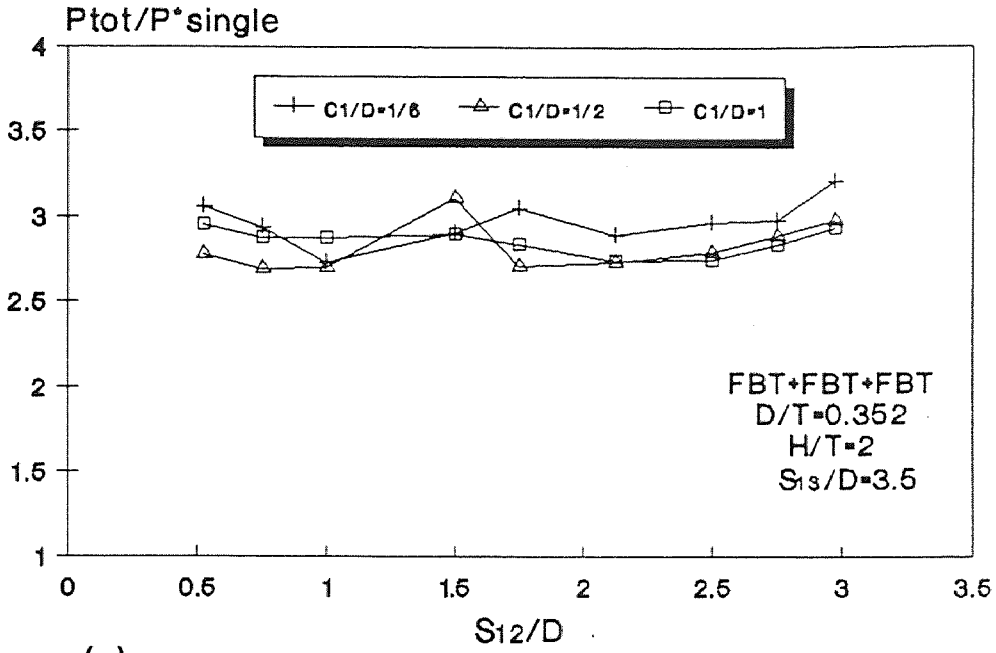

(a)

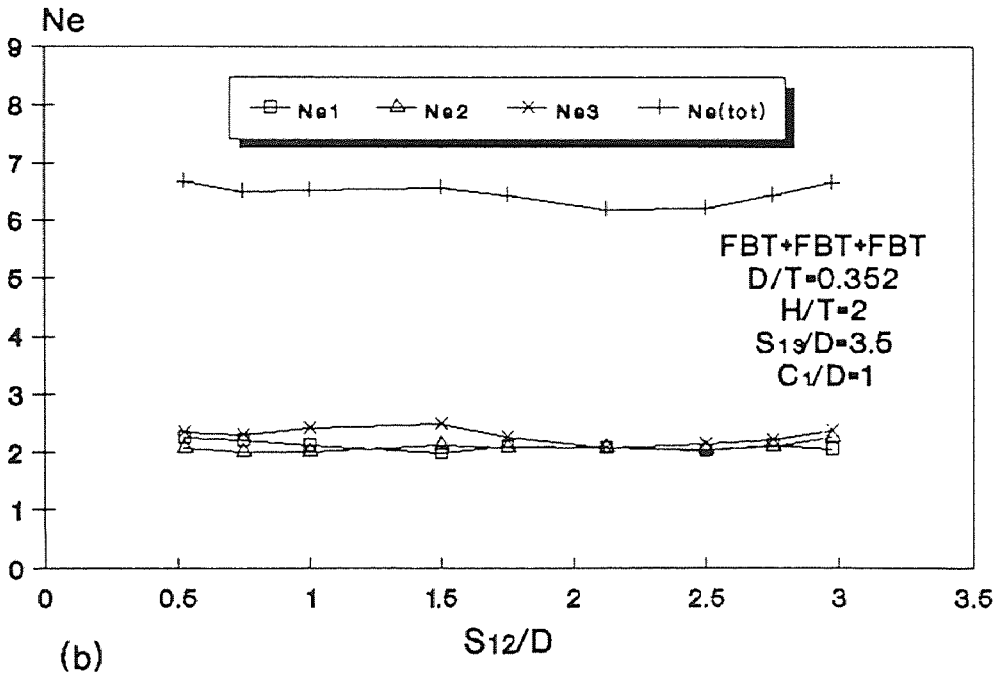

(b)

Figure 41 Effect of S on Ptot and Ne

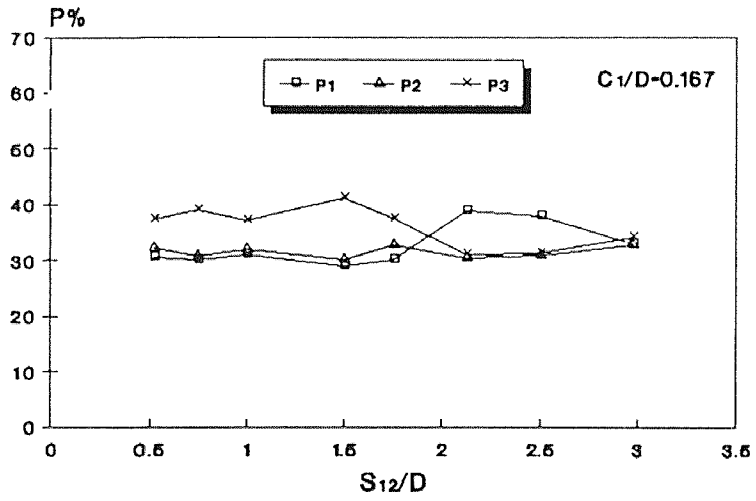

(a)

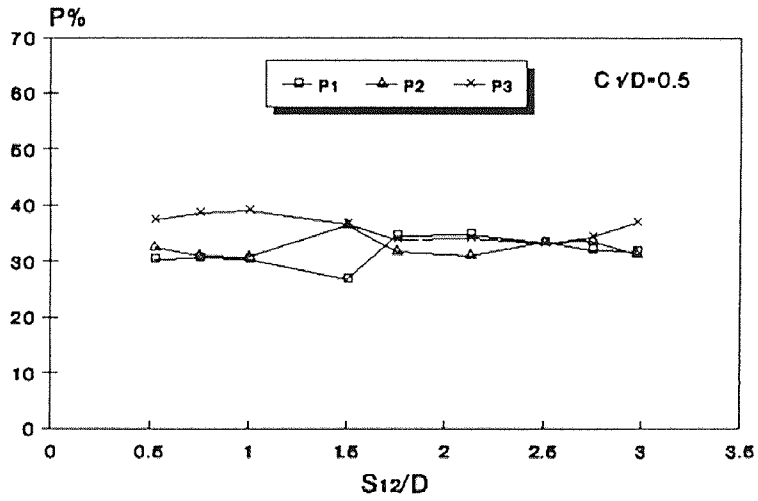

(b)

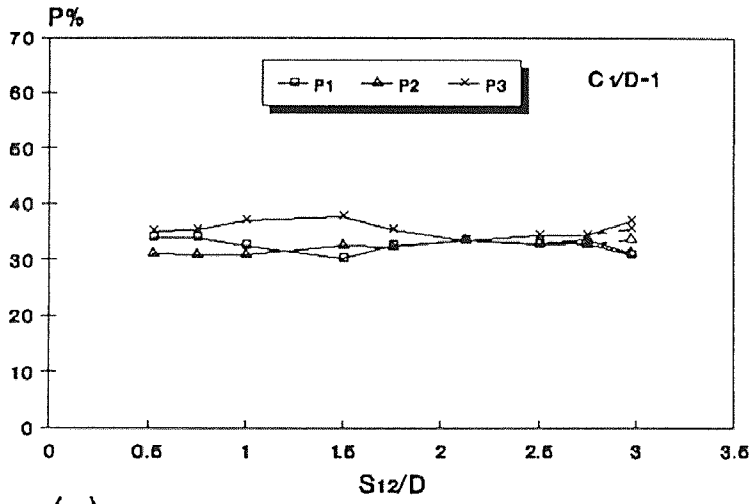

(c)

FBT+FBT+FBT
D/T=0.352
H/T=2
S_{13} /D=3.5

Figure 42 Effect of S on PI

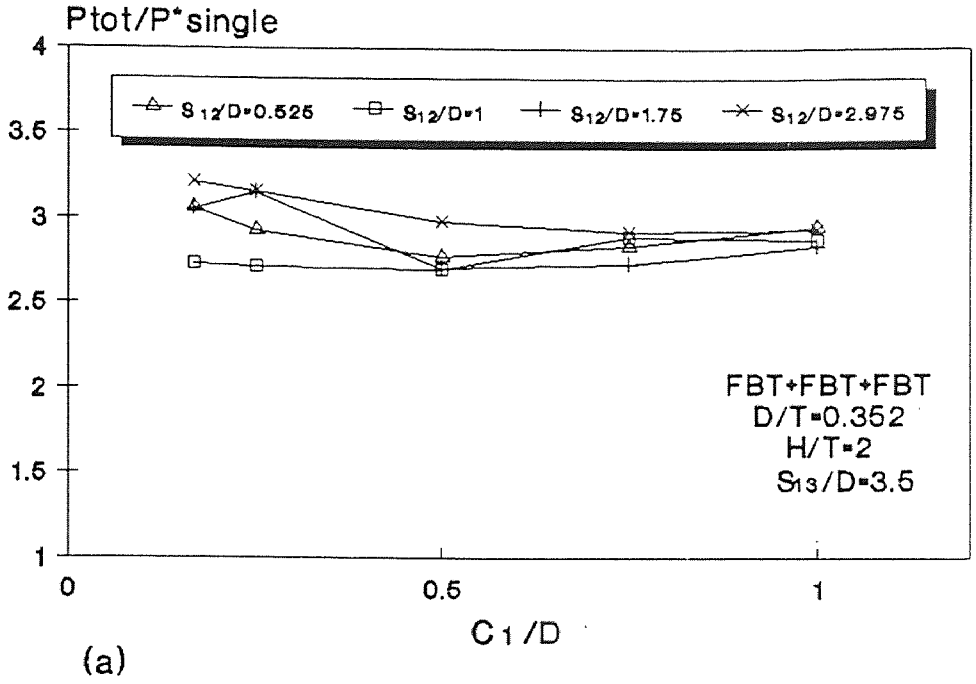

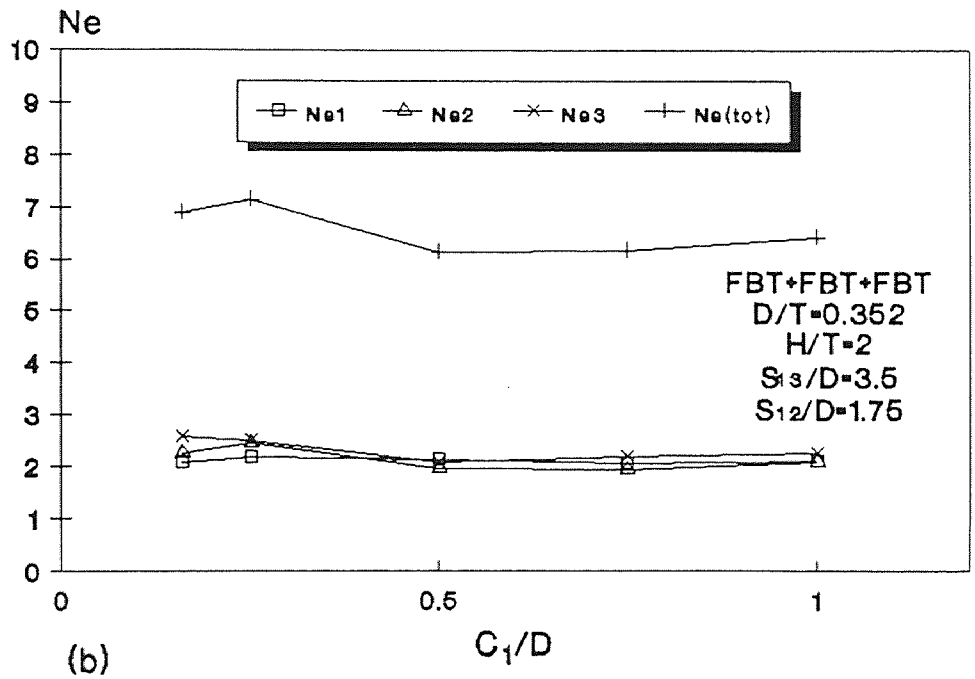

Figure 43 Effect of C_1 on Ptot and Ne

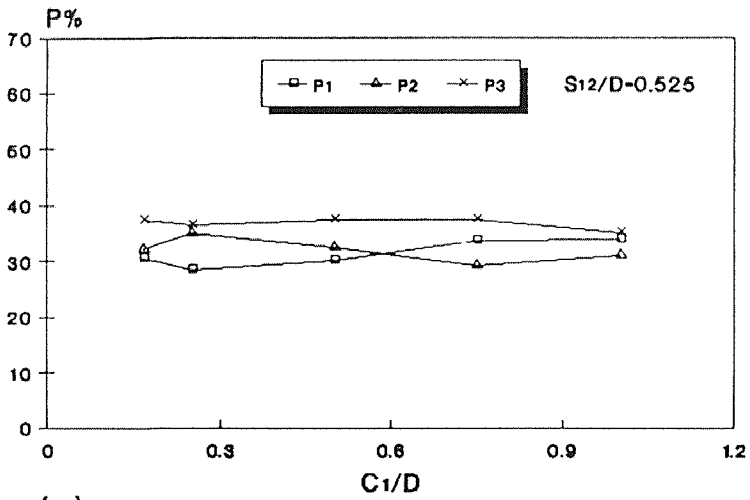

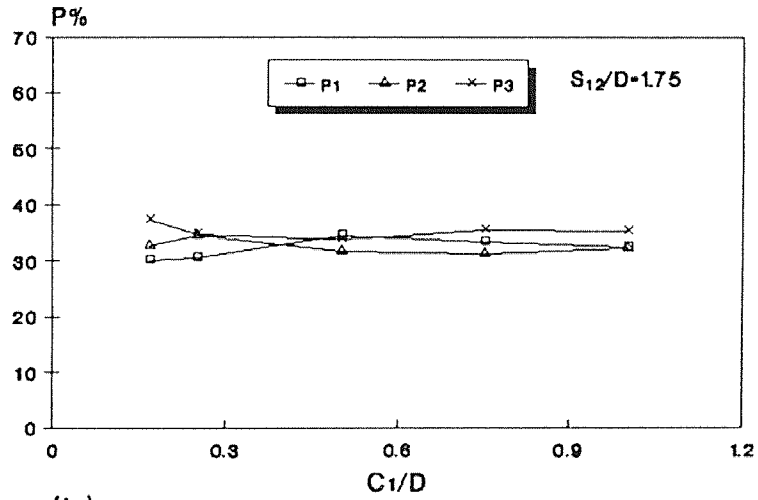

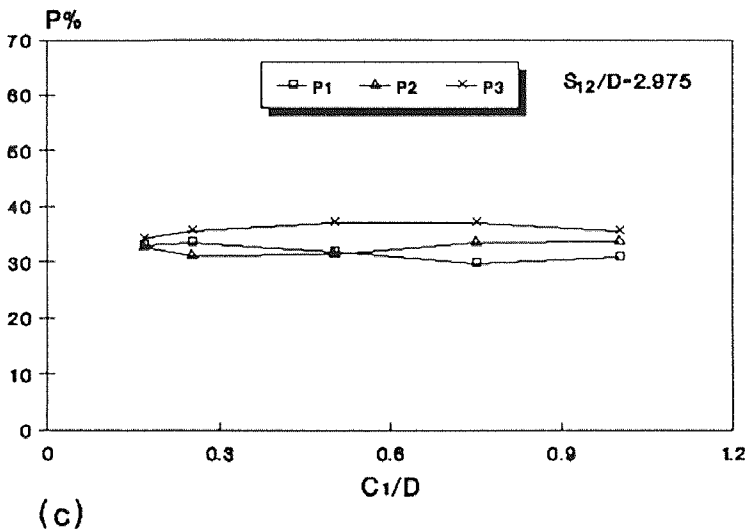

FBT+FBT+FBT
D/T=0.352
H/T=2
S_{13} /D=3.5

Figure 44 Effect of C_1 on PI

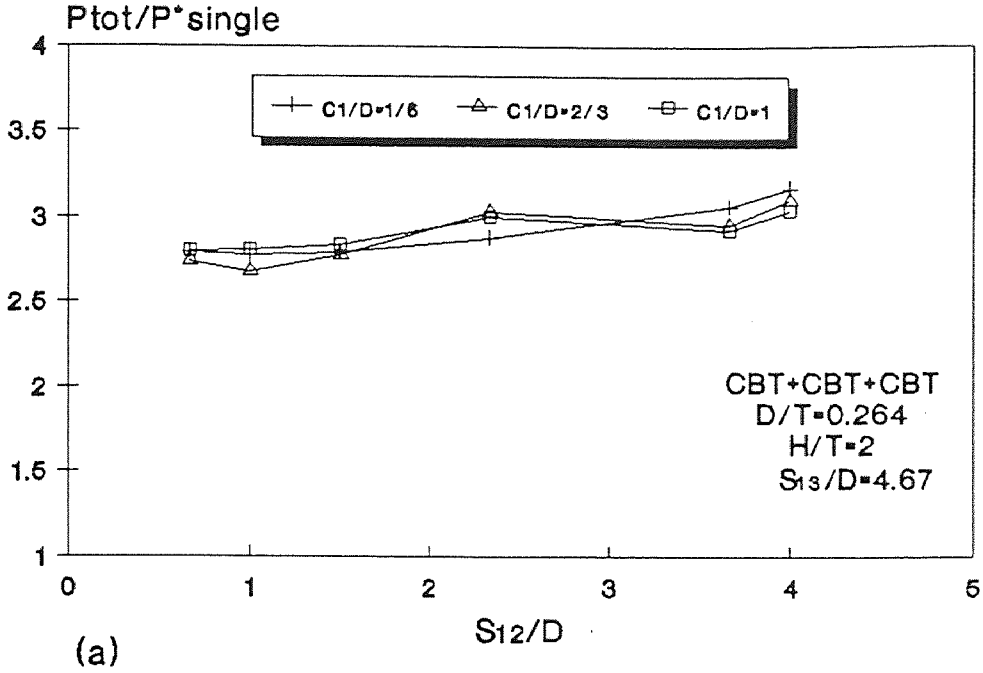

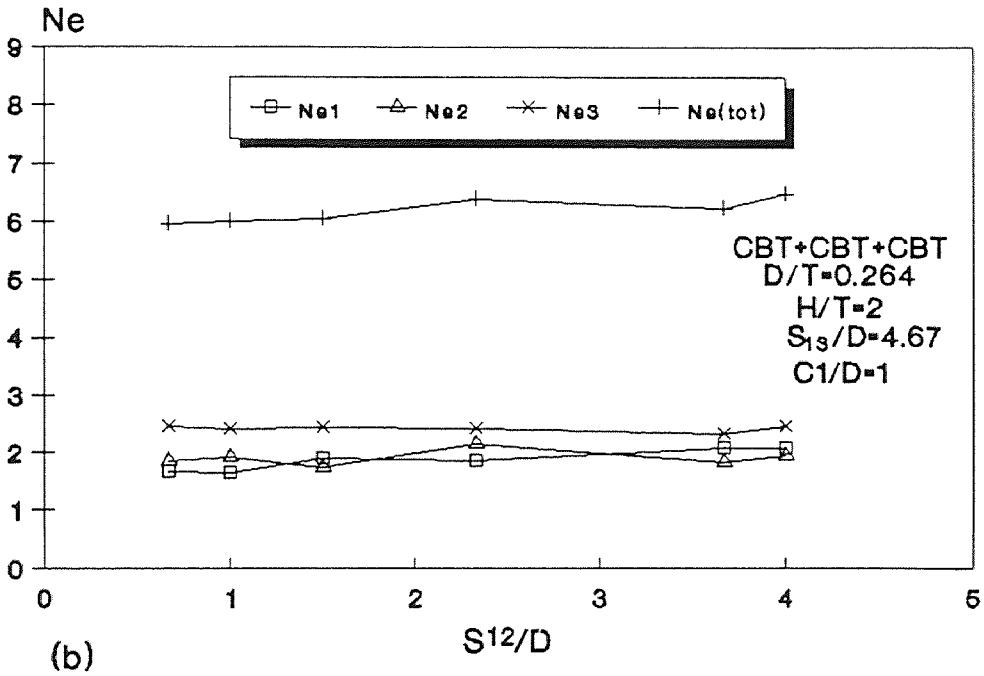

Figure 45 Effect of S on Ptot and Ne

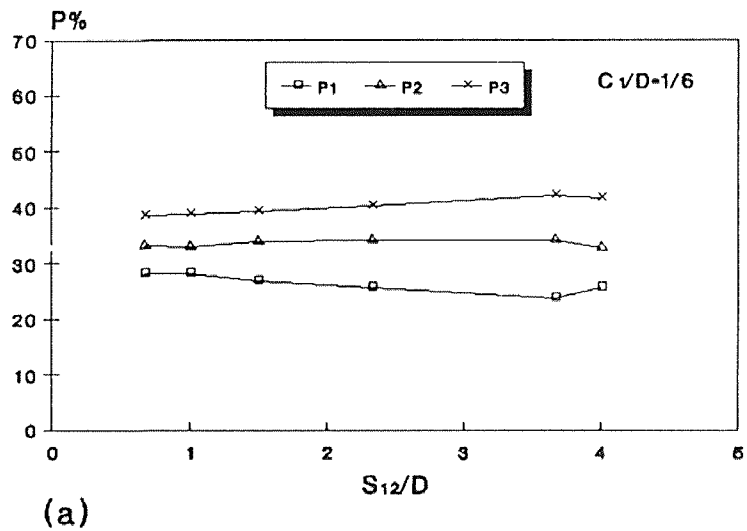

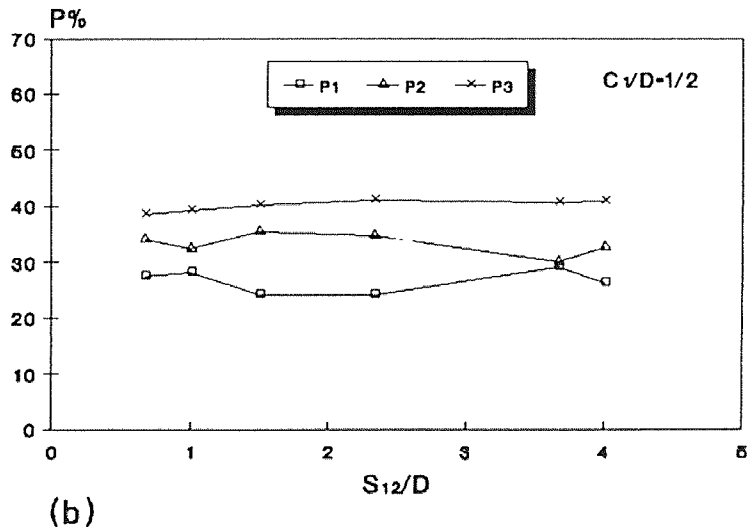

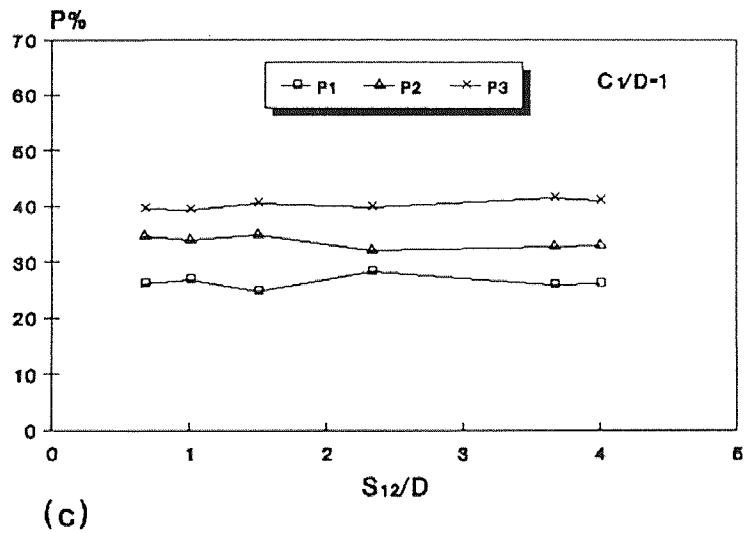

CBT+CBT+CBT
D/T=0.264
H/T=2
S_{13} /D=4.67

Figure 46 Effect of S on PI

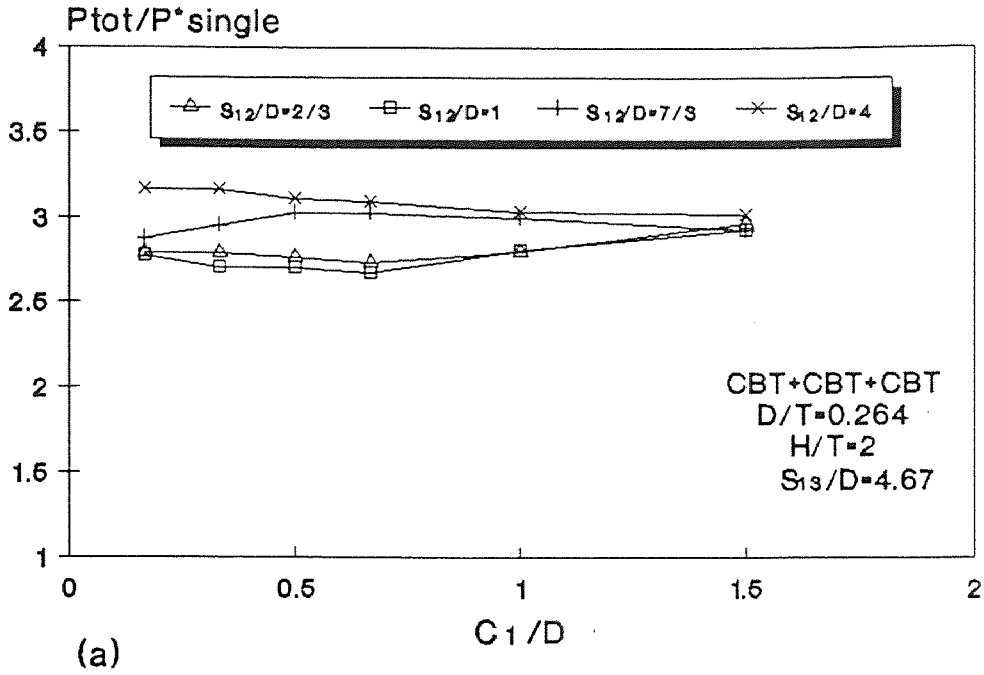

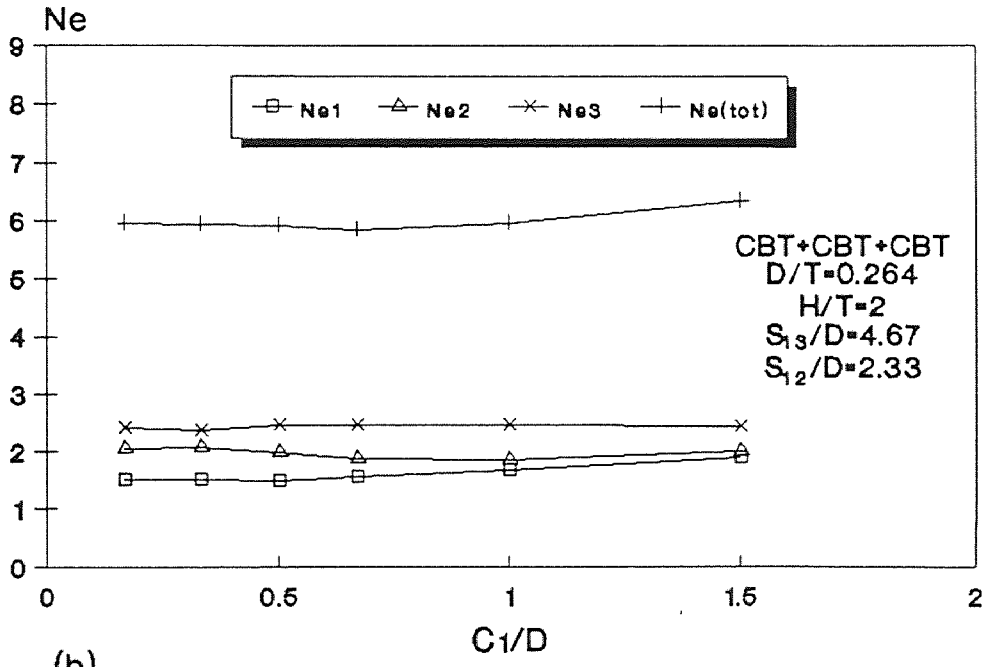

Figure 47 Effect of C_1 on Ptot and Ne

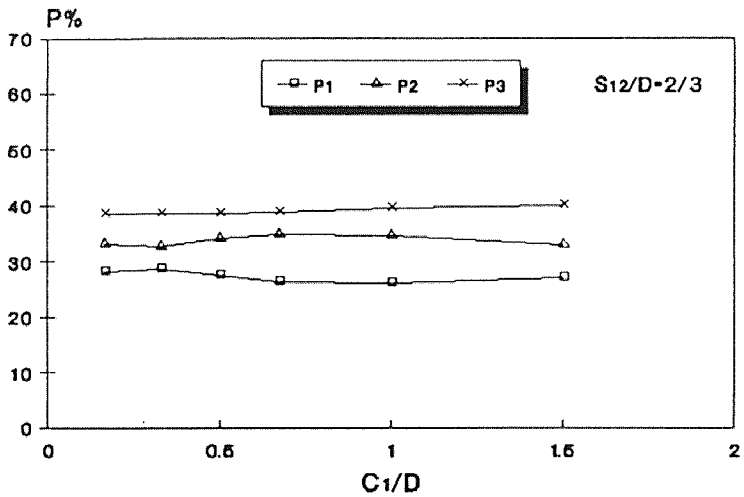

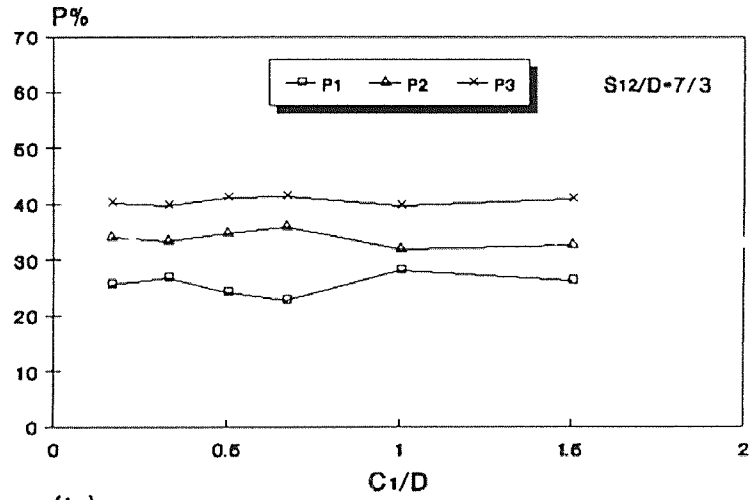

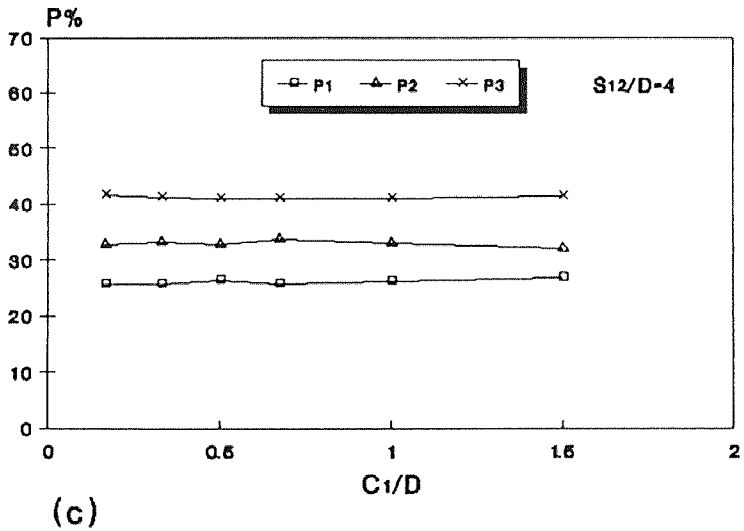

CBT+CBT+CBT
D/T=0.264
H/T=2
S_{13} /D=4.67

Figure 48 Effect of C_1 on PI

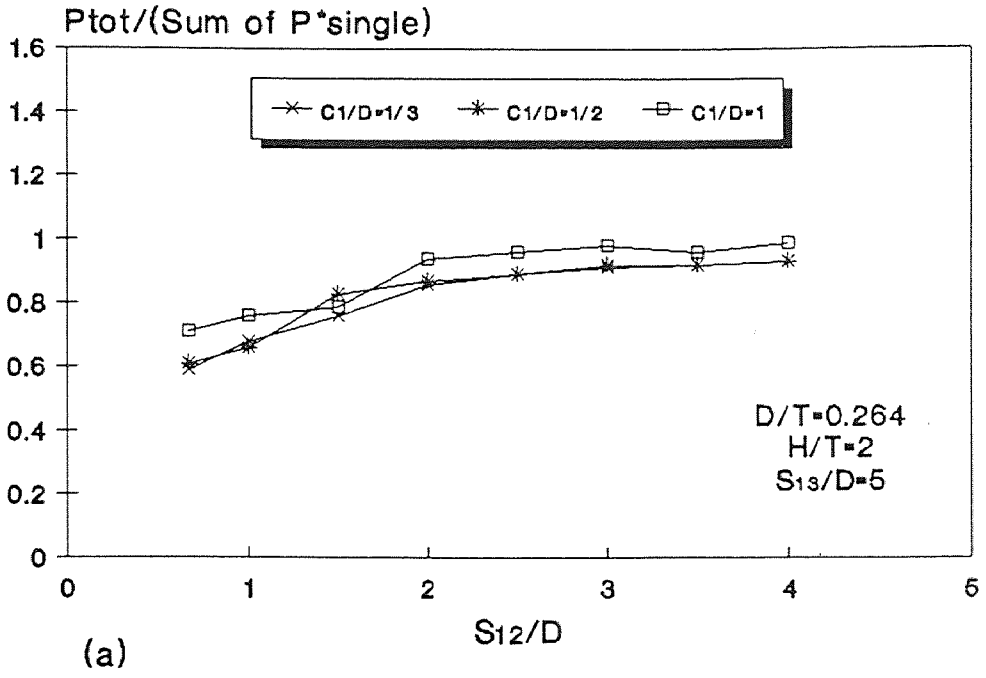

PBT(top)+DT(middle)+DT(bottom)

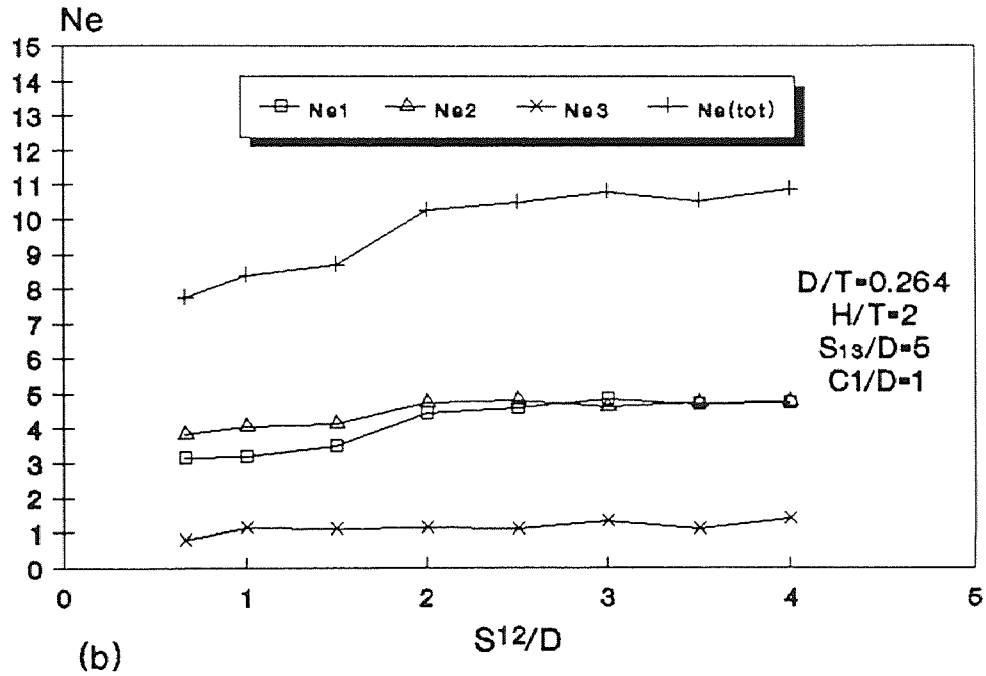

Figure 49 Effect of S on Ptot and Ne

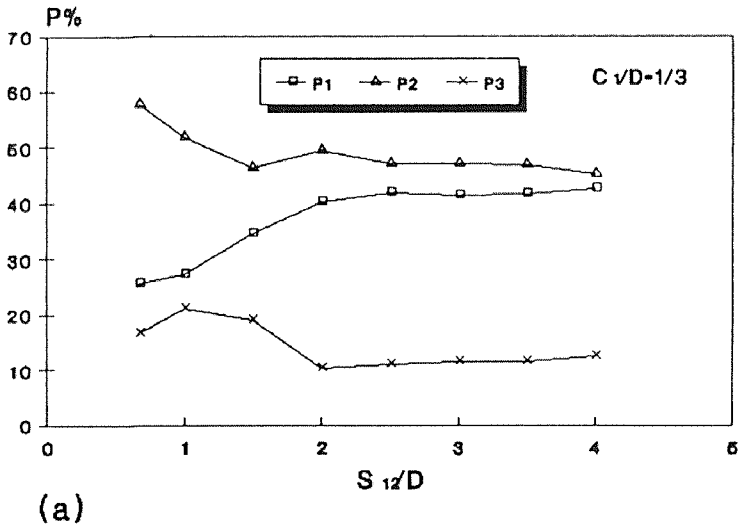

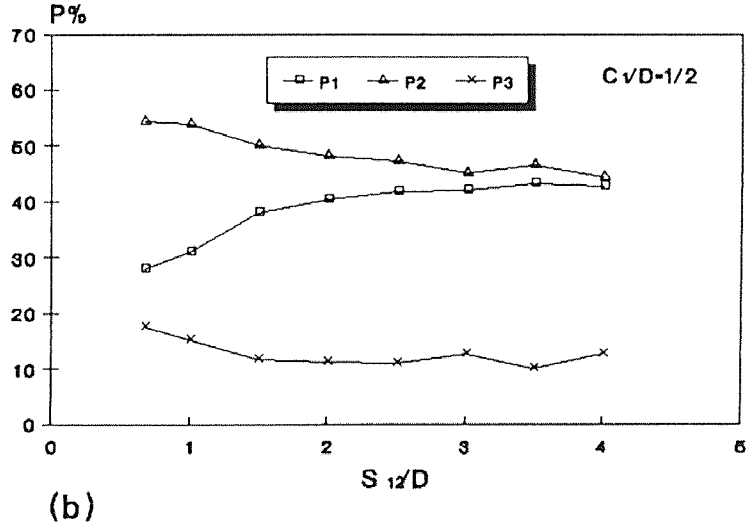

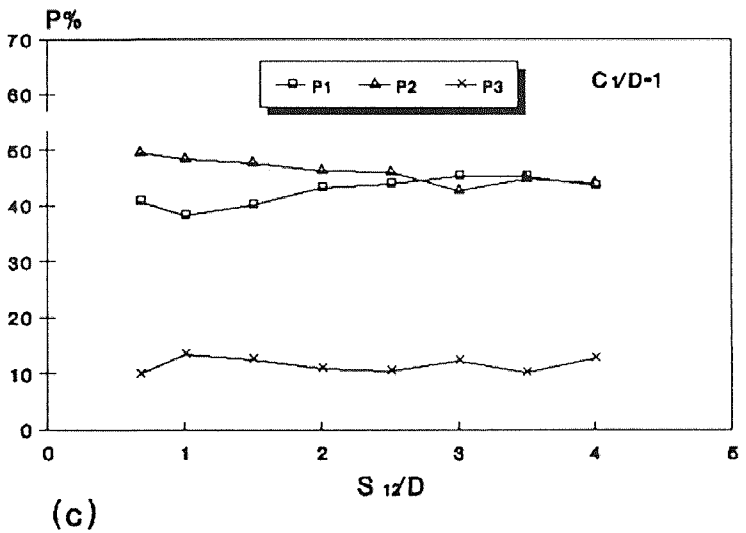

PBT(top)+DT(middle)+DT(bottom)
D/T=0.264
H/T=2
$S_{13}/D=5$

Figure 50 Effect of S on PI

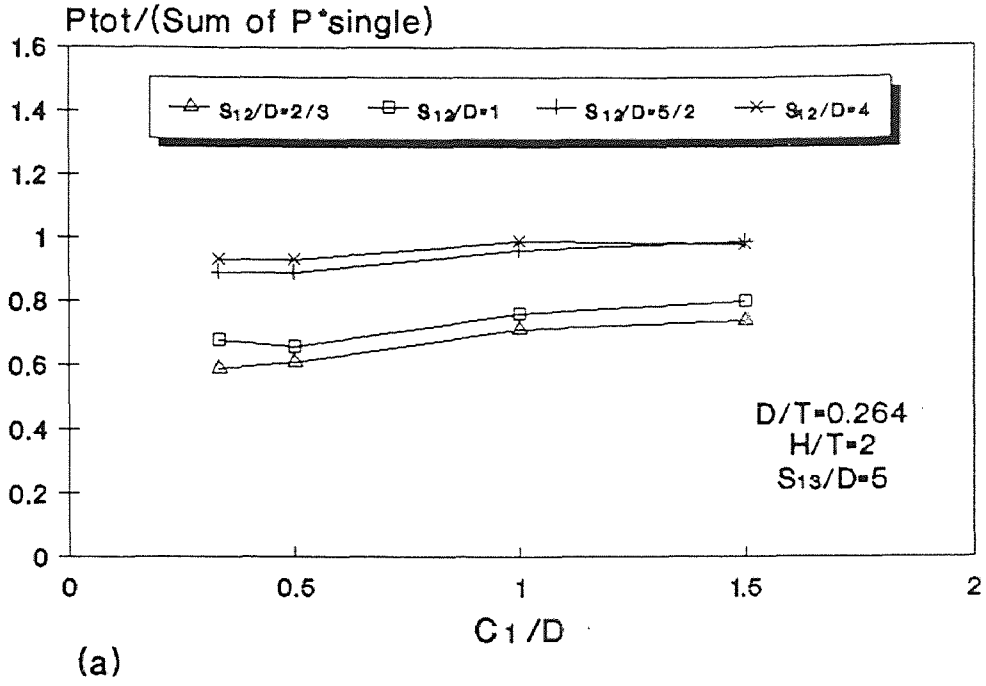

PBT(top)+DT(middle)+DT(bottom)

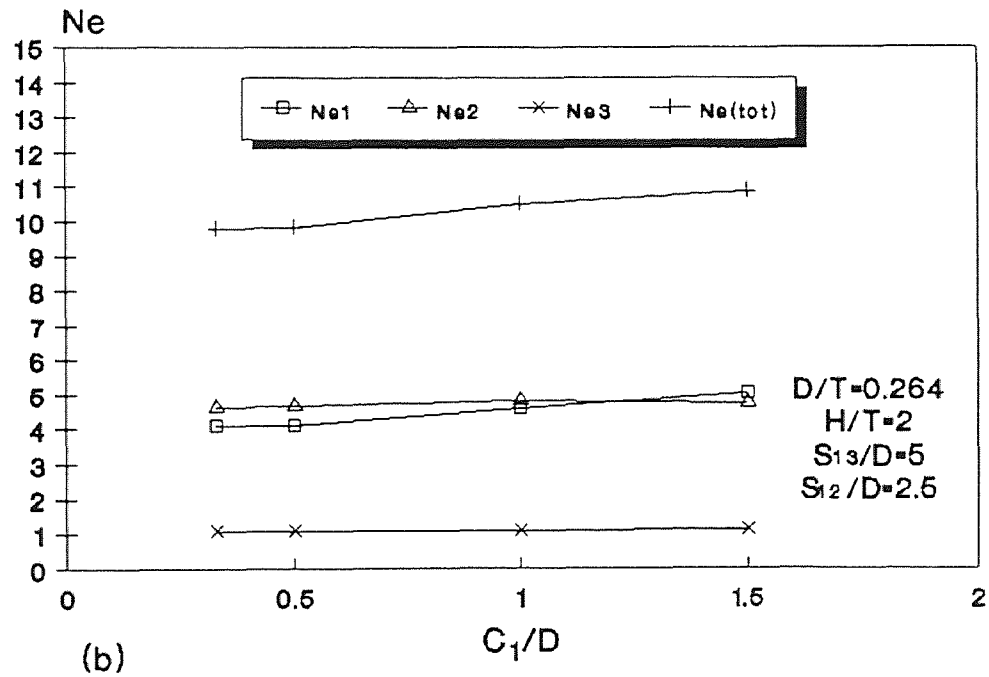

Figure 51 Effect of C_1 on Ptot and Ne

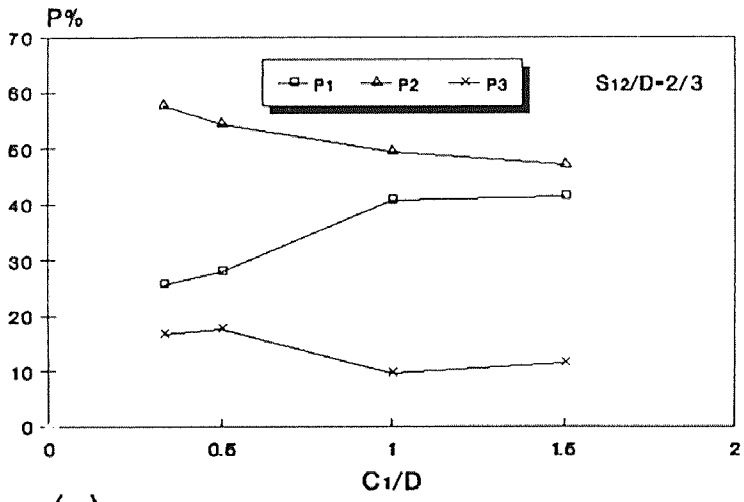

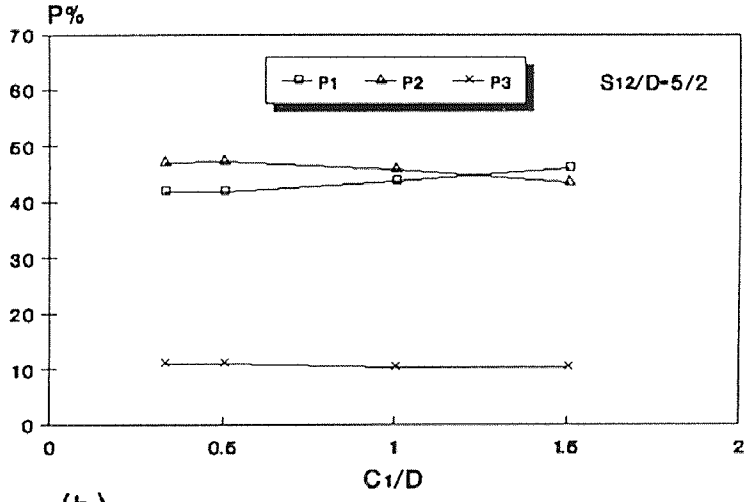

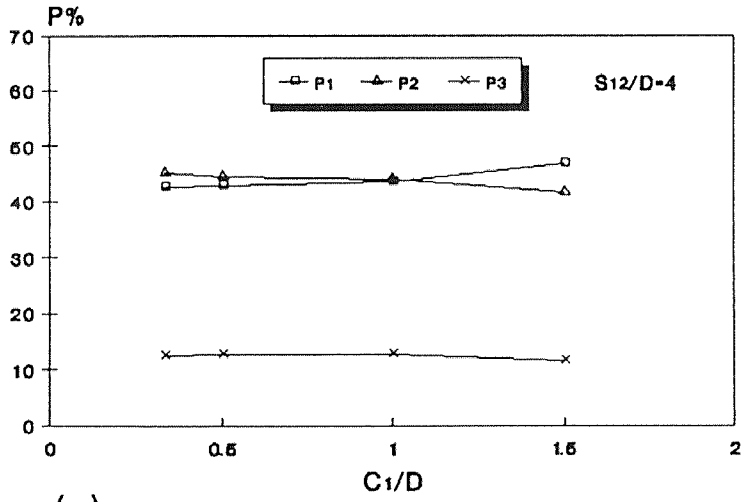

PBT(top)+DT(middle)+DT(bottom)
D/T=0.264
H/T=2
$S_{13}/D=5$

Figure 52 Effect of C_1 on PI

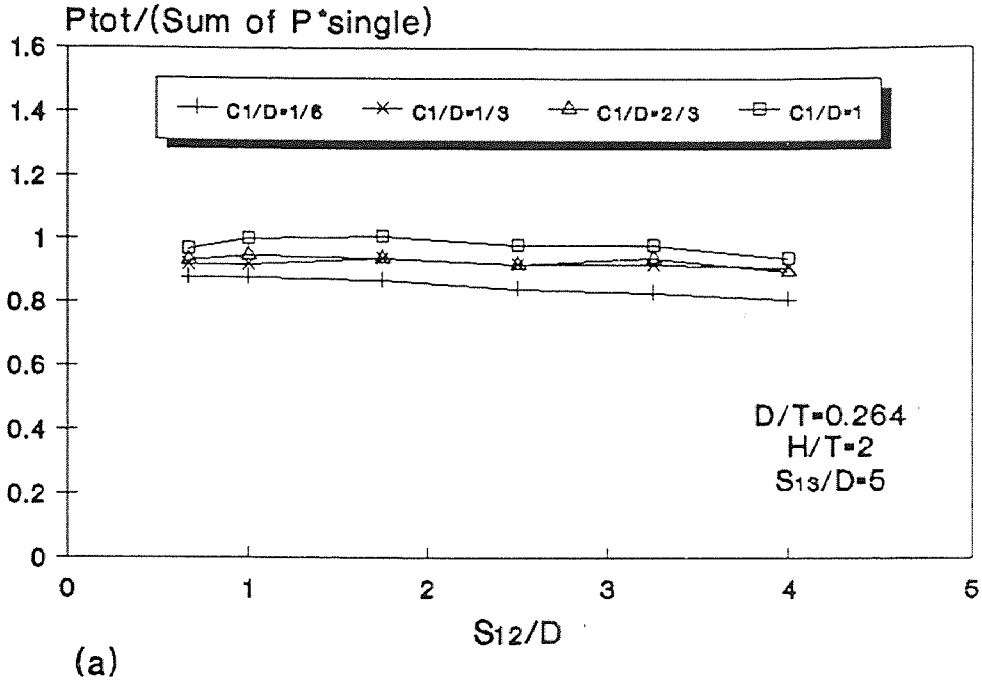

DT(top)+PBT(middle)+DT(bottom)

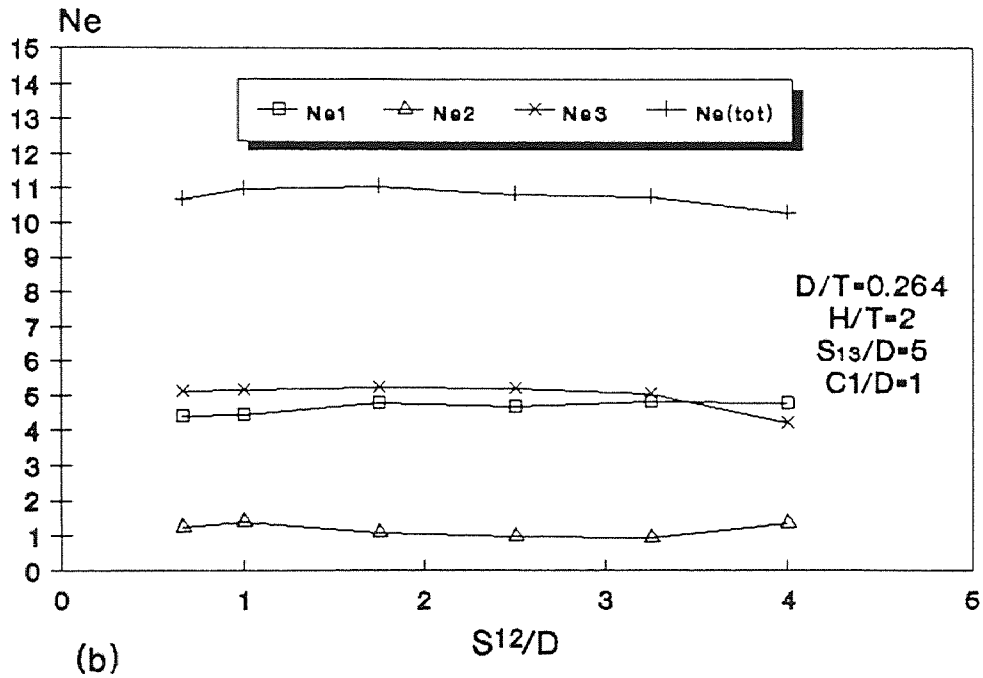

Figure 53 Effect of S on Ptot and Ne

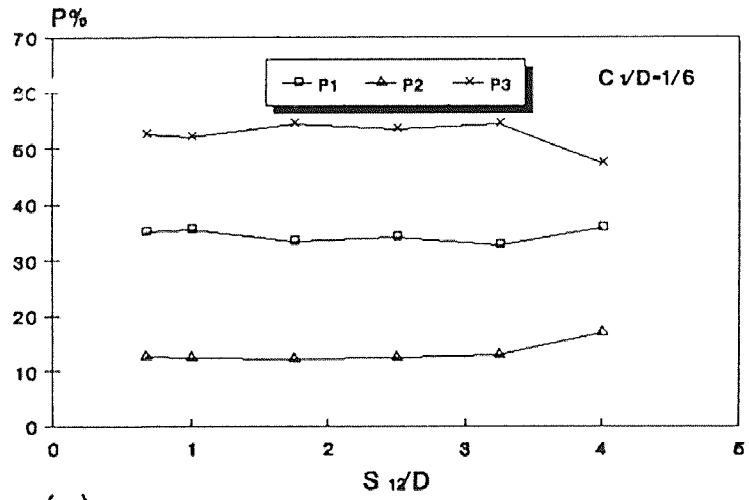

(a)

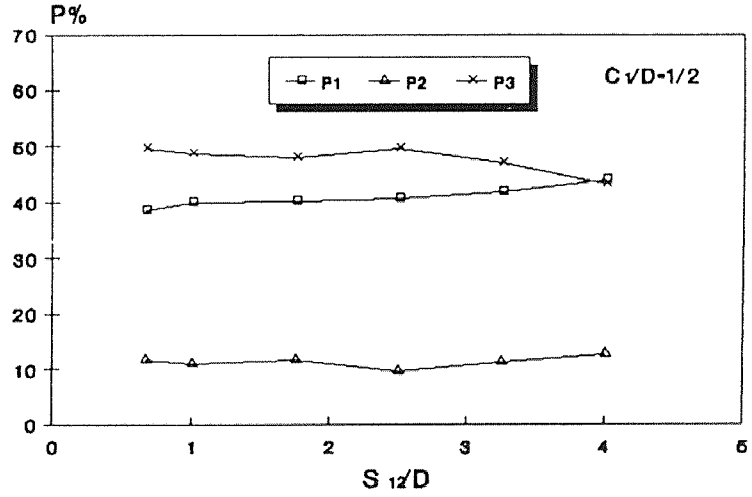

(b)

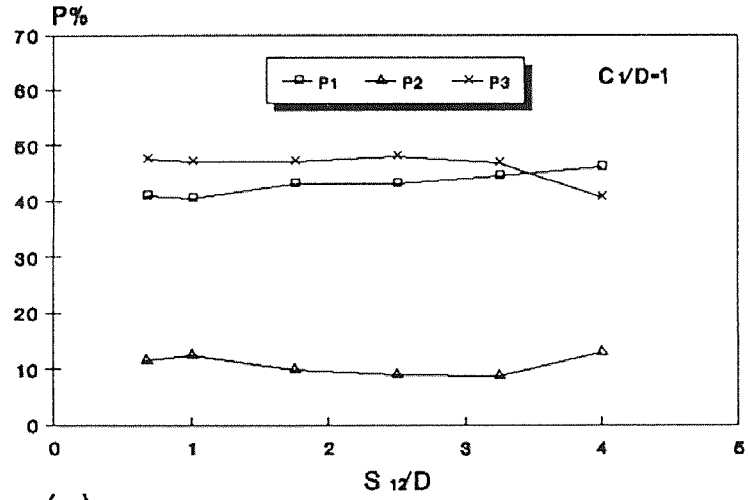

(c)

DT(top)+PBT(middle)+DT(bottom)
D/T=0.264
H/T=2
$S_{13}/D=5$

Figure 54 Effect of S on PI

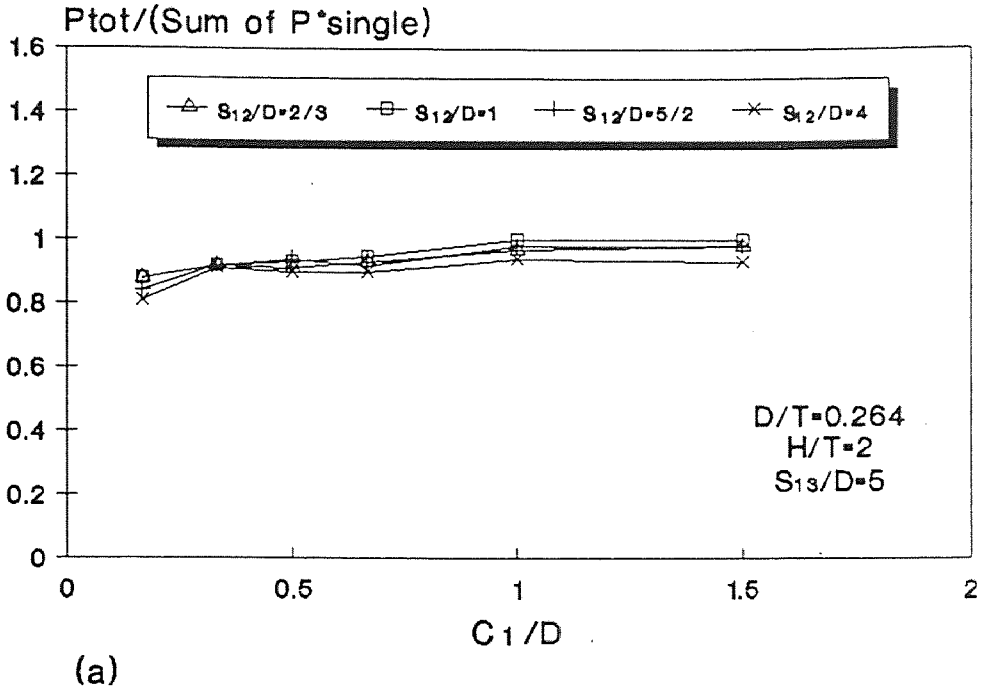

(a)

DT(top)+PBT(middle)+DT(bottom)

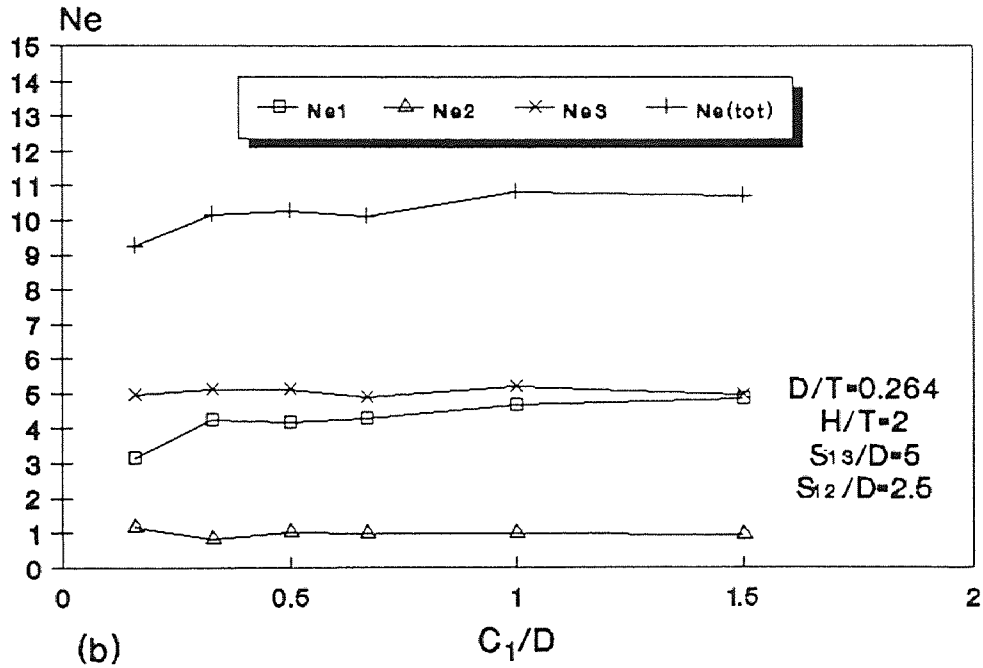

(b)

Figure 55 Effect of C_1 on Ptot and Ne

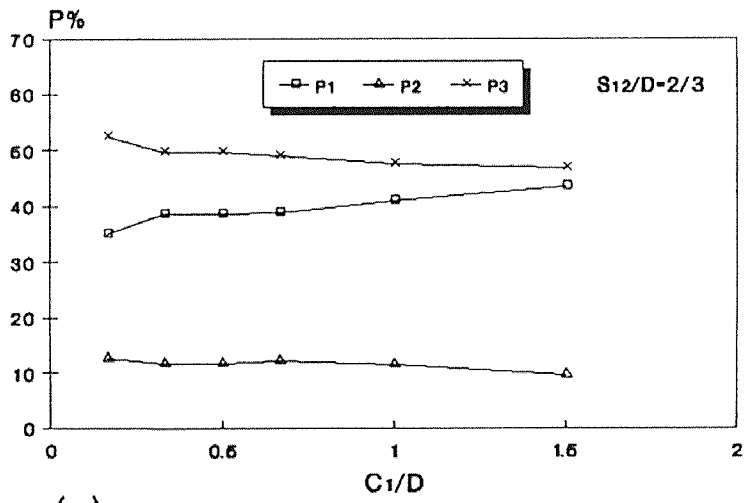

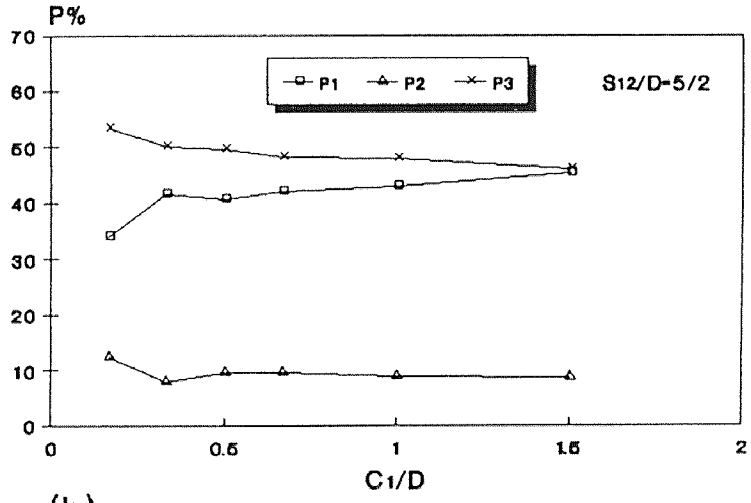

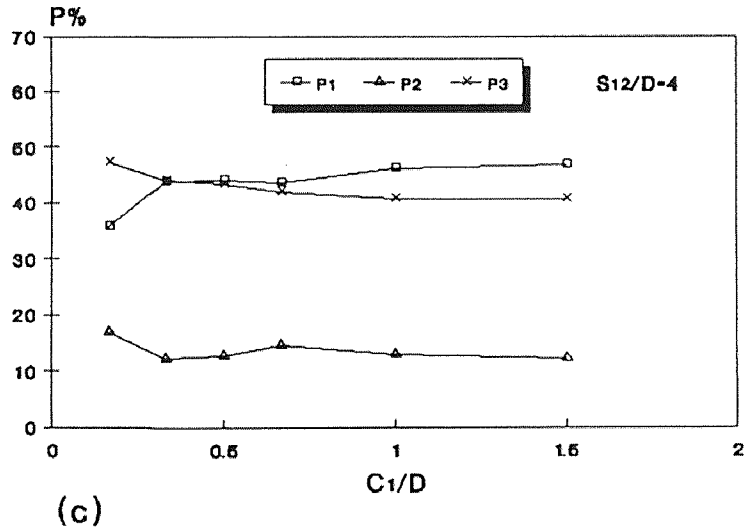

DT(top)+PBT(middle)+DT(bottom)
D/T=0.264
H/T=2
$S_{13}/D=5$

Figure 56 Effect of C_1 on PI

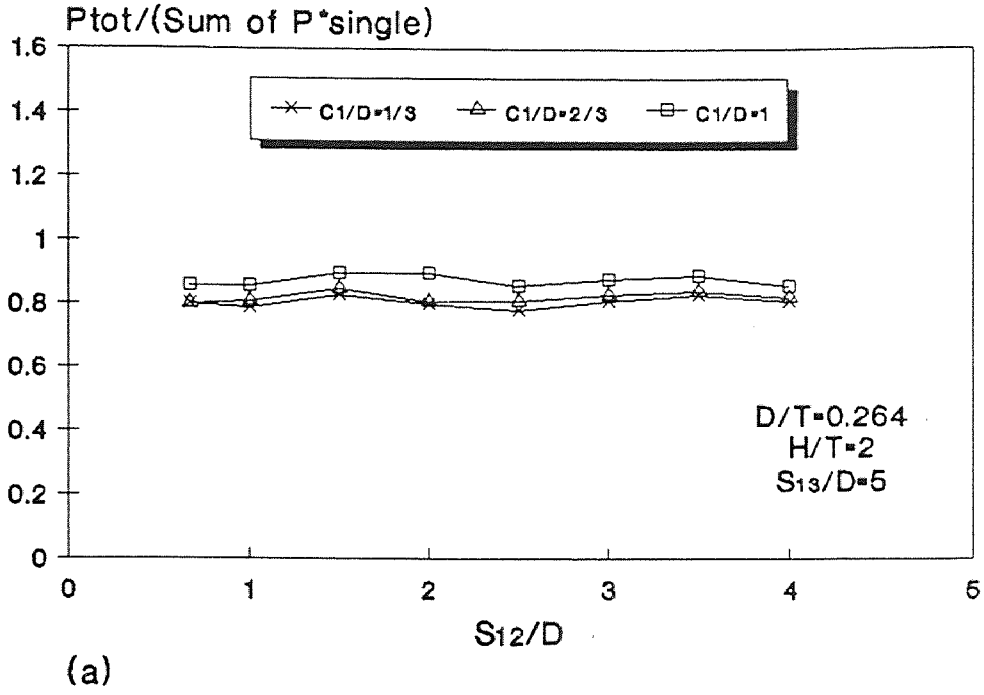

PBT(top)+PBT(middle)+DT(bottom)

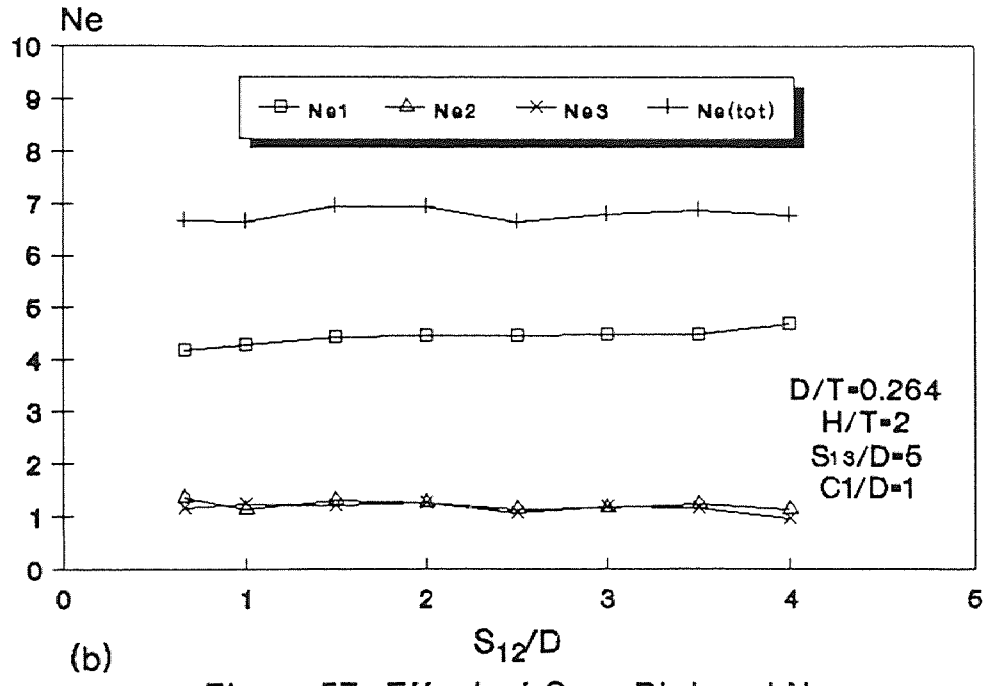

Figure 57 Effect of S on Ptot and Ne

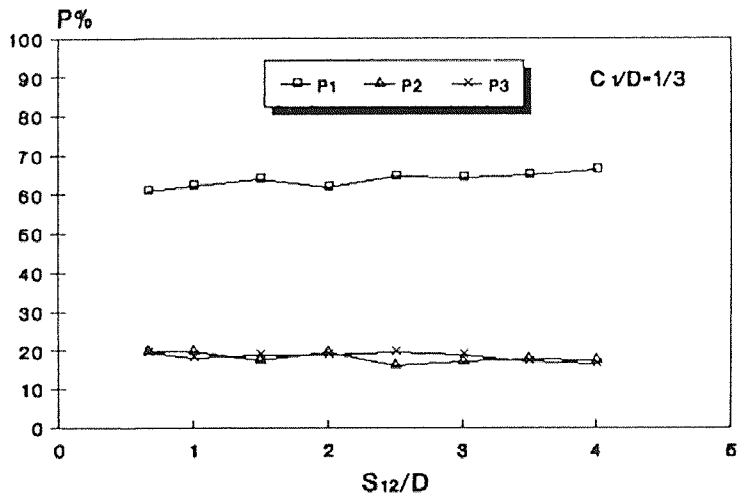

(a)

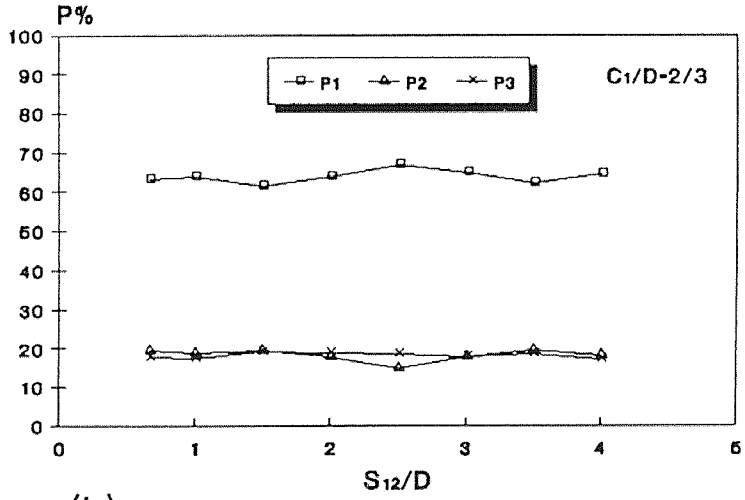

(b)

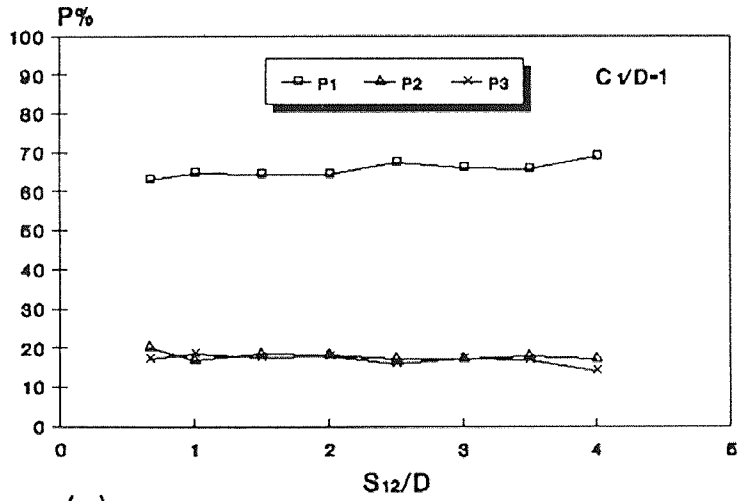

(c)

PBT(top)+PBT(middle)+DT(bottom)
D/T=0.264
H/T=2
$S_{13}/D=5$

Figure 58 Effect of S on PI

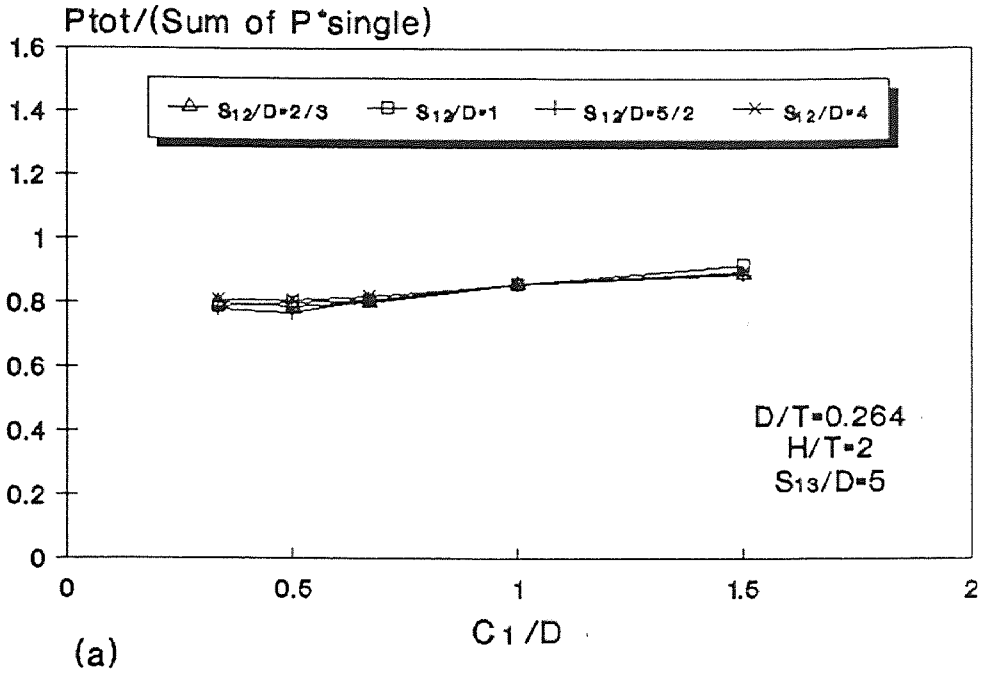

PBT(top)+PBT(middle)+DT(bottom)

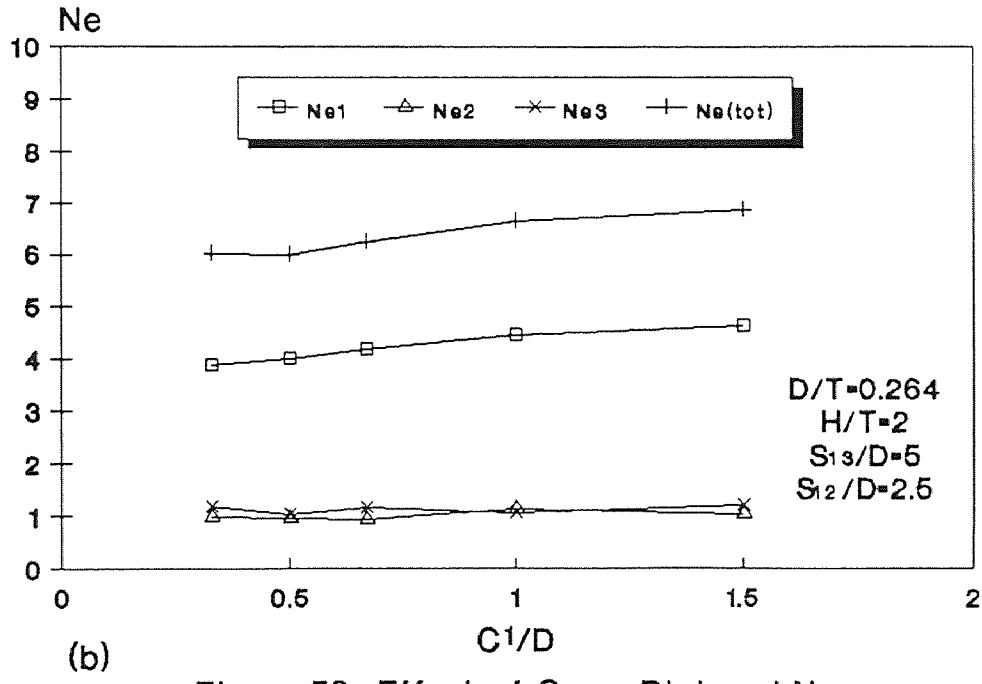

Figure 59 Effect of C on Ptot and Ne

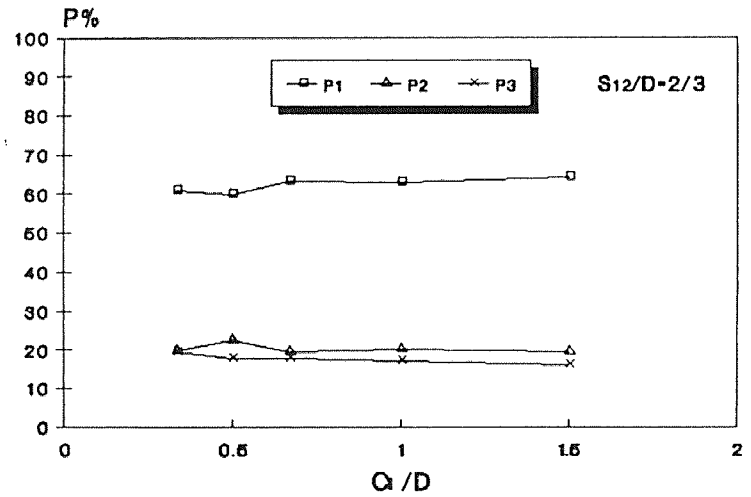

(a)

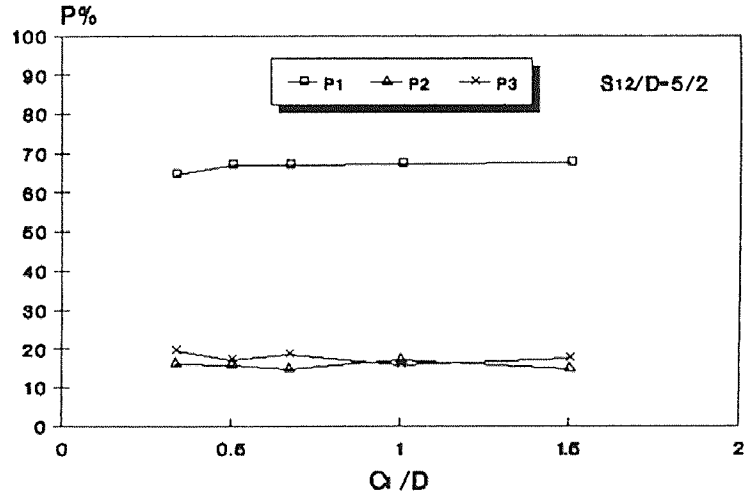

(b)

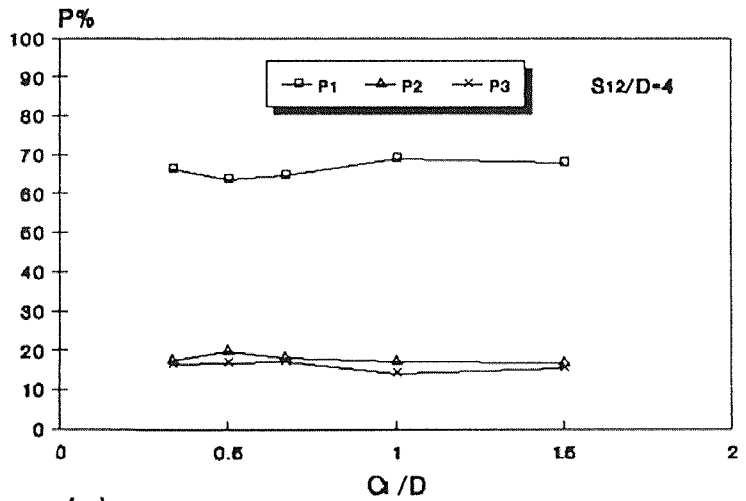

(c)

PBT(top)+PBT(middle)+DT(bottom)
D/T=0.264
H/T=2
$S_{13}/D=5$

Figure 60 Effect of C_1 on PI

APPENDIX B

EXPERIMENTAL DATA FOR MULTIPLE-IMPELLER SYSTEMS

This appendix tabulates the experimental data for the results in both dual- and triple-impeller systems. For the dual-impeller systems, the effects of impeller spacing and off-bottom clearance on power consumption are shown in Table 9 to Table 14. For the triple-impeller systems, these effects are shown in Table 15 to Table 21.

Table 9 Effect of C_1 and S on Power Consumption (Dual-DT Systems)

H/T=1, D/T=0.264

S/D	C_1/D	Ne_1	Ne_2	P_2 / P_1	Ptot/P*single
0.667	0.167	1.18	3.84	3.27	1.02
	0.33	1.41	3.73	2.65	1.05
	0.5	1.77	3.66	2.07	1.11
	0.667	3.02	3.99	1.32	1.43
	1	3.45	3.97	1.15	1.51
	1.33	3.55	3.97	1.12	1.54
	1.67	3.91	3.94	1.01	1.6
	2	3.96	3.88	0.98	1.6
	2.33	4.08	3.76	0.92	1.6
1	0.167	1.46	4.22	2.89	1.16
	0.33	1.86	3.96	2.13	1.19
	0.5	2.21	3.93	1.78	1.25
	0.667	3.37	3.92	1.16	1.49
	1	3.51	4.09	1.17	1.55
	1.33	3.7	4	1.08	1.57
	1.67	4.01	3.91	0.97	1.62
1.333	0.167	2.49	5.05	2.03	1.54
	0.33	3.24	4.73	1.46	1.63
	0.5	3.49	4.78	1.37	1.69
	0.667	3.72	5	1.34	1.78
	1	3.57	4.21	1.18	1.59
	1.33	3.95	3.89	0.98	1.6
1.5	0.167	2.58	4.78	1.85	1.5
	0.33	3.38	4.78	1.41	1.67
	0.5	3.63	5	1.38	1.76
	0.667	3.85	4.92	1.28	1.79
	1	3.72	4.13	1.11	1.6
	1.33	4	3.82	0.96	1.6
1.667	0.167	2.77	4.82	1.74	1.55
	0.33	3.78	4.93	1.3	1.78
	0.5	3.8	5.03	1.32	1.8
	0.667	3.9	4.96	1.27	1.81
	1	4.27	4.77	1.12	1.84
	1.33	4.53	4.46	0.99	1.84
2	0.167	2.98	4.79	1.61	1.59
	0.33	3.86	5.08	1.32	1.83
	0.5	3.89	5.01	1.29	1.82
	0.667	4.08	4.99	1.22	1.85
	1	4.47	4.68	1.05	1.87
2.33	0.167	3.04	5.04	1.66	1.65
	0.33	3.95	4.9	1.24	1.81
	0.5	3.97	4.61	1.16	1.75
	0.667	4.09	4.8	1.17	1.81

Table 10 Effect of C_1 and S on Power Consumption (Dual-PBT Systems)

H/T=1, D/T=0.264

S/D	C_1/D	Ne_1	Ne_2	P_2 / P_1	Ptot/P*single
0.667	0.33	1.11	1.29	1.16	1.61
	0.5	0.83	1.52	1.84	1.57
	0.667	0.93	1.32	1.42	1.51
	1	0.97	1.39	1.42	1.58
	1.5	0.95	1.27	1.37	1.49
	2	1.02	1.24	1.21	1.52
1	0.33	1.33	1.24	0.94	1.72
	0.5	1.26	1.18	0.94	1.64
	0.667	1.26	1.35	1.07	1.75
	1	1.36	1.15	0.85	1.68
	1.5	1.27	1.06	0.83	1.57
	2	1.27	1.12	0.88	1.6
1.33	0.33	1.48	1.14	0.77	1.76
	0.5	1.49	1.23	0.83	1.82
	0.667	1.42	1.27	0.89	1.8
	1	1.34	1.16	0.87	1.68
	1.5	1.3	0.97	0.75	1.52
1.5	0.33	1.58	1.45	0.92	2.03
	0.5	1.55	1.15	0.74	1.81
	0.667	1.47	1.27	0.86	1.83
	1	1.37	1.11	0.81	1.66
	1.5	1.3	1.05	0.8	1.58
1.667	0.33	1.67	1.33	0.8	2.01
	0.5	1.55	1.06	0.68	1.75
	0.667	1.53	1.07	0.7	1.74
	1	1.4	1	0.72	1.61
	1.5	1.34	0.78	0.58	1.42
2	0.33	1.55	1.2	0.77	1.84
	0.5	1.48	1.29	0.87	1.86
	0.667	1.51	0.97	0.64	1.66
	1	1.35	1.03	0.77	1.6

Table 11 Effect of C_1 and S on Power Consumption (Dual-FBT Systems)

H/T=2, D/T=0.264

S/D	C_1/D	Ne_1	Ne_2	P_2 / P_1	Ptot/P*single
0.667	0.167	1.22	1.95	2.37	2
	0.33	0.98	2.06	2.01	1.88
	0.5	0.92	2.03	1.86	1.8
	0.667	0.97	1.97	1.91	1.8
	0.83	0.89	2.05	1.82	1.79
	1	0.99	2.15	2.14	1.99
	1.5	1.15	2.1	2.41	2.09
1	0.167	1.1	1.93	2.12	1.88
	0.33	1.14	1.84	2.1	1.82
	0.5	0.96	1.92	1.84	1.74
	0.667	1.14	1.8	2.05	1.78
	0.83	1.02	2.07	2.1	1.93
	1	1.17	1.96	2.3	1.97
	1.5	0.99	2.07	2.03	1.9
1.5	0.167	0.94	2.06	1.93	1.85
	0.33	0.94	1.97	1.85	1.77
	0.5	1.24	1.66	2.06	1.73
	0.667	0.95	1.98	1.89	1.79
	0.83	0.92	2.16	1.99	1.93
	1	1.06	2.07	2.2	1.97
2	0.167	0.93	2.06	1.91	1.84
	0.33	0.95	2.04	1.94	1.84
	0.5	1.02	2.07	2.12	1.94
	0.667	0.88	2.13	1.87	1.85
	1	1.02	2.05	2.09	1.91
2.3	0.167	0.98	2.15	2.09	1.96
	0.5	0.85	2.25	1.9	1.92

Table 12 Effect of C_1 and S on Power Consumption (Dual-CBT Systems)

H/T=2, D/T=0.264

S/D	C_1/D	Ne_1	Ne_2	P_2 / P_1	Ptot/P*single
0.667	0.167	1.43	2.06	1.44	1.7
	0.33	1.54	2.01	1.31	1.72
	0.5	1.53	1.91	1.25	1.67
	0.667	1.57	1.68	1.08	1.58
	1	1.86	2.04	1.1	1.89
	1.5	1.97	2.17	1.1	2.01
	2	2.07	2.24	1.09	2.09
1	0.167	1.5	2.02	1.35	1.71
	0.33	1.61	1.85	1.15	1.68
	0.5	1.68	1.64	0.98	1.61
	0.667	1.69	2.04	1.16	1.81
	1	1.9	1.97	1.04	1.88
	1.5	2.02	1.94	0.96	1.92
	2	1.99	1.97	0.99	1.92
1.5	0.167	1.56	1.92	1.24	1.69
	0.33	1.62	1.91	1.18	1.72
	0.5	1.6	1.85	1.16	1.67
	0.667	1.59	1.85	1.17	1.67
	1	1.8	2.05	1.14	1.87
2	0.167	1.72	2.01	1.17	1.81
	0.33	1.68	1.96	1.17	1.77
	0.5	1.75	2.14	1.22	1.89
	0.667	1.72	2	1.18	1.8

Table 13 Effect of C_1 and S on Power Consumption
(Combination of a PBT and a DT Systems)

PBT (top), DT (bottom), H/T=1, D/T=0.264

S/D	C_1/D	Ne_1	Ne_2	P_2 / P_1	Ptot/P*single
0.667	0.167	3.07	1.29	0.42	0.68
	0.33	3.66	1.23	0.33	0.77
	0.5	3.71	1.23	0.33	0.77
	0.667	3.71	1.32	0.36	0.79
	1	4.21	1.27	0.3	0.86
	1.5	4.37	1.32	0.3	0.89
	2	4.82	1.11	0.23	0.93
1	0.33	3.83	1.09	0.28	0.77
	0.5	3.88	1.07	0.28	0.77
	0.667	3.97	1.09	0.27	0.79
	1	4.41	1.11	0.25	0.86
	1.5	4.7	1.11	0.24	0.91
	2	4.73	1.08	0.23	0.91
1.33	0.33	3.81	1.21	0.32	0.78
	0.5	4.05	1.05	0.26	0.8
	0.667	4.02	1.07	0.27	0.8
	1	4.39	1.14	0.26	0.87
	1.5	4.68	1.11	0.24	0.91
	2	4.73	0.76	0.16	0.86
1.5	0.33	4	1.18	0.3	0.81
	0.5	4.12	0.95	0.23	0.79
	0.667	4.05	0.97	0.24	0.79
	1	4.46	1.06	0.24	0.86
	1.5	4.68	0.85	0.18	0.87
1.667	0.33	4.01	1.12	0.28	0.8
	0.5	4.04	1.02	0.25	0.79
	0.667	4.06	0.96	0.24	0.79
	1	4.5	1.09	0.24	0.87
	1.5	4.6	0.84	0.18	0.85
2	0.33	3.94	1.07	0.27	0.78
	0.5	4.02	0.99	0.25	0.78
	0.667	4.07	0.97	0.24	0.79
	1	4.55	1.01	0.22	0.87

Table 14 Effect of C_1 and S on Power Consumption
(Combination of a PBT and a FBT Systems)

PBT (top), FBT (bottom), H/T=1, D/T=0.264

S/D	C_1/D	Ne_1	Ne_2	P_2 / P_1	Ptot/P*single
0.667	0.167	0.49	2.57	1.26	1.05
	0.33	0.43	2.55	1.1	1
	0.5	0.7	2.11	1.47	0.98
	0.667	0.61	2.16	1.31	0.95
	0.83	0.56	2.22	1.24	-
	1	0.6	2.13	1.28	0.93
	1.5	0.43	2.39	1.04	0.94
1	0.167	0.46	2.55	1.18	1.02
	0.33	0.58	2.31	1.32	0.99
	0.5	0.56	2.26	1.27	0.97
	0.667	0.59	2.17	1.28	0.95
	0.83	0.47	2.25	1.06	-
	1	0.52	2.18	1.15	0.91
	1.5	0.51	2.38	1.22	0.99
1.5	0.167	0.52	2.43	1.28	1.02
	0.33	0.56	2.29	1.28	0.98
	0.5	0.62	2.13	1.32	0.94
	0.667	0.65	2.07	1.34	0.93
	1	0.52	2.2	1.16	0.92
2	0.167	0.46	2.44	1.12	0.98
	0.33	0.61	2.1	1.28	0.92
	0.5	0.57	2.04	1.15	0.87
	0.667	0.55	2.06	1.14	0.87

Table 15 Effect of C_1 and S_{12} on Power Consumption (Triple-DT Systems)

H/T=2, D/T=0.264, S_{13}/D=5

S_{12}/D	C_1/D	Ne_1	Ne_2	Ne_3	Ptot/P*single	P_1%	P_2%	P_3%
0.667	0.33	1.68	3.81	4.82	2.18	16.3	37	46.8
	0.5	1.8	3.58	4.78	2.14	17.7	35.2	47
	0.667	2.2	3.4	4.81	2.2	21.2	32.6	46.2
	1	3.13	3.91	4.91	2.52	26.2	32.7	41.1
1	0.33	1.76	4.03	5.3	2.34	15.9	36.4	47.8
	0.5	2.09	3.99	5.19	2.38	18.5	35.4	46.1
	1	2.99	4.47	5.37	2.71	23.3	34.8	41.9
	1.5	3.77	3.95	5.18	2.72	29.2	30.6	40.2
1.5	0.33	3.48	4.81	5.38	2.88	25.4	35.2	39.4
	0.5	3.65	5.04	5.4	2.97	25.9	35.8	38.3
	1	3.37	4.35	5.22	2.73	26	33.6	40.3
	1.5	3.77	4.54	5.1	2.83	28.1	33.9	38
2	0.33	3.79	4.93	5.24	2.95	27.2	35.3	37.5
	0.5	4.02	4.82	5.32	2.99	28.4	34.1	37.6
	1	4.19	4.97	5.35	3.06	28.9	34.2	36.9
	1.5	4.38	4.94	5.39	3.1	29.8	33.6	36.7
2.5	0.33	3.93	5.06	5.14	2.98	27.8	35.8	36.4
	0.5	3.87	5.12	5.27	3.01	27.1	35.9	37
	1	4.37	5.12	5.35	3.13	29.5	34.5	36
	1.5	4.56	5.03	5.22	3.12	30.8	34	35.3
3	0.33	3.95	4.97	5.24	2.99	27.9	35.1	37
	0.5	4.03	4.98	5.27	3.01	28.2	34.9	36.9
	1	4.48	4.87	5.28	3.09	30.6	33.3	36.1
3.5	0.33	4.24	4.15	4.59	2.74	32.7	32	35.4
	0.5	4.12	4.34	4.44	2.72	31.9	33.6	34.4
	1	4.45	4.54	4.39	2.82	33.2	34	32.8
	1.5	4.78	4.18	4.2	2.77	36.3	31.8	31.9
4	0.33	3.93	4.42	4.26	2.66	31.2	35	33.8
	0.5	4.31	3.96	4.29	2.65	34.3	31.5	34.2
	1	4.57	4.27	4.25	2.76	34.9	32.6	32.4
	1.5	4.76	4.22	4.01	2.74	36.6	32.5	30.9

Table 16 Effect of C_1 and S_{12} on Power Consumption (Triple-PBT Systems)

H/T=2, D/T=0.264, S_{13}/D=5

S_{12}/D	C_1/D	Ne_1	Ne_2	Ne_3	Ptot/P*single	P_1%	P_2%	P_3%
0.667	0.167	1.31	1.57	1.16	2.7	32.4	39	28.6
	0.33	1.06	1.59	1.3	2.64	26.9	40.2	32.9
	0.5	1.03	1.53	1.36	2.61	26.2	39	34.7
	1	1.12	1.42	1.31	2.57	29.2	36.9	33.9
	1.5	1.18	1.09	1.49	2.51	31.6	28.8	39.6
1	0.167	1.45	1.57	1.26	2.86	33.9	36.6	29.5
	0.33	1.39	1.41	1.34	2.76	33.6	34.1	32.3
	0.5	1.31	1.5	1.39	2.8	31.1	35.8	33.1
	1	1.25	1.38	1.27	2.61	32.1	35.3	32.6
	1.5	1.22	1.16	1.29	2.45	33.1	31.6	35.2
1.5	0.167	1.67	1.46	1.34	2.99	37.4	32.7	29.9
	0.33	1.47	1.56	1.27	2.88	34.1	36.3	29.5
	0.5	1.51	1.34	1.33	2.79	36.2	32.1	31.7
	1	1.37	1.05	1.45	2.58	35.5	27.2	37.4
	1.5	1.14	1.32	1.43	2.6	29.2	33.9	36.8
2	0.167	1.71	1.28	1.4	2.93	38.9	29.1	32
	0.33	1.49	1.36	1.3	2.78	35.9	32.8	31.3
	0.5	1.39	1.3	1.3	2.67	34.8	32.6	32.6
	1	1.34	1.16	1.4	2.6	34.3	29.9	35.8
2.5	0.167	1.84	0.96	1.41	2.82	43.7	22.9	33.4
	0.33	1.42	1.24	1.47	2.76	34.4	30	35.6
	0.5	1.3	1.34	1.33	2.65	32.8	33.7	33.5
	1	1.19	1.39	1.33	2.61	30.6	35.4	34
	1.5	1.27	1.26	1.37	2.6	32.6	32.3	35.1
3.5	0.167	1.72	1.37	1.15	2.83	40.5	32.4	27.1
	0.33	1.61	1.36	1.23	2.81	38.3	32.4	29.3
	0.5	1.57	1.35	1.21	2.76	38.1	32.7	29.2
	1	1.39	1.36	1.25	2.67	34.8	34	31.2
	1.5	1.29	1.31	1.21	2.55	33.9	34.3	31.8
4	0.167	1.76	1.25	1.26	2.86	41.1	29.3	29.6
	0.33	1.65	1.29	1.38	2.89	38.3	29.9	31.8
	0.5	1.57	1.33	1.35	2.84	37	31.3	31.7
	1	1.4	1.3	1.34	2.7	34.6	32.3	33.1
	1.5	1.23	1.3	1.4	2.62	31.3	33	35.6

Table 17 Effect of C_1 and S_{12} on Power Consumption (Triple-FBT Systems)

H/T=2, D/T=0.352, S_{13}/D=3.5

S_{12}/D	C_1/D	Ne_1	Ne_2	Ne_3	Ptot/P*single	P_1%	P_2%	P_3%
0.525	0.167	2.11	2.22	2.58	3.06	30.6	32.1	37.3
	0.25	1.88	2.32	2.42	2.93	28.4	35	36.5
	0.5	1.9	2.03	2.35	2.78	30.2	32.4	37.4
	0.75	2.15	1.86	2.4	2.84	33.6	29.1	37.4
	1	2.25	2.08	2.34	2.95	33.8	31.1	35.1
0.75	0.167	2	2.05	2.6	2.94	30.1	30.8	39.1
	0.25	2.01	2.02	2.34	2.82	31.5	31.7	36.8
	0.5	1.86	1.89	2.34	2.69	30.5	31	38.5
	0.75	2.15	1.88	2.38	2.84	33.5	29.3	37.2
	1	2.2	2	2.3	2.88	33.8	30.8	35.4
1	0.167	1.91	1.97	2.3	2.73	31	31.9	37.2
	0.25	1.9	1.97	2.28	2.72	30.9	32	37.1
	0.5	1.85	1.88	2.39	2.7	30.2	30.7	39
	0.75	2.23	1.84	2.46	2.89	34.1	28.2	37.7
	1	2.11	2	2.4	2.88	32.5	30.7	36.8
1.5	0.167	1.89	1.97	2.71	2.91	28.8	30	41.2
	0.25	1.87	2.07	2.66	2.92	28.4	31.3	40.3
	0.5	1.89	2.56	2.57	3.11	26.9	36.5	36.6
	0.75	2	2.44	2.61	3.12	28.4	34.6	37.1
	1	1.97	2.12	2.47	2.9	30	32.4	37.6
1.75	0.167	2.08	2.25	2.57	3.05	30.1	32.6	37.3
	0.25	2.18	2.46	2.49	3.15	30.6	34.5	34.9
	0.5	2.12	1.94	2.08	2.71	34.5	31.7	33.9
	0.75	2.05	1.93	2.18	2.73	33.3	31.3	35.4
	1	2.09	2.07	2.26	2.84	32.5	32.3	35.2
2.125	0.167	2.53	1.98	2.02	2.89	38.7	30.4	31
	0.25	2.36	1.97	2.02	2.81	37.2	31.1	31.7
	0.5	2.15	1.92	2.11	2.73	34.9	31	34.1
	0.75	2.1	1.94	2.01	2.68	34.7	32	33.3
	1	2.06	2.06	2.07	2.74	33.3	33.3	33.4
2.5	0.167	2.54	2.08	2.09	2.97	37.9	30.9	31.2
	0.25	2.43	2.02	2.13	2.91	37	30.7	32.3
	0.5	2.11	2.1	2.09	2.79	33.5	33.3	33.2
	0.75	2.07	2.07	2.15	2.78	32.9	32.9	34.2
	1	2.03	2.05	2.13	2.75	32.7	33	34.3
2.975	0.167	2.39	2.38	2.47	3.21	33	32.8	34.1
	0.25	2.4	2.22	2.53	3.16	33.5	31.1	35.4
	0.5	2.14	2.11	2.49	2.98	31.8	31.3	36.9
	0.75	1.96	2.21	2.45	2.92	29.6	33.4	37
	1	2.04	2.24	2.37	2.94	30.7	33.7	35.5

Table 18 Effect of C_1 and S_{12} on Power Consumption (Triple-CBT Systems)

H/T=2, D/T=0.264, S_{13}/D=4.67

S_{12}/D	C_1/D	Ne_1	Ne_2	Ne_3	Ptot/P*single	P_1%	P_2%	P_3%
0.667	0.167	1.5	2.05	2.4	2.79	28.3	33.1	38.6
	0.33	1.51	2.07	2.36	2.79	28.7	32.7	38.6
	0.5	1.48	1.97	2.45	2.77	27.4	34.1	38.5
	0.67	1.54	1.86	2.45	2.74	26.3	34.7	38.9
	1	1.66	1.85	2.45	2.8	26.1	34.5	39.4
	1.5	1.89	2	2.44	2.97	27	32.9	40.1
1	0.167	1.53	2.03	2.37	2.78	28.3	33	38.8
	0.33	1.63	1.87	2.27	2.71	27.3	33.2	39.5
	0.5	1.57	1.95	2.25	2.71	28.3	32.5	39.2
	0.67	1.61	1.73	2.36	2.68	25.6	34.9	39.5
	1	1.65	1.92	2.42	2.81	26.9	33.8	39.3
	1.5	2	1.79	2.46	2.93	24.9	34.2	40.8
1.5	0.167	1.63	1.91	2.41	2.79	26.8	33.9	39.3
	0.33	1.63	1.7	2.57	2.77	24.1	36.5	39.3
	0.5	1.78	1.66	2.42	2.75	24.3	35.5	40.3
	0.67	1.77	1.65	2.5	2.78	23.7	36.1	40.1
	1	1.88	1.73	2.44	2.84	24.7	34.8	40.5
	1.5	1.91	2.01	2.24	2.89	28.2	31.3	40.5
2.33	0.167	1.85	1.83	2.45	2.88	25.6	34.2	40.2
	0.33	1.82	1.98	2.49	2.95	26.7	33.5	39.8
	0.5	2.13	1.78	2.55	3.03	24.2	34.7	41.2
	0.67	2.15	1.67	2.63	3.03	22.8	32	39.8
	1	1.84	2.13	2.42	3	28.2	32	39.8
	1.5	2	1.88	2.35	2.93	26.3	32.8	40.9
3.67	0.167	2.32	1.73	2.46	3.06	23.8	34	42.2
	0.33	2.15	1.92	2.42	3.04	26	32.8	41.2
	0.5	2	2.12	2.18	2.96	29.2	30.1	40.7
	0.67	2.15	1.83	2.29	2.95	25.9	32.5	41.7
	1	2.08	1.83	2.31	2.92	25.9	32.7	41.4
	1.5	2.01	2.04	2.26	2.96	28.1	31.2	40.8
4	0.167	2.32	1.95	2.47	3.17	25.7	32.6	41.7
	0.33	2.22	1.98	2.55	3.17	25.7	33.1	41.2
	0.5	2.13	2.01	2.48	3.11	26.4	32.7	40.9
	0.67	2.12	1.94	2.55	3.1	25.5	33.6	40.9
	1	2.08	1.94	2.45	3.04	26.1	33	40.9
	1.5	2.14	1.96	2.34	3.02	26.8	31.9	41.3

Table 19 Effect of C_1 and S_{12} on Power Consumption
(Combinations of DTs and PBTs Systems)

PBT (top), DT (middle), DT (bottom), H/T=2, D/T=0.264, S_{13}/D=5

S_{12}/D	C_1/D	Ne_1	Ne_2	Ne_3	Ptot/$\sum$ P*single	P_1%	P_2%	P_3%
0.667	0.33	1.67	3.75	1.08	0.59	25.7	57.6	16.6
	0.5	1.88	3.66	1.19	0.61	27.9	54.4	17.7
	1	3.15	3.83	0.76	0.71	40.8	49.5	9.7
	1.5	3.37	3.84	0.95	0.74	41.3	47.1	11.6
1	0.33	2.04	3.89	1.58	0.68	27.2	51.8	21.1
	0.5	2.23	3.87	1.09	0.66	31	53.8	15.2
	1	3.2	4.05	1.13	0.76	38.2	48.3	13.5
	1.5	3.78	3.89	1.14	0.8	42.9	44.2	13
	2	4.17	3.72	1.07	0.83	45.1	42.4	12.5
1.5	0.33	2.9	3.85	1.56	0.76	34.7	46.3	19
	0.5	3.49	4.59	1.06	0.83	38.2	50.2	11.6
	1	3.47	4.12	1.09	0.79	40	47.5	12.5
	1.5	4.03	3.91	1.21	0.83	44.1	42.7	13.2
	2	4.56	4.47	1.02	0.92	45.4	44.5	10.1
2	0.33	3.8	4.68	0.98	0.86	40.2	49.5	10.3
	0.5	3.88	4.62	1.08	0.87	40.5	48.3	11.3
	1	4.42	4.74	1.11	0.94	43	46.1	10.8
	1.5	4.75	4.62	1.1	0.95	45.4	44.1	10.5
	2	4.95	4.58	0.88	0.95	47.6	44	8.4
2.5	0.33	4.09	4.6	1.09	0.89	41.8	47	11.1
	0.5	4.1	4.64	1.07	0.89	41.8	47.3	10.9
	1	4.58	4.82	1.09	0.96	43.7	45.9	10.4
	1.5	5.02	4.72	1.12	0.99	46.2	43.5	10.3
	2	5.04	4.71	1.03	0.98	46.8	43.7	9.5
3	0.33	4.14	4.71	1.14	0.91	41.5	47.1	11.4
	0.5	4.27	4.58	1.28	0.92	42.2	45.2	12.6
	1	4.86	4.6	1.32	0.98	45.1	42.7	12.2
	2	4.99	4.69	1.08	0.98	46.4	43.6	10.1
3.5	0.33	4.21	4.73	1.16	0.92	41.7	46.8	11.5
	0.5	4.35	4.68	1.02	0.92	43.3	46.6	10.2
	1	4.77	4.73	1.08	0.96	45.1	44.7	10.2
	1.5	4.82	4.82	1.17	0.98	44.6	44.6	10.8
	2	4.94	4.52	0.89	0.94	47.7	43.7	8.6
4	0.33	4.33	4.59	1.27	0.93	42.5	45.1	12.5
	0.5	4.36	4.53	1.3	0.93	42.8	44.5	12.7
	1	4.72	4.77	1.38	0.99	43.4	43.9	12.7
	1.5	5.01	4.48	1.25	0.98	46.7	41.7	11.6
	2	5.06	4.45	1.1	0.97	47.7	42	10.4

Table 20 Effect of C_1 and S_{12} on Power Consumption
(Combinations of DTs and PBTs Systems)

DT (top), PBT (middle), DT (bottom), H/T=2, D/T=0.264, S_{13}/D=5

S_{12}/D	C_1/D	Ne_1	Ne_2	Ne_3	Ptot/$\sum$ P*single	P_1%	P_2%	P_3%
0.667	0.167	3.38	1.22	5.07	0.88	35	12.6	52.4
	0.33	3.89	1.18	5.01	0.92	38.6	11.7	49.7
	0.5	3.86	1.18	4.98	0.91	38.5	11.8	49.7
	0.67	3.99	1.25	5.02	0.93	38.8	12.2	48.9
	1	4.38	1.23	5.09	0.97	40.9	11.5	47.6
	1.5	4.65	1.03	5.02	0.98	43.5	9.6	46.9
1	0.167	3.42	1.19	5.03	0.88	35.5	12.4	52.1
	0.33	3.95	1.18	4.99	0.92	39	11.7	49.3
	0.5	4.1	1.13	4.99	0.93	40.1	11.1	48.8
	0.67	4.1	1.37	4.92	0.95	39.5	13.2	47.3
	1	4.44	1.37	5.15	1	40.5	12.5	47
	1.5	4.77	1.13	5.03	1	43.7	10.3	46
1.75	0.167	3.18	1.16	5.17	0.87	33.4	12.2	54.4
	0.33	4.22	1.24	4.85	0.94	40.9	12.1	47
	0.5	4.17	1.22	4.96	0.94	40.3	11.8	47.9
	0.67	4.34	1.02	4.95	0.94	42.1	9.9	48
	1	4.77	1.08	5.21	1.01	43.1	9.8	47.1
	1.5	4.89	1.11	5.07	1.01	44.2	10	45.8
2.5	0.167	3.15	1.15	4.94	0.84	34.1	12.4	53.5
	0.33	4.24	0.82	5.1	0.92	41.7	8	50.2
	0.5	4.17	1	5.1	0.94	40.6	9.7	49.6
	0.67	4.27	0.96	4.89	0.92	42.2	9.5	48.3
	1	4.66	0.97	5.18	0.98	43.1	9	47.9
	1.5	4.85	0.93	4.94	0.98	45.3	8.6	46.1
3.25	0.167	3	1.18	4.97	0.83	32.8	12.9	54.3
	0.33	4.24	1.05	4.76	0.92	42.2	10.4	47.4
	0.5	4.2	1.12	4.73	0.92	41.8	11.2	47.1
	0.67	4.42	0.97	4.87	0.94	43.1	9.5	47.5
	1	4.77	0.92	5.03	0.98	44.5	8.6	46.9
	1.5	4.85	0.99	4.86	0.98	45.3	9.3	45.4
4	0.167	3.16	1.48	4.2	0.81	35.8	16.8	47.4
	0.33	4.37	1.22	4.38	0.91	43.8	12.3	43.9
	0.5	4.34	1.25	4.24	0.9	44.1	12.7	43.2
	0.67	4.3	1.43	4.13	0.9	43.6	14.5	41.9
	1	4.76	1.34	4.2	0.94	46.2	13	40.8
	1.5	4.8	1.26	4.17	0.93	46.9	12.3	40.7

Table 21 Effect of C_1 and S_{12} on Power Consumption
(Combinations of DTs and PBTs Systems)

PBT (top), PBT (middle), DT (bottom), H/T=2, D/T=0.264, S_{13}/D=5

S_{12}/D	C_1/D	Ne_1	Ne_2	Ne_3	Ptot/$\sum$ P*single	P_1%	P_2 %	P_3 %
0.667	0.33	3.74	1.22	1.19	0.8	60.9	19.8	19.3
	0.5	3.65	1.36	1.08	0.79	59.9	22.3	17.8
	0.667	3.89	1.19	1.08	0.8	63.1	19.3	17.6
	1	4.19	1.34	1.14	0.86	62.8	20.1	17.1
	1.5	4.42	1.34	1.12	0.89	64.3	19.4	16.2
1	0.33	3.82	1.22	1.1	0.79	62.2	19.8	18
	0.5	3.83	1.3	1.07	0.8	61.8	20.9	17.2
	0.667	3.98	1.17	1.09	0.81	63.8	18.7	17.4
	1	4.28	1.12	1.23	0.86	64.6	16.9	18.6
	1.5	4.55	1.37	1.21	0.92	63.8	19.2	16.9
1.5	0.33	4.11	1.12	1.21	0.83	63.8	17.4	18.7
	0.5	4.02	1.25	1.22	0.84	61.9	19.3	18.8
	0.667	4.03	1.28	1.25	0.85	61.4	19.5	19.1
	1	4.44	1.29	1.2	0.9	64.1	18.6	17.3
	1.5	4.63	1.27	1.17	0.92	65.4	18	16.6
2	0.33	3.84	1.21	1.16	0.8	61.8	19.5	18.7
	0.5	3.86	1.15	1.13	0.79	62.9	18.7	18.4
	0.667	4.01	1.11	1.17	0.81	63.8	17.6	18.6
	1	4.45	1.25	1.24	0.9	64.1	18	17.9
2.5	0.33	3.87	0.97	1.17	0.78	64.4	16.2	19.4
	0.5	4.01	0.95	1.03	0.77	67	15.8	17.1
	0.667	4.18	0.92	1.14	0.81	66.9	14.8	18.3
	1	4.47	1.13	1.04	0.86	67.3	17	15.7
	1.5	4.64	1.02	1.2	0.89	67.7	14.8	17.5
3	0.33	4.02	1.08	1.17	0.81	64.1	17.2	18.7
	0.5	4.16	1.03	1.17	0.82	65.4	16.2	18.3
	0.667	4.13	1.13	1.12	0.83	64.7	17.7	17.6
	1	4.48	1.15	1.16	0.88	65.9	17	17.1
3.5	0.33	4.16	1.14	1.1	0.83	65	17.8	17.2
	0.667	4.06	1.26	1.2	0.84	62.2	19.3	18.5
	1	4.49	1.22	1.15	0.89	65.5	17.7	16.8
4	0.33	4.15	1.1	1.03	0.81	66.1	17.4	16.5
	0.5	3.97	1.24	1.05	0.81	63.4	19.8	16.7
	0.667	4.1	1.16	1.1	0.82	64.5	18.2	17.2
	1	4.6	1.13	0.94	0.86	68.9	17	14.1
	1.5	4.74	1.17	1.07	0.9	68	16.7	15.3

REFERENCES

Abradi, V., Rovero, G., Sicardi, S., Baldi, G., and Conti, R., 1988. "Sparged Vessels Agitated by Multiple Turbines." *6th Euro. Conf. on Mixing*, 329-336.

Abradi, V., Rovero, G., Sicardi, S., Baldi, G., and Conti, R., 1990. "Hydrodynamics of a Gas-Liquid Reactor Stirred with a Multiple-Impeller System." *Trans IChem E*, 68, Part A: 516-522.

Bates, R. L., Fondy, P. L., and Corpstein, R. R., 1963. "An Examination of Some Geometric Parameters of Impeller Power." *I & EC Proc. Des. and Dev.*, 2: 310-314.

Chiampo, F., Guglielmetti, R. Manna,L., and Conti, R., 1991. "Gas-Liquid Mixing in a Multiple Impellers Stirred Vessel." *7th Euro. Conf. on Mixing*, 2:333-341.

Chudacek, M. W., 1985. "Impeller Power Numbers and Impeller Flow Numbers in Profiled Bottom Tanks." *Ind. Eng. Chem. Des. Dev.*, 24: 858-867.

Fajner, D., Magelli, F., and Pasquali, G., 1982. "Modelling of Non-standard Mixers Stirred with Multiple Impellers." *Chem. Eng. Commun.*, 17: 285-295.

Gray, D. J., Treybal, R. E., and Barnett, S. M., 1982. "Mixing of Single and Two Phase Systems: Power Consumption of Impellers." *AIChE Journal*, 28: 195-199.

Greaves, M. and Kobbacy, K. A. H., 1981. "Surface Aeration in Agitated Vessels." *IChemE Symposium Series*, 64: H1-H22.

Hudcova, V., Machon, V., and Nienow, A.W., 1989. "Gas-Liquid Dispersion with Dual Rushton Turbine Impellers." *Biotech. and Bioeng*, 34: 617-628.

Kuboi, R., and Nienow, A. W., 1982. "The Power Drawn by Dual Impeller Systems under Gassed and Ungassed Conditions." *4th Euro. Conf. on Mixing*, G2: 247-261.

Li, T., 1991. "Solid-Liquid Suspension in Agitated Vessels Provided with Multiple Impellers." Master's Thesis, New Jersey Institute of Technology.

Lu, W. -M., and Yao, C, -L., 1991. "Gas Dispersion in a Multi-Stage Impeller Stirred Tank." *7th Euro. Conf. on Mixing*, 2: 351-357.

Machon, V., Mcfarlane, C. M., and Nienow, A. W., 1991. "Power Input and Gas Hold up in Gas Liquid Dispersions Agitated by Axial Flow Impellers." *7th Euro. Conf. on Mixing*, 2: 243-249.

Machon, V., Vlcek, J., and Skrivanek, J., 1985. "Dual Impeller Systems for Aeration of Liquids: An Experimental Study." *5th Euro. Conf. on Mixing*, 155-169.

Mahmoudi, S. M., Yianneskis, M., 1991. "The Variation of Flow Pattern and Mixing Time with Impeller Spacing in Stirred Vessels with Two Rushton Impellers." *7th Euro. Conf. on Mixing*, 1: 17-24.

Mhaisalkar, V. A., Paramasivam, R., and Bhole, A. G., 1986. "An Innovative Technique for Determining Velocity Gradient in Coagulation-Flocculation Process." *Wat. Res.*, 20: 1307-1314.

Nienow, A. W., and Lilly, M. D., 1979. "Power Drawn by Multiple Impellers in Sparged Agitated Vessels." *Biotech. and Bioeng.*, 21: 2341-2345.

Nocentini, M., Magelli, F., Pasquali, G., and Fajner, D., 1988. "A Fluid-Dynamic Study of a Gas-Liquid, Non-standard Vessel Stirred by Multiple Impellers." *The Chem. Eng. J.*, 37: 53-59.

O'Connell, F. P., and Mack, D. E., 1950. "Simple Turbines in Fully Baffled Tanks, Power Characteristics." *Chem. Eng. Prog.*, 46: 359-362.

Oldshue, J. Y., 1983. *Fluid Mixing Technology*. McGraw-Hill Pub. Co., New York, NY

O'Okane, K., 1974. "The Effect of Geometric Parameters on the Power Consumption of Turbine Impellers Operating in Non-viscous Fluids." *1st Euro. Conf. on Mixing*, A3: 23-31.

Rao, K. S. M. S., and Joshi, J. B., 1988. "Liquid Phase Mixing in mechanically Agitated Vessels" *Chem. Eng. Comm.*, 74: 1-25.

Rewatkar, V. B., Rao, K. S. M. S. R., and Joshi, J. B., 1990. "Power Consumption in Mechanically Agitated Contactors Using Pitched Bladed Turbine Impellers." *Chem. Eng. Prog.*, 88: 69-90.

Roustan, M., 1985. "Power Consumed by Rushton Turbines in Non-Standard vessels under Gassed Conditions." *5th Euro. Conf. on Mixing*, 127-141.

Rushton, J. H., Costich, E.W., and Everett, H. J., 1950. "Power Characteristics of Mixing Impellers, Part I." *Chem. Eng. Prog.*, 46: 395-404.

Rushton, J. H., Costich, E.W., and Everett, H. J., 1950. "Power Characteristics of Mixing Impellers, Part II." *Chem. Eng. Prog.*, 46: 467-476.

Shiue, S. J., and Wong, C, W., 1984. "Studies on Homogenization Efficiency of Various Agitators in Liquid Blending." *Can. J. Chem. Eng.*, 62: 602-609.

Smith, J. M., Warmoeskerken, M. M. C. G., and Zeef, E., 1987. "Flow Conditions in Vessels Dispersing Gases in Liquids with Multiple Impellers." *Biotechnology Process*, AIChE, New York, N. Y.

Tatterson, G. B., 1991. *Fluid Mixing and Gas Dispersion in Agitated Tanks*. McGraw-Hill, Inc.

White, A. M. and Brenner, E., 1934. "Studies in Agitation, V. The Correlation of Power Data." *Trans American Institute of Chemical Engineers*, 30: 585-597.